DEVELOPMENT OF MODIFIED BIOPOLYMER ADSORBENTS FROM NATURAL POLYSACCHARIDES FOR RENEWAL OF ABATTOIR WASTEWATER

ERNESTINE ATANGANA

Thesis submitted in fulfilment of the requirements for the Degree

DOCTOR PHILOSOPHIAE:

ENVIRONMENTAL HEALTH

in the

Department of Life Sciences

Faculty of Health and Environmental Sciences

at the

Central University of Technology, Free State

Promoter: **Dr. T.T. CHIWESHE** (PhD. Chemistry)

Co-promoter: **Dr. H.A. ROBERTS** (D. Tech. Environmental Health)

BLOEMFONTEIN

2019

DECLARATION OF INDEPENDENT WORK

.

I, ERNESTINE ATANGANA, student number , do hereby declare that this research project submitted to the Central University of Technology, Free State for the Degree Doctor Philosophiae: Health and Environmental Science, is my own independent work and that it complies with the Code of Academic Integrity as well as other relevant policies, procedures, rules and regulations of the Central University of Technology, Free State. The manuscript has not been submitted before to any institution by myself or any other person in fulfilment (or partial fulfilment) of the requirements for the attainment of any qualification.

_____
SIGNATURE OF STUDENT

JANUARY 2019
DATE

ACKNOWLEDGEMENTS

This work was conducted at the department of Life Sciences, Central University of Technology, Free State, Bloemfontein, during 2016 − 2018.

I would like to express my sincere gratitude and appreciation to my saviour, Jesus Christ, for giving me life, good health and the spiritual resources I needed to undertake this study.

I did not attempt this challenge alone as I stood on the shoulders of giants whom I want to thank. I wish to express my deepest appreciation to the following people:

My Supervisor, Dr. T.T. Chiweshe, for your positive attitude and guidance throughout the research project. You were helpful and I learnt so much from you. I thank you for your relentless but compassionate supervision, advice, inspiration, indefatigable assistance, willingness to help, guidance, encouragement and constant reassurance. Your recommendations and suggestions greatly improved my thesis writing abilities.

My co-Supervisor, Dr. H. Roberts. Thank you so much for the review of my work and information regarding the paper work, and for your guidance and encouragement.

My special thanks to the following staff members in the Centre of Applied Food Security and Biotechnology lab. Thank you for being helpful and supportive towards my research project.

- Prof J.F.R. Lues,
- Dr. N.L. Malebo (The Head of Department)
- Dr. I. Manduna and
- Dr.O de Smith and

Dr. L. Deysel, thank you for your kindness and for making it possible to complete this research.

The Physics Department of the University of the Free State is also thanked for the FTIR analysis and the National Research Foundation (NRF) for the financial assistance.

My special gratitude goes to Prof. A. Atangana, my loving, intelligent, God-fearing and caring husband. Thank you for your financial support, constant prayers, advice, inspiration, indefatigable assistance, guidance, encouragement, constant faith and companionship. You gave me the courage to complete this work.

I also wish to thank my two sons, Melchizedek and Diophantine Atangana, for your love and support, as well as my family and extended family members for your prayers and encouragement.

> ''The Lord is my shepherd, I shall not want. He makes me lie down in green pastures. He leads me beside the still waters. He restores my soul. He leads me in the paths of righteousness, for His name's sake. Yea, though I walk through the valley of the shadow of death, I shall fear no evil, for Thou are with me. Thy rod and Thy staff they comfort me. Thou prepare a table before me in the presence of mine enemies. Thou anoint my head with oil; my cup run over. Surely goodness and mercy shall follow me all the days of my life and I shall dwell in the house of the Lord forever.''
>
> **(Psalm 23:1-6, Bible, King James Version)**

ABSTRACT

The wastewater effluents produced by poultry and the red meat industries were analysed in the quest to detect the presence of heavy metals in abattoir wastewater and to establish and optimize alternative methods of purifying wastewater from Bloemfontein abattoirs in an effort to reduce water pollution. Water samples were randomly collected from two categories of local abattoirs in Bloemfontein, namely poultry and red meat abattoirs. The samples were found to contain high levels of alkali and alkaline earth metals (Ca, Mg, K and Na) at rates above 100 mg/ℓ. Other elements present in the wastewater samples that were analyzed included Cr, Ni, Cu and Pb, which are elements that have been reported to cause devastating effects in animals and the environment. Analyses of the Cr, Ni, Cu and Pb using ICP-OES showed the presence of ultra-trace levels (0.05 – 0.2 mg/ℓ) in both wastewater solutions. These elements confirmed the presence of heavy metals in the water bodies at the abattoirs. A chromatographic technique using different chitosan products as adsorbents was developed.

Some cross-linked chitosan products were synthesized from different chitin (mussel, prawn, pang and silver) products. The modified chitosan products were obtained from cross-linking the chitin with glutaraldehyde, formaldehyde, epichlorohydrine, maleic anhydride, *p*-benzoquinone, poly (ethylene) glycol diglycidyl ether (PEG diglycidyl ether), 1-vinyl-2-pyrrolidone, 1,3-dichloroaceone, acrylic acid and s-methyl-benzylamine. Characterization of these cross-linked chitosan products was performed using FTIR, SEM and viscometer assessments. The results obtained from the analyses using SEM spectroscopy revealed that the different products had different morphological structures. The results of the analyses showed significant adsorption rates of alkali and alkaline earth metals (Ca, Mg, K and Na) using shrimp chitosan that was cross-linked with maleic anhydride (J1) and shrimp chitosan that was cross-linked with acrylic acid (I2) chitosan products. The shrimp and crab chitosan starch that was cross-linked with formaldehyde (C1 and C2) was also shown to effectively adsorb the alkali and alkaline earth metals present in the waste samples. Lower concentrations of heavy metals were recovered (0.05 - 0.2 mg/ℓ) for Cr, Ni, Cu and Pb using these chitosan products. Although no complete adsorption of these elements was achieved

in both the wastewater samples, the results showed a substantial improvement of the water eluted which demonstrated the effectiveness of the method using synthesized chitosan products.

TABLE OF CONTENTS

LIST OF FIGURES

LIST OF TABLES

LIST OF SCHEME

LIST OF ABBREVIATIONS

General terms

RMAA: Red meat abattoir association

Analytical spectrometry equipment

ICP-OES: Inductive coupled plasma-optical emission spectroscopy

FTIR: Fourier transform infrared spectroscopy

SEM: Scanning electron microscope

Cps: Centipoise

PEG: poly-ethylene glycol diglycidyl ether

KEYWORDS

Chitin

Chitosan

Abattoir wastewater effluent

Heavy metals

Qualitative and quantitative analysis

Spectrometric analysis

1 INTRODUCTION

1.1 General background and motivation for this study

Chemical water pollution due to heavy metals in industrial waste remains a serious environmental and public concern. The most common source of surface water pollution in South Africa is waste from industrial abattoirs which contributes to ‘’up to’’ 85% of water pollution in this country. Industrial wastewater from abattoirs contains mixtures of solid particles and liquid wastes that include blood, carcasses, hides, carcass trimmings, grease, feathers, manure, grit, undigested feed, bones, horns, hair, fat, bile, urine and dissolved chemicals. These waste products, together with other heavy metals from chemical waste in abattoirs, pollute fresh water sources (e.g., rivers, dams and boreholes) and ultimately spread sickness and diseases such as typhoid and cholera (Chukwu *et al*. 2011). Moreover, heavy metals in wastewater have been found to severely affect human cellular organelles, particularly the cell membrane, endoplasmic reticulum, nuclei, mitochondrial, lysosome and some enzymes involved in the detoxification toxins in the body (Wang & Shi, 2001).

The liquid waste (or effluent) from industrial abattoirs contains a variety of dissolved chemicals, heavy metals ions, aromatic compounds such as phenolic derivatives and polycyclic aromatic compounds, dyes and humic pigments (Rio & Delebarre, 2003) that often result in coloured effluents. When these effluents are disposed of in and then washed down river streams, the effects are devastating and range from immediate to long-term damage to humans and the environment. Heavy metals are not biodegradable and tend to accumulate in living organisms, thereby causing immediate ill effects in animals (Van der Oost *et al.* 2003). Humic substances and some persistent organic micro-pollutants found in effluents are also harmful to organisms and to human health (Irshad, 2013). Other pigments such as synthetic dyes that are extensively used in the textile industry for dyeing, paper printing and additives in petroleum products are recalcitrant organic molecules that also strongly colour wastewater. These pigments are the most common contaminants in wastewater and are regarded as carcinogenic.

The effective disposal of abattoir wastewater (Figure 1.1) is therefore a matter of severe concern because most current techniques do not completely address the issue of heavy metals due to the complexity of the chemistry involved and problems associated with waste separation techniques (Adeyemo, 2002).

Figure 1.1: Abattoir effluent released in the environment

Source: Irshad, 2013

Several techniques have been used to treat industrial effluents in an attempt to prevent water pollution. These techniques include the use of conventional methods such as activated carbon, precipitation, coagulation-flocculation, and the application of synthetic polymers (Brostow *et al.* 2009). Treatment of wastewater using these techniques is divided into primary, secondary and tertiary treatment categories (Massé & Massé, 2000). Primary treatment predominantly targets the removal of suspended solid particles, the separation of floating and heavy solids using screens or catch basins, dissolved air floatation, flow equalization, oil and grease removal, and settlers for the recovery of proteins and fats. Secondary treatment mainly involve the removal of organic matter using biological treatment methods such as aerobic and anaerobic lagoons, facultative lagoons, activated sludge systems, extended aeration, oxidation ditches and sequencing batch reactors. The tertiary treatment stage involves the removal of nitrate, phosphate and heavy metals.

1.2 Motivation for the study

Fresh water supplies in South Africa are increasingly becoming scarcer due to water pollution that is derived mainly from abattoirs. The recent drought that ravaged Cape Town in 2018 and the persistent drought in other inland areas have highlighted the need to recycle wastewater from abattoirs and to establish ways to minimize water pollution (Otto and Wolski, 2018). The availability of clean water from already scarce sources is threatened by the continuous addition of abattoir wastes and contaminated industrial waste chemicals into watercourses (Lvovich, 1979). Techniques to effectively recycle wastewater, disinfect micro-organisms in water and isolate heavy metals are still a major challenge in South Africa.

Conventional wastewater treatment methods such as chemical precipitation and coagulation-flocculation systems using inorganic materials, activated carbon, synthetic polymers or natural biopolymers are the most commonly used techniques for purifying industrial wastewater. However, the application of these techniques in the treatment of wastewater has been shown to produce inconsistent results, and each technique has been reported to have its pros and cons depending on the nature of the water analysed. The flocculation technique has been widely used for removing suspended particles (flocculants) in wastewater. However, this technique has the drawback of leaving large volumes of sludge that strongly affect the pH of the medium when excess amounts of salts (flocculants) remain (Brostow *et al*., 2009). Other disadvantages of using flocculation are the effects caused by temperature variations, particle size of the flocculants used, and the water chemistry (matrix) (Vijayaraghavan *et al.*, 2011). Activated-carbon flocculants have also been used and have been shown to be non-selective and costly (Crini, 2005; Ali *et al*., 2012).

Other commonly used techniques for wastewater treatment include the use of natural biopolymers (polysaccharides). Biopolymers such as chitosan that were used in the past in commercial applications − particularly in the biomedical, food and chemical industries − have recently received increased attention in wastewater treatment (Knorr, 1984; Muzzarelli, 1973; Sandford & Hutchings, 1987). Chitosan is a modified, natural carbohydrate polymer derived by deacetylation of chitin (Figure 1.2), which is a major component in the shells of *crustacea* such as crab, prawn and crayfish. It is the second most abundant natural biopolymer after cellulose (No & Meyers, 1989).

Chitosan with high free amino groups can effectively function as a coagulant and as an adsorbent in wastewater treatment (Peniston & Johnson, 1970).

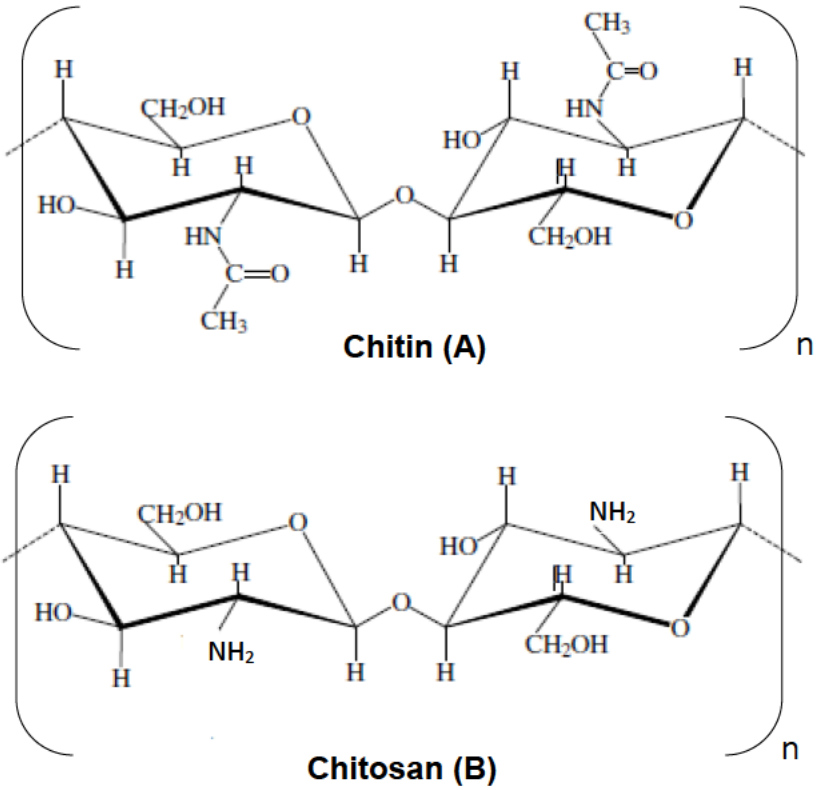

Figure 1.2: Chemical structures of chitin and chitosan

Source: No et al., 2000

However, although the use of chitosan may be considered a method of choice, it is not without drawbacks. Amongst some of the common problems associated with the use of chitosan is its insoluble nature which renders it ineffective in an acidic medium (Brostow *et al.*, 2009; Crini, 2005). Synthetic polymers are also very efficient flocculants; however, they are not shear resistant (Singh *et al.*, 2000) and the presence of the residual monomers in treated water is undesirable because of their neurotoxicity and strong carcinogenic properties (Vijayaraghavan *et al.*, 2013).

Based on the above discussion, it was argued that the use of chitosan for the modification of its operational conditions might be beneficial in the purification of wastewater from abattoirs. It was also clear that the advantages of using chitosan as

a flocculent would be its availability, cost effectiveness, and ease to be regenerated after use. A cost-effective technique using different types of chitosan was therefore designed with the intention of providing an effective method to curb water pollution, particularly with reference to the Mangaung (Bloemfontein) Metropolitan Municipality's abattoir effluents. The effectiveness of each synthetic modified chitosan was tested in the laboratories with respect to its ability to effectively purify and isolate heavy metals in the effluent of selected abattoirs.

1.3 Aim of this study

The aim of the study was to detect heavy metals in abattoir effluent and to establish an alternative method of purifying wastewater from Bloemfontein abattoirs in an effort to reduce water pollution.

To achieve this, the following objectives had to be achieved:

- Identify raw materials (domestic waste) such as fish scales (silver and pang scales), Crustacean shells (crab), and Mollusk shells (oyster, prawns) for the preparation of chitin and chitosan products to be used for wastewater treatment;

- Synthesize a variety of absorbents from chitin and chitosan biopolymers obtained from fish scales and prawn, crab, oyster, and mussel shells for wastewater purification;

- Characterize these adsorbents using spectroscopy techniques such as solubility tests, viscometer determinations, degree of acetylation, and SEM and FTIR spectroscopy; and

- Sample abattoir wastewater and investigate the effectiveness of the modified product(s) in purifying these wastewater effluents through comparative studies with commercially available adsorbents such as chitosan beads, chitins, natural polysaccharides, and Amberlite resins.

2 PRODUCTION AND DISPOSAL OF WASTEWATER FROM ABATTOIRS – A LITERATURE SURVEY

2.1 Introduction

The meat industry is often subdivided into two categories, namely the red meat sector that processes beef, mutton and pork and the white meat sector that processes poultry. The white meat industry has the highest consumption of water (6 to 10 million m^3 per annum) compared to the red meat processing industry that consumes approximately 4 to 5 million m^3 of water per annum (Steffen *et al.* 1989). The production of wastewater, particularly by the red meat processing industry, has increased at an alarming rate (Kieppar, 2001) which, by implication, has also resulted in an increase in water pollution. A detailed literature study was thus conducted to determine the source of water pollution and the effects it has caused. The main objective of this chapter is thus to illuminate the composition and quantity of wastewater generated by the red meat and poultry processing industries and to assess the impact that their wastewater has on the environment.

2.2 Distribution of abattoirs in South Africa

South Africa is amongst the highest meat producing countries in the world, with an estimated 13.5 million cattle, 29 million sheep and 6.6 million goats slaughtered each year (Van Zyl, 1995). Most of the agricultural land in South Africa is used for livestock farming (ca. 80%) with sheep and goat farming occupying approximately 590 000 km^2 of land. According to statistics, the provinces with the highest meat production are the Eastern Cape (22.9%), KwaZulu-Natal (20.3%) and the Free State (16.5%) (Van Zyl, 1995) (Figure 2.1).

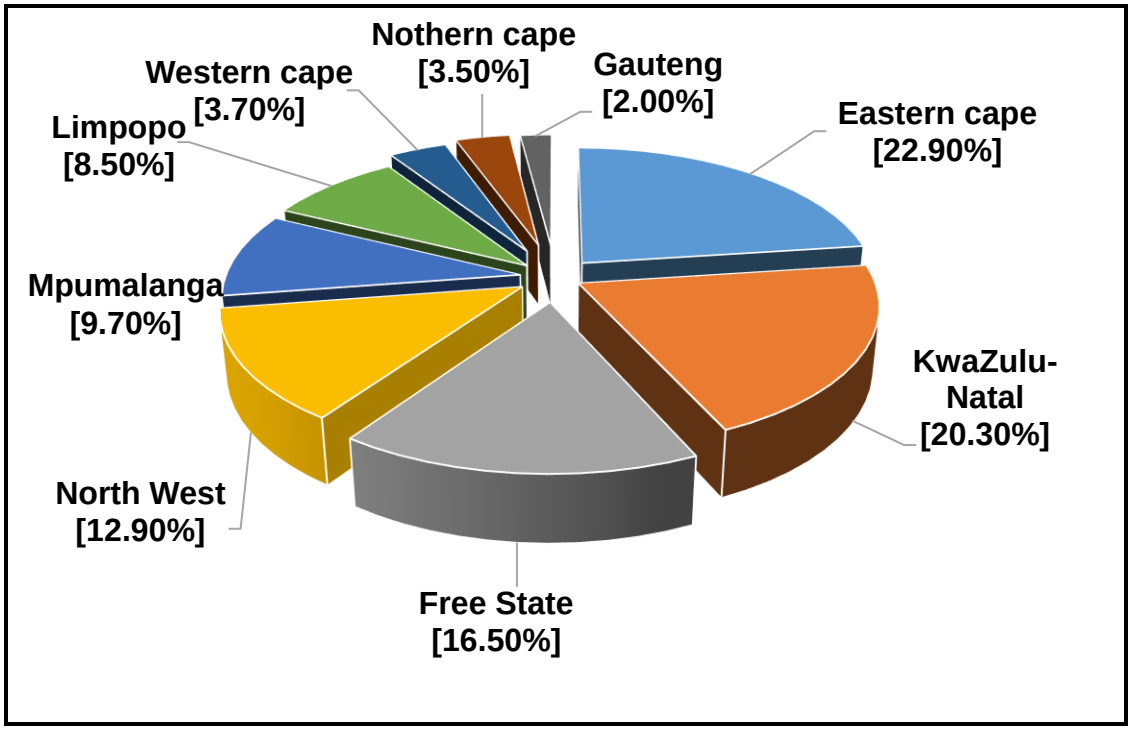

Figure 2.1: Cattle production per province in South Africa
Source: Van Zyl, 1995

Increasing demands on meat production locally and internationally have led to the increase in the number of abattoirs where animals are slaughtered. Ironically, the Free State Province has the highest number of meat processing centres compared to the Eastern Cape and KwaZulu-Natal (KZN), where more meat is produced (Table 2.1). The large number of abattoirs in the Free State Province thus makes it one of the highest water consumers with an estimated of 96.91 million m^3 per annum water consumption (Department of Water Affair, 2011). High per annum water consumption rates are also reported for the Eastern Cape (149.61 million m^3) and KwaZulu-Natal (299.80 million m^3), and these high rates suggest a correlation between water consumption and pollution. The Free State Province has been experiencing an increase in water pollution due to increased industrial activities (Coleman, 2015), and it is inevitable that the meat processing industry contributes significantly to this plight.

Table 2.1: Distribution of registered abattoirs in South African per province (Red Meat Abattoir Association, 2003)

Province	Registered Abattoirs	RMAA*
Gauteng	41	19
Limpopo	31	11
North West	30	11
Free State	85	26
KZN	49	19
Eastern Cape	83	21
Western Cape	69	24
Mpumalanga	40	20
Northern Cape	64	20
Total:	492	171

2.3 Chemical composition of wastewater

The effluent from red meat abattoirs contains various soluble and insoluble materials that are disposed of as waste from the abattoir (Scheme 2.1). The composition of the waste was of significance in this study as it plays a critical role in determining the ideal methods for recovering essential elements and paving ways to curb pollution. During the slaughtering process in the meat processing industry, a lot of water (6 to 10 million m^3 per annum) is used mainly for washing the animals and cleaning the meat, which makes abattoirs one of the biggest water consumption industries in the country. The solid and liquid wastes are washed down drains where they are often filtered to remove the insoluble material. The effluent waste constitutes nearly 90% of the soluble substances which, amongst others, include blood, urine, organic lipids and chemicals. Suspended material constitutes nearly 10% of the red meat effluent waste and mainly consists of fat and oils (Figure 2.2).

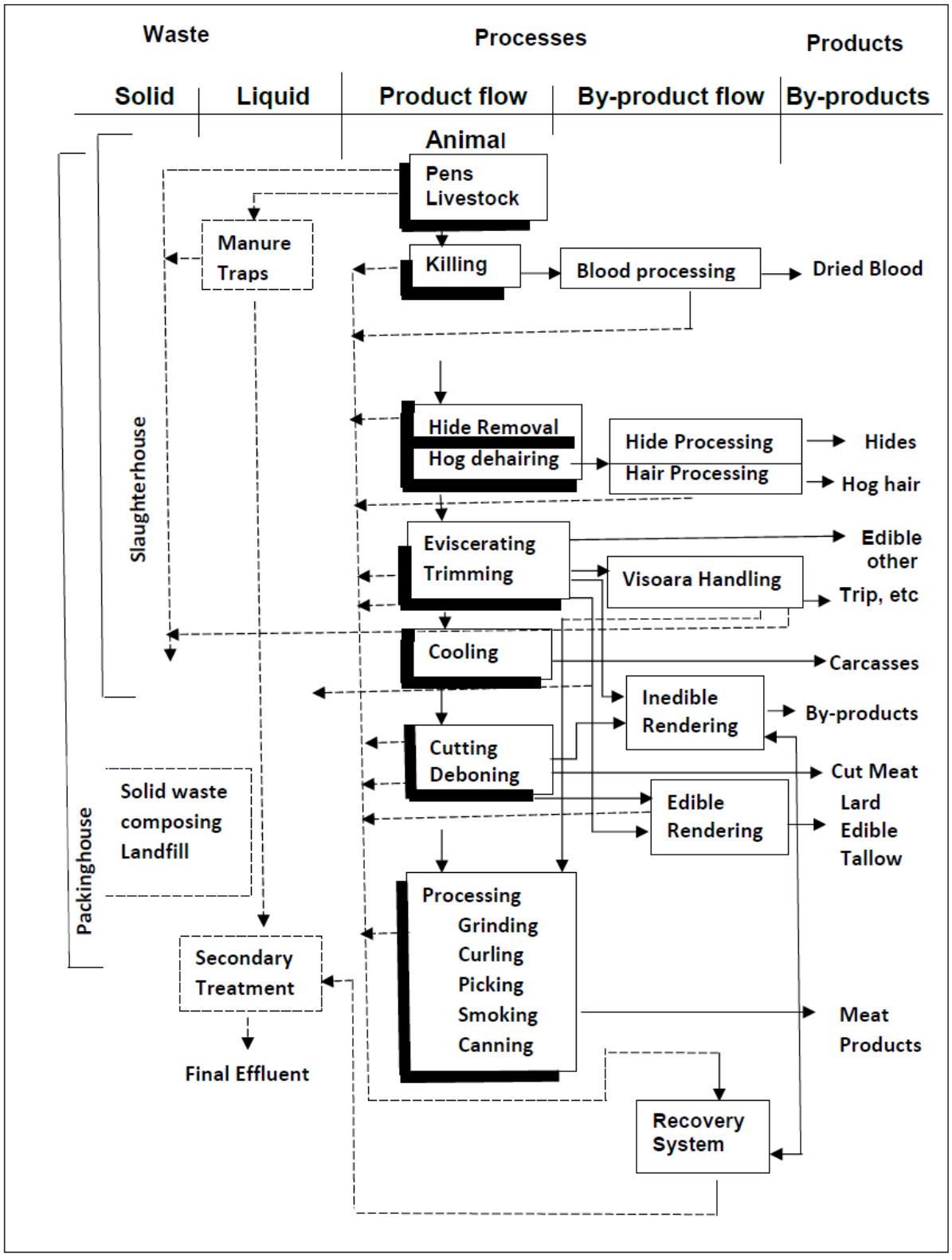

Scheme 2.1: Wastewater production (effluent) in the red meat processing industry

Source: Verheijen *et al*., 1996

Figure 2.2: Effluent from a red meat processing abattoir

Source: Aniebo *et al*., 2009

2.4 Effects of the soluble components in effluent wastewater

The wastewater from meat abattoirs, but particularly from red meat abattoirs, contains numerous soluble substances that, amongst others, include heavy metals, dyes, humic substances and organic pollutants. The effects caused by these substances are discussed below.

2.4.1 Effects of heavy metals in wastewater

The source of elements and heavy metals in wastewater is often attributed to the washing of intestines and a variety of chemicals used in the meat processing industry (US Environmental Protection Agency [USEPA], 2005). Some of the common elements found in wastewater include iron (Fe), copper (Cu), zinc (Zn), lead (Pb) nickel (Ni), selenium (Sn), mercury (Hg), chromium (Cr), arsenic (As), aluminium (Al), and cadmium (Cd) which are all reported to be present in the range of 0.023 to 0.50 mg/kg (Nkansah & Ansah, 2014; Ubwa *et al*. 2013). Anthony and Kozlowski (1982) reports of the environmental effects caused by these elements are due to their toxicity that affects aquatic life and disrupts the ecological balance in the aquatic environment. The latent fatal effects of heavy metals in wastewater that is discharged into fresh water bodies are devastating. These effects are dependent on the quantity and composition

of the discharges (Owuli, 2003; Akpor & Muchie, 2011). Heavy metals are easily absorbed by aquatic species and the effects thereof have been shown to inhibit growth and reproduction, which eventually leads to the extinction of aquatic life forms. Amongst the common metals found in effluent are Cr(VI) ions from the oxidation of Cr(III) compounds that affect the health and survival of aquatic species (Saikia *et al*., 2014). Khansari *et al*. (2005) found an accumulation of mercury and arsenic in human tissues. Substantial concentrations of these metals result in health problems such as damage to the nervous system, the kidneys and the cardiovascular system (Järup, 2003).

Contamination of fresh water bodies by wastewater is very common in South Africa, particularly in the outskirts of Bloemfontein in the Free State where most of the abattoirs in this province are located (Benotti et al., 2009). Most of the effluent from abattoirs is carried into the river streams where it pollutes these fresh water bodies. The effects of heavy metals have also been reported to have severe adverse effects on humans as they cause diseases like gastrointestinal disorders, diarrhoea, stomatitis, haemoglobinuria, ataxia, paralysis, convulsion, vomiting, depression and pneumonia. A study by Salem, Eweida and Farag (2000) on the effects of lead in humans showed severe damage to the nervous system of the human body. The study also indicated that the ingestion of large quantities of lead (up to 12 mg/ℓ) is fatal to human health and also results in diminution in haemoglobin production. It also affects the kidneys and the cardiovascular system (Nolan, 1983; Galadima & Garba, 2012; Okegye & Gajere, 2015).

Disposal of wastewater that contains heavy metals can alter the chemical composition of the soil where it is discarded, which ultimately affects the growth of plants. Morso, Khan *et al.* (2015) studied the effects of heavy metals on plants and report that a large quantity of heavy metals in soil inhibits growth, uptake of nutrients and water, and physiological and metabolic processes (Guala *et al.*, 2010). According to Gardea-Torresdey *et al*. (1998), the presence of heavy metals in plants can also decrease seed germination, enzyme activity, chlorophyll production and inhibit photosynthesis which will ultimately lead to yield depression.

2.4.2 The effects of dyes (colorants)

Most wastewater contains a significant percentage (estimated between 2 to 20%) of dye which is often used in abattoirs for meat packaging and for textile and paper printing. These compounds are often the major components responsible for the formation of coloured effluents. The most common types of dyes used in the meat processing industry are synthetic dyes that are used to colour meat products (Aksu, 2005). There are various derivatives of synthetic dyes which include anionic, non-ionic and cationic dyes. Non-ionic dyes do not ionize in aqueous environments and are less soluble, unlike the anionic dyes that are soluble. The anionic dyes are very common in abattoir effluent due to their bright colour and solubility in water. Congo red (Figure 2.3) and Orange 16 azo dye are commonly known anionic dyes that are used in abattoirs for colouring, and these dyes are often detected in abattoir wastewater due to their brilliant colours.

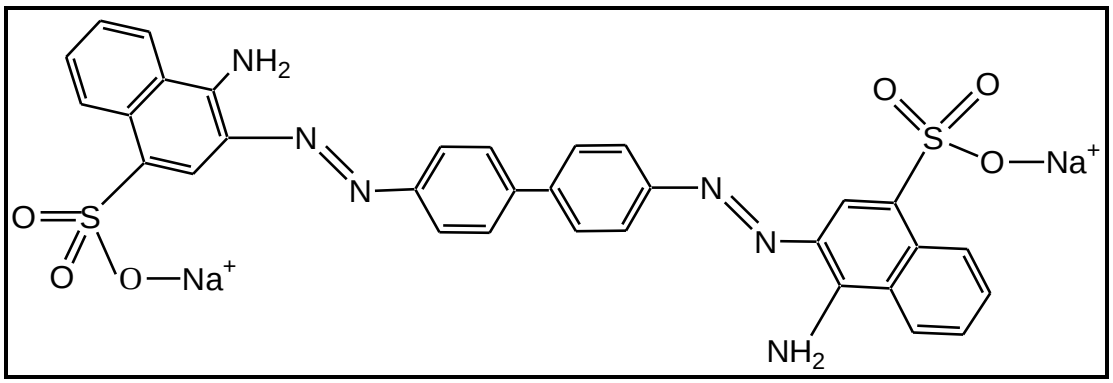

Figure 2.3: Structure of Congo red dye and anionic dye

Source: Jabbar *et al*., 2014

Non-ionic dyes such as disperse red 1 (Figure 2.4) are also brightly coloured and insoluble in water and often form emulsion in most effluent waste.

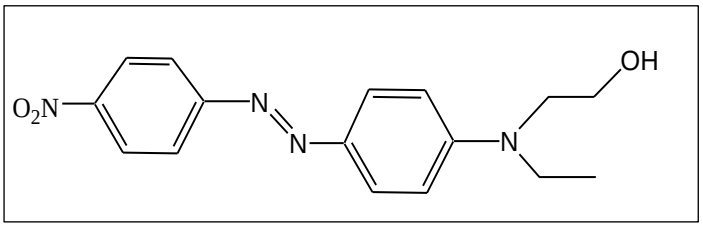

Figure 2.4: Structure of disperse red 1, a non-ionic dye

Source: Attla, Girgis & Fathy, 2008

The presence of dyes in effluent causes an unpleasant appearance and the colourant and other breakdown products impact aquatic life forms negatively. The decomposed structures of dyes also contain aromatic compounds that, in the presence of light, can form radicals which can be toxic to aquatic life. The dyes present in effluent give persistent colour to the receiving streams and interfere with photosynthesis in aquatic life (Cunningham & Saigo, 2001). Research by Crini and Badot (2008) and Pagga and Brown (1986) on the effects of synthetic dyes showed that highly coloured effluent blocks the penetration of sunlight and oxygen in water. This causes the destabilization of biological activity and reduces photosynthetic processes. Most dyes are non-biodegradable with carcinogenic action, causing allergies and dermatitis in humans as their synthetic nature and structure are aromatics (Carmen & Daniela, 2012).

2.4.3 Organic and humic substances

Effluents from abattoirs have also been reported to contain soluble and suspended organic particles and other decayed substances like humic substances (Figure 2.5). Humic substances are usually dark-brown mixtures of complex organic compounds with high molecular weight ranges which are often derived from decomposed organic debris.

Figure 2.5: Organic waste substances from abattoirs that contain humic substances

Source: Aniebo *et al*., 2009

These decomposed organic substances often randomly coil to form macromolecules, micelles or pseudo-micelles in wastewater. The degradation of animal waste materials often results in the formation of acidic compounds such as fulvic and humic acids (Figure 2.6) (Senn & Kingman, 1973). These substances contain a number of conjugated unsaturated bonds that are capable of absorbing light (Corin *et al*., 1998).

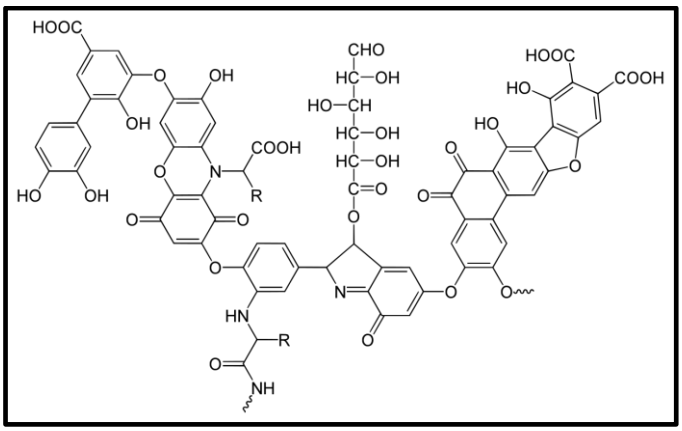

Figure 2.6: Organic structure of humic acid

Source: Steveson, 1994

Abattoir waste products have also been shown to contain a wide variety of persistent organic pollutants (POP) that, amongst others, include polycyclic aromatic hydrocarbons and polychlorinated biphenyls that are the by-products of the decomposition or degradation of organic matter. Recent investigations have estimated the concentrations of polycyclic aromatic hydrocarbons and polychlorinated biphenyls in raw abattoir wastewaters to be in the range of 250 to 1 250 µg/L. The solubility, semi-volatility, biodegradability and lipophilicity of POP enable their widespread, environmental transportation and bioaccumulation. The effects of these aromatic derivative compounds also add to the toxicity of wastewater (Badmus et *al*, 2018).

Abattoir waste such as blood (haemoglobin) decomposes into small, persistent organic compounds such as maleimide and dipyrrole (Figure 2.7). Haemoglobin often undergoes autoxidation to form superoxide (O^{2-}) in the presence of light which then undergoes dis-mutation to produce hydrogen peroxide. These series of reactions triggers a cascade of secondary oxidative reactions that decompose to form toxic products (Alayash, 2004).

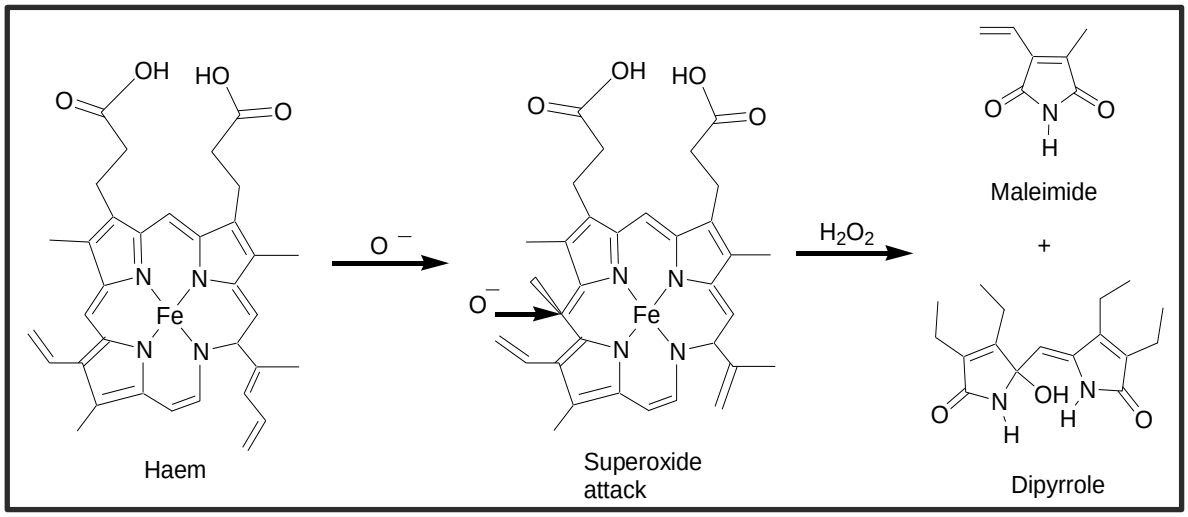

Figure 2.7: Degradation of haemoglobin in wastewater

Source: Alayash, 2004

2.5 Conclusion

It can be concluded that wastewater from abattoirs contributes significantly to water pollution and the meat processing industry is one of the biggest water polluter. This wastewater is known to have heavy metals, dyes and organic and humic substances, and it was shown that the effects of heavy metals are devastating in animals and plants. It was also shown that heavy metals alter the chemical composition of the soil where they are deposited and that this ultimately affects the growth of plants. It was also argued that the effects of other components such as organic and humic substances are not immediate, but ultimately devastating.

3 Techniques used in the separation of heavy metals from wastewater − Literature Survey

3.1 Introduction

The discourse in the previous chapters elucidated the fact that wastewater from the red meat processing industry contributes significantly to water pollution in South Africa. Wastewater from the meat industry undeniably contains heavy metals, dyes, organic and humic substances and an accumulation of these substances in fresh water bodies such as rivers, dams and lakes causes devastating effects on both animals and plants (Grozes *et al*., 1995; Gongwala *et al*., 2014). The effects of the accumulation of heavy metals in wastewater are critical as the pollution of water due to heavy metals causes more serious effects compared to other pollutants. The literature revealed that several techniques had been used to separate heavy metals from wastewater. These methods included gravimetric, chromatographic and solvent extraction (Adeniji et al. 2017), but it is clear that none of these methods have had the desired effect of curbing water and hence environmental pollution. Therefore, in order to develop an effective method for the removal of heavy metals from abattoir wastewater, it was deemed crucial to explore the challenges associated with current techniques in order to illuminate possible opportunities for improvement. An in-depth literature study was therefore conducted as a springboard for refreshing old methods and developing new techniques to optimize the efficiency of decontaminating poultry and red meat abattoir effluent.

3.2 Gravimetric techniques

Gravimetric methods are amongst the oldest analytical techniques used in the separation and quantification of heavy metals. There are four major types of gravimetric analysis strategies/methods used in the extraction of heavy metals, namely physical gravimetry, thermo gravimetry, precipitative gravimetric analysis (often called chemical precipitation), and electrodeposition. The most commonly used technique to separate heavy metals from industrial effluent is the chemical precipitation method. This method involves the use of different chemicals called precipitation reagents to precipitate analyte species. The advantages of using this method are that it requires a simple operation and costs are low. However, the

drawbacks of this technique are that it is time consuming, tedious, labour intensive, and involves a number of stages such as pre-separation of the interfering substances and pre-concentration of the analyte species. However, the simplicity of the chemical precipitation method has rendered this technique both desirable and versatile amongst researchers. The success of this technique has often been attributed to the precipitation rate, temperature, pH of the wastewater, the solubility product (K_{sp}) of the metals involved, and the equilibrium constant of the metal-hydroxide complexes. Different precipitation reagents such as hydroxide, carbonate, sulphide and phosphate have been used in the isolation of heavy metals from wastewater (Charerntanyarak, 1999). The formed precipitates are removed as sludge after coagulation, flocculation, sedimentation and filtration. The use of hydroxides as a precipitation reagent in the removal of heavy metals in solutions has been widely advocated as a method of choice due to a number of reasons, such as its low cost and simplicity and ease of automatic pH control (Mirbagheri & Hosseini, 2004; Aziz *et al.*, 2008). Moreover, the solubility of various metal hydroxides is minimized for pH in the range of 8.0 to 11.0.

The process of precipitating heavy metals using the chemical precipitation technique is achieved by producing an insoluble precipitate from the solution. Once the metals precipitate and form solids, they can then easily be removed and the water, now with low metal concentrations, can be discharged or reused. The mechanism of this process is centred on promoting conditions that favour the precipitation of soluble metal ions using a precipitating agent like hydroxide salts or any chelating agent. Percentage recoveries of metal ions in solution have also been shown to be improved by adjusting parameters such as the pH, temperature initial concentration, and charge of the ions. The precipitation of heavy metals using hydroxides in wastewater effluent has also been reported to occur according to Equation 1 below:

$$M^{n+} + 2(OH)^{-} \leftrightarrow M(OH)_n \downarrow \quad \ldots 1$$

Where M^{n+} = metal ions; and

$M(OH)_n$ is the insoluble metal hydroxide precipitate.

Heavy metals that are often found in wastewater i.e. Cd, Cu, Cr, Ni, Pb and Zn – reportedly cause devastating effects in both plants and animals (Nkansah & Ansah, 2014). Unlike organic contaminants, heavy metals are not biodegradable and tend to accumulate in living organisms and cause several health issues. To ensure the cleanliness of water and a healthy environment, these elements must be removed completely from all effluent. Several research studies have been conducted using the chemical precipitation technique such as the work done by (Mirbagheri and Hosseini, 2004), who successfully isolated Cu(II) and Cr(IV) in the presence of ferrous sulphate from wastewater using $Ca(OH)_2$ and NaOH as a precipitate agent. They reported that complete removal of these metals from the solution required the correct pH adjustment in achieving a complete precipitation. Maximum precipitation of Cr(III) as $Cr(OH)_3$ was achieved at a pH of 8.7, which significantly reduced concentration of chromium in the wastewater from 30 to 0.01 mg/ℓ. However, the removal of copper was successfully achieved at a pH of 12 using the same precipitating reagents. Substantial reduction in copper concentration in the wastewater from 48.51 to 0.694 mg/ℓ was achieved.

Studies have also shown that selective precipitation of various metals occurs at various pH levels depending on the precipitating agent used. Chemical precipitation of various metals has been shown to occur at different pH values using hydroxides. Selective isolation of different metals in solution was also achieved using these differences in pH and K_{sp} values for metal ions (Suponik, 2010). A theoretical pH range for the precipitation of various metals using hydroxides is presented in Figure 3.1.These findings were based on the solubility product K_{sp} of the metal hydroxide (Nkansah & Ansah, 2014).

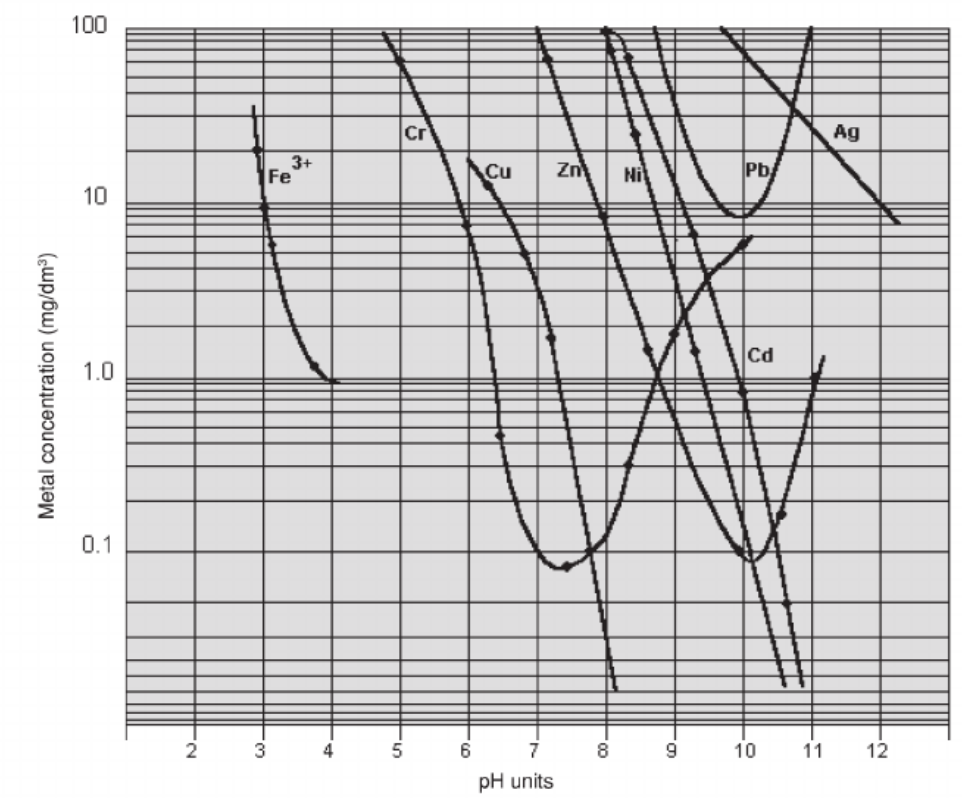

Figure 3.1: Metal hydroxide solubility as a function of its concentration and pH
Source: Suponik, 2010

Analyses by Mirbagheri and Hosseini (2004) were corroborated by the predicted pH values by (Suponik, 2010) as presented in Figure 3.1, which shows the chromium species to be quantitatively isolated at pH between 7 and 8. Further research on the isolation of heavy metals using hydroxides showed that lead and zinc could be successfully isolated using $Ca(OH)_2$ and NaOH at a pH range of 10 to 11. The results also showed a significant reduction of lead and zinc metals concentrations in the effluent from 100.0 to 0.45 mg/ℓ respectively. The success of this method was attributed to the use of coagulants such as alum (hydrated potassium hyfroxide), organic polymer and iron salt to facilitate the precipitation process (Charentanyarak, 1999). The biggest challenge in using this technique has been ascribed to the huge quantities of chemicals (precipitants) that are required to reduce metals to an acceptable level for discharge.

In the water treatment process, chemical precipitation using hydroxides is currently being employed in municipal water treatment for the removal of heavy metals in wastewater (Figure 3.2). The use of hydroxide in the removal of heavy metals by chemical precipitation has been shown to significantly improve metal recovery using

pH between 9 and 11. Caustic (sodium hydroxide) and lime (calcium hydroxide) are amongst the commonly employed precipitant agents used due to their availability and low cost. In municipal wastewater treatment systems, lime is often preferred due to its lower cost, whereas in small wastewater treatment systems caustic soda is used due to ease of handling. In cases where fluoride or phosphate removal from the wastewater is required, lime is used for pH adjustment. The use of lime or caustic soda seems to have no great effect on the rate of sedimentation, but the volume of sludge will be twice as large when using lime compared to using caustic soda (Wang and Shi, 2004).

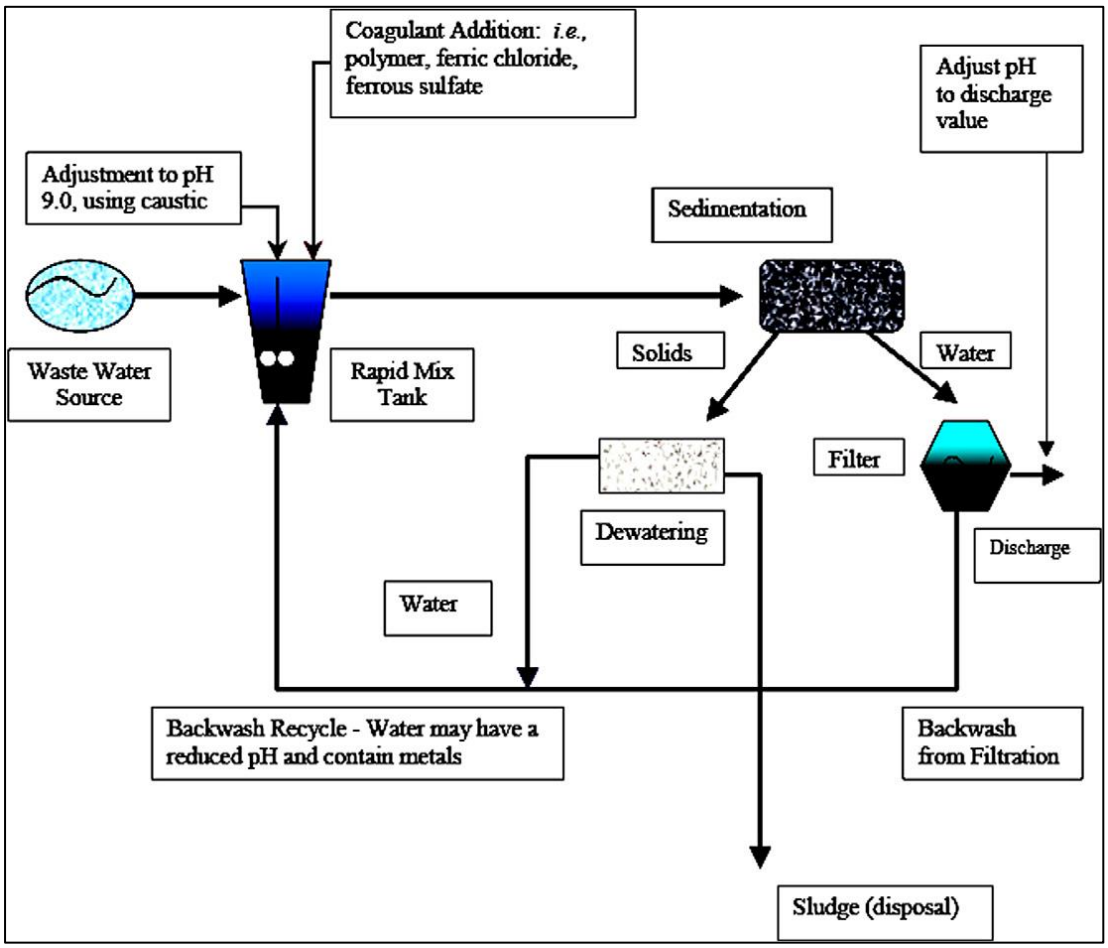

Figure 3.2: Chemical precipitation processes used in wastewater treatment plants

Source: Wang and Shi, 2004

3.2.1 Isolation of heavy metals using chelating agents as precipitating agents

Removal of heavy metals from wastewater has also been achieved by using different chelating agents. The use of chelating agents seemingly improves selectivity and sensitivity compared to the use of hydroxides. The commonly used chelating agents in the purification of wastewater are ethylene diamine tetra acetic acid (EDTA) (Figure 3.3), citric acid (CA), nitriliacetic acid (NTA), diethylene triaminentaacetic (DTPA), and oxoic acids (OA). EDTA is the preferred ligand and has been reported to form stable complexes with the transition elements due to its ability to form a hexadentate ligand which results in chelate or complex metals ions in the ratio 1:1 (metal to EDTA complex).

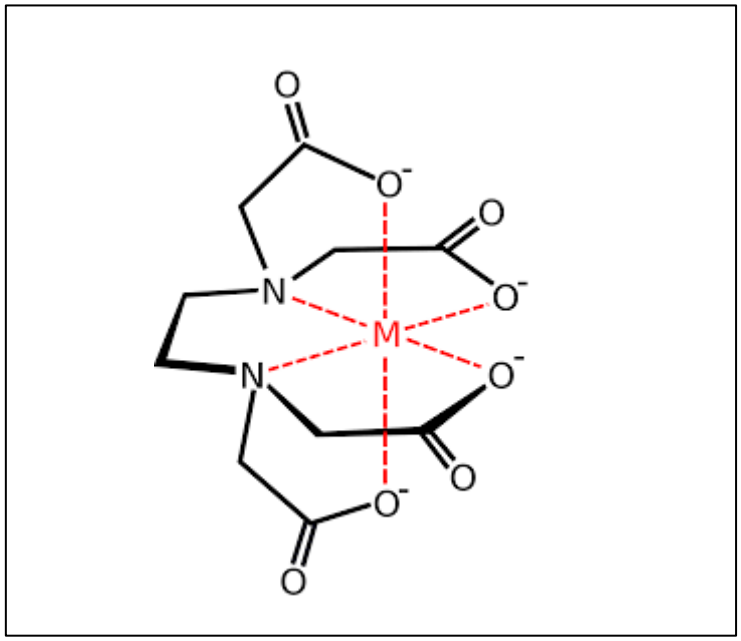

Figure 3.3: EDTA metal structure

Source: Sun *et al*., 2001

Factors influencing the choice of the chelating agents include the K_{sp} values of the metal-ligand complex and the ability of the formed complex to liberate the metal ion. The common problem encountered in the selection of the chelating agent is the removal of chelated metals (i.e., metal liberation from the complex molecule). In its deprotonated form, EDTA has been shown to form hexadentate ligand whilst CA and OA form tridentate and bidentate ligands respectively (Al-Qahtani, 2017). These

ligands bind with the metal cation in a ratio of 1:1 respectively according to the following equations:

M^{n+} + EDTA → Metal - EDTA Complex

M^{n+} + OA → Metal - OA Complex

M^{n+} + CA → Metal - CA Complex

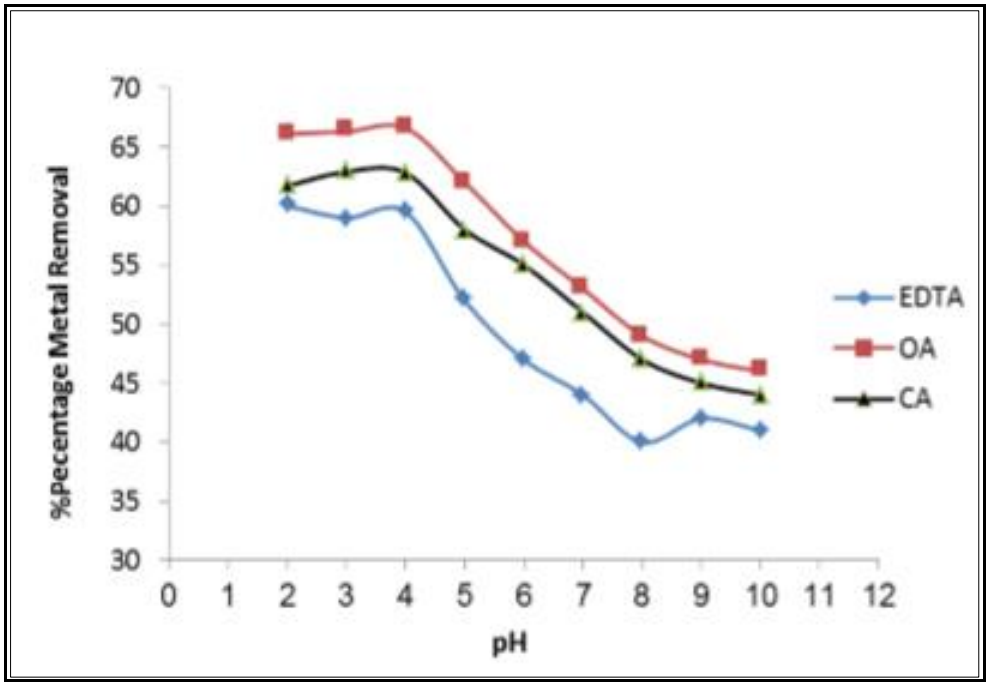

Figure 3.4: Influence of pH on the removal of copper and mercury from wastewater using 0.1 M of EDTA, OA and CA at room temperature

Source: Al-Qahtani, 2017

In a study that was conducted by Dupare (2015), the effectiveness of EDTA and CA as chelating agents in isolating Zn, Cu, Cd, Pd and As from wastewater was demonstrated. In this latter study, the effects of increasing the chelating concentration were analysed. The effectiveness of these chelating reagents were also studied at a constant pH (5.2) and at room temperature. The metal concentration was held constant whilst the chelating concentration was varied. The effect of increasing the concentration of the chelating agent was determined by analysing the amount of the metal ions isolated. Results obtained in this study latter (Tables 3.1 to 3.3) showed that higher percentage recoveries of the metal ions were obtained using 0.1 M of the chelating agent (EDTA and CA). The highest concentration recoveries at lower EDTA and CA concentrations (0.01 M) were in the order Zn>Cd>Cu>Pb>As and

Zn>Cu>Cd>Pb>As respectively. At higher concentration (0.1 M) of the chelating agents, the recoveries of EDTA were in the same order as CA and increased from Zn>Cu>Cd>Pb>As.

Table 3.1: Recoveries of metal ions from wastewater samples using 0.01 M EDTA and 0.01 M citric acid (CA) at pH 5.2 (Dupare, 2015)

Wastewater sample	mg/dm^3									
	Zn (II)		Cu (II)		Cd (II)		As (II)		Pb (II)	
	EDTA	CA	EDTA	CA	EDTA	CA	EDTA	CA	EDTA	CA
S1	212	302	78	58	82	52	32	26	44	32
S2	220	304	76	56	84	54	32	24	48	30
S3	210	306	78	59	83	56	36	24	55	32
S4	222	310	80	60	85	55	30	20	60	40

Table 3.2: **Recoveries of metal ions from wastewater samples using 0.05 M EDTA and 0.05 M citric acid (CA) at pH 5.2** (Dupare, 2015)

Wastewater sample	mg/dm^3									
	Zn (II)		Cu (II)		Cd (II)		As (II)		Pb (II)	
	EDTA	CA	EDTA	CA	EDTA	CA	EDTA	CA	EDTA	CA
S1	228	332	206	312	162	208	88	56	112	92
S2	230	334	208	316	168	206	83	58	114	94
S3	234	336	204	314	172	211	84	54	116	96
S4	248	340	210	320	180	215	90	60	120	98

Table 3.3: Recoveries of metal ions from wastewater samples using 0.10 M EDTA and 0.10 M citric acid (CA) at pH 5.2 (Dupare, 2015)

Wastewater sample	mg/dm^3									
	Zn (II)		Cu (II)		Cd (II)		As (II)		Pb (II)	
	EDTA	CA	EDTA	CA	EDTA	CA	EDTA	CA	EDTA	CA
S1	230	374	186	342	162	264	91	71	112	111
S2	232	368	186	348	164	268	92	74	114	113
S3	228	372	184	344	168	263	94	76	116	114
S4	232	330	200	380	170	265	95	80	120	120

Although significant research has been done to isolate heavy metals using chelating agents, the use of this technique has shown to be expensive compared to the use of hydroxides. Moreover, the use of chelating agents requires optimum conditions that sometimes take long to achieve and it often takes longer for the metal and ligand to complex. The cost of using this technique is further increased by the use of excess chelating reagents in order to attain the best recoveries, as can be observed in the above data.

3.3 Ion exchange technique

The ion exchange technique involves the use of an ion exchange resin or agent (the stationery phase) and metal ions present in the wastewater sample (the mobile phase). This technique has been used extensively in the separation of heavy metals from wastewater. Various synthetic and naturally occurring ion exchangers (zeolites) have been used in the isolation of different metal ions. Synthetic ion exchanges are preferred because of their effectiveness and ability to uptake the majority of the targeted metal ions from the solution (Álvarez-Ayuso *et al.*, 2003). The ion exchange technique has also shown to effectively treat inorganic effluent waste within a relatively wide range of metal ion concentrations of up to 100 mg/ℓ (Sapari *et al.*, 1996). Despite these advantages, this technique has also some limitations in the treatment of wastewater that is laden with heavy metal ions as, quite often, suitable ion exchange resins are not available for all heavy metal ions and the capital and operational costs are high.

Metal cations affecting the purity of water such as those identified in Chapter 2 Section 2.3 pass through the ion exchanger (stationery phase) where these positively charged

ions are exchanged with the positively charged ions from the resins such as hydrogen and sodium ions (Figure 3.5). The same concept is also used for the separation of negatively charged anions present in a wastewater solution where sulfate, nitrate and chromate ions that are released replace the hydroxyl and chloride ions from the resins. The resins are therefore categorized as either cation or anion exchangers depending on the charges of the ions exchanged. The efficiency of this technique has been reported to depend highly on pH, temperature, metal concentrations and contact time between the metal ion and the stationery phase (Fenglian & Wang, 2011).

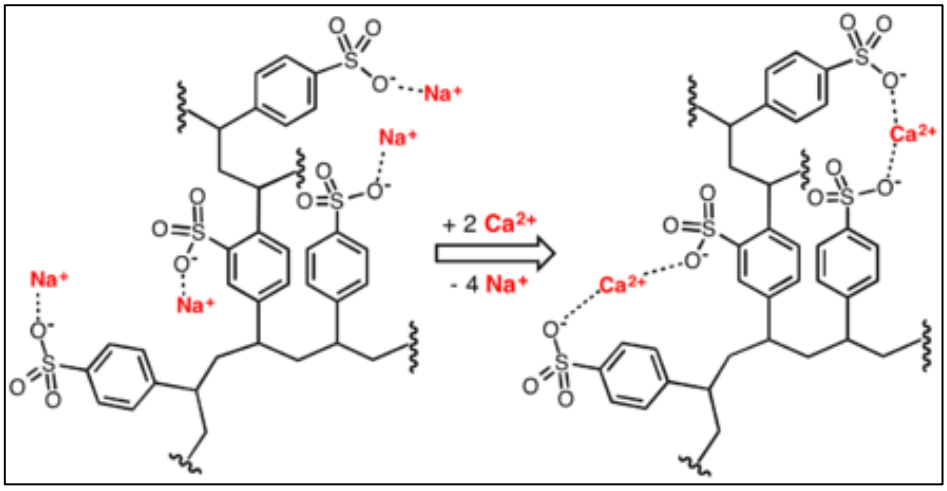

Figure 3.5: The displacement of Na^+ ions by the Ca^{2+} ion in a cationic exchange ion resin

Source: Lower, 2007

The widely used strong cation exchanges have a sulfonic acidic group ($-SO_3H$) whilst the weak cationic exchangers have carboxylic acid groups (-COOH) that are attached to them and that function as shown in Equations 2 and 3:

$$nR - SO_3H + M^{n+} \longrightarrow (R\text{-}SO_3^-)_n\ Mn^+ + nH^+ \quad \ldots 2$$

$$nR - COOH + M^{n+} \longrightarrow (R\text{-}COO^-)_n\ Mn^+ + nH^+ \quad \ldots 3$$

A research study that was conducted by Shaidan, Eldemerdash, and Awad (2012) in which they used strong acidic cation exchange resin (Ceralite IR 120) to extract nickel from wastewater showed excellent recoveries of as high as 97%. The use of Ceralite IR 120 had the advantages of being effective and also being capable of treating large volumes of effluent at the same time. The replacement of the H^+ ions on the resin by the Ni^{2+} ions was reportedly dependent on the pH of the solution. The results showed that the optimum pH for Ni^{2+} isolation was about 5 as shown in Figure 3.6. Excessive protonation of the active sites of the resin was reported for pH below 3 and this resulted in no formation of links between Ni^{2+} ion and the active site. It was also observed that, at moderate pH values between 3 and 6, the H^+ ions were released from the active sites creating room for the Ni^{2+} to bind, hence increasing the percentages of recovery.

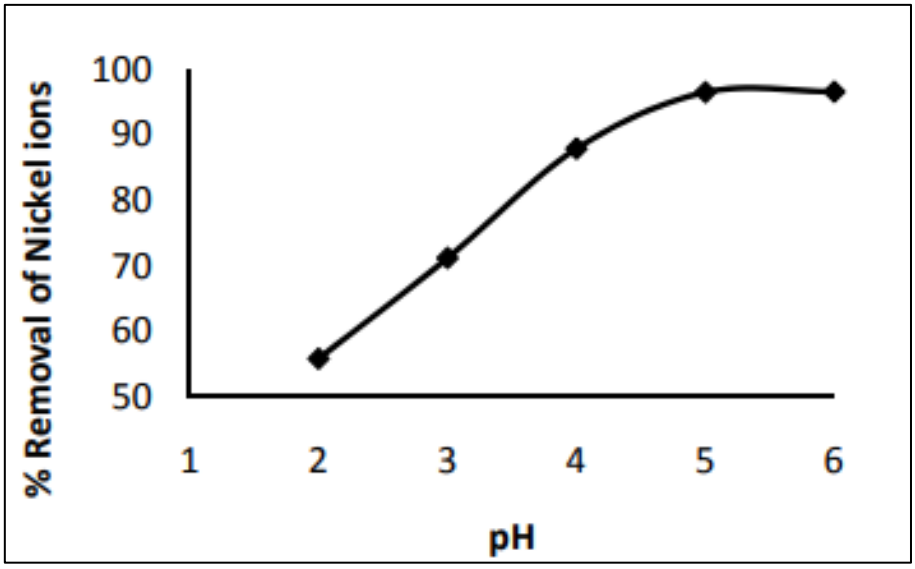

Figure 3.6: Effects of pH in nickel recovery using cation exchange resin (Ceralite IR 120)

Source: Shaidan *et al*., 2012

The effect of the Ni^{2+} concentration used was also investigated and the results obtained showed that the percentage nickel recovered decreased with a concomitant increase in nickel concentration from 100 to 500 mg/ℓ (Figure 3.7). The optimum concentration for nickel removal was 100 mg/ℓ with a recovery rate of 96.42%. The decrease in the percentage recovery of nickel was almost 91.02% and was attributed to the blockage of the active sites of the resin by the nickel ions. The results obtained by Shaidan *et al*. (2012) correlated with those of Sapari *et al.* (1996) who reported that the ion exchange technique was effective with metal ion concentrations of up to 100 mg/ℓ.

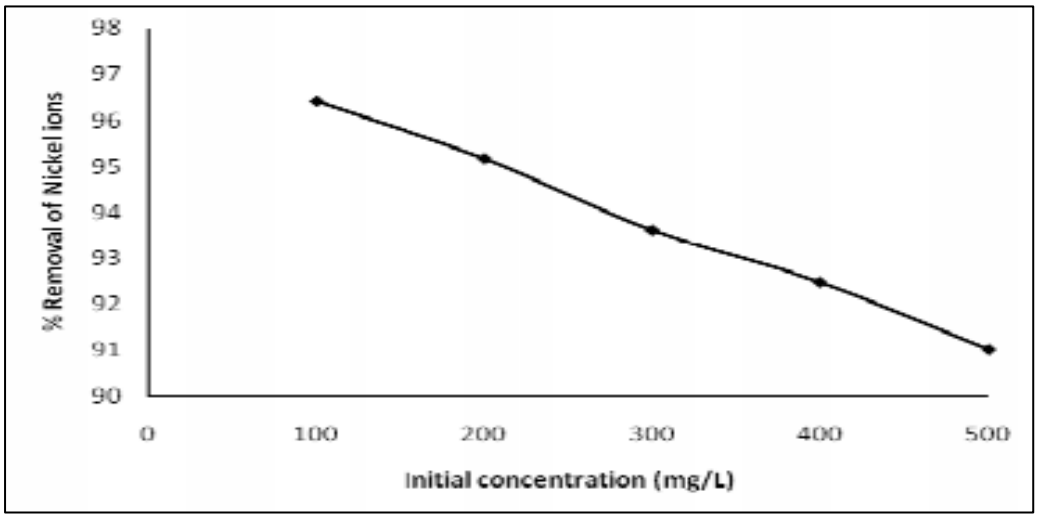

Figure 3.7: Effects of the metal concentration in the recovery of Ni^{2+} using cation exchange resin (Ceralite IR 120)

Source: Shaidan *et al*., 2012

Various types of ion exchange resins have been used for the selective removal of heavy metals in wastewater. It has been shown that precise selection of the resin is crucial for the complete removal of the targeted metal ion. Amongst the notable resins used is Purolite C100, which has been used for the selective removal of Pb^{2+} ions with a 99.71% recovery rate. Other types of resin used by several researchers for the removal of different metals in wastewater are summarised in Table 3.4 below.

Table 3.4: Summary of the ion exchange resins used in the removal of heavy metals in wastewater effluents

Heavy metal	Initial metal conc. (mg/ℓ)	Resin	Optimum pH	Removal Efficiency (%)	References
Cu, Zn and Cd	-	Amberlite IR	-	-	Lee *et al*. (2007)
Pb	-	Purolite C100	-	99	Badawy *et al*. (2009)
Cu	50 – 150	Indion 225H	6.3-6.5	-	Thakare & Jana (2015)
Ni and Pb	800 − 1 250	Amberjet1200	-	98	Zewail & Yousef (2015)
Hg and As	-	-	-	99	Oehmen *et al*. (2006)
Ni	1800 – 3 800	Acidic cation exchange resin	3-7	97	Shaidan *et al*. (2012)
Cd and Pb	100 – 6 000	Sargassum muticum loaded with calcium	5	-	*Carro et al.* (2015)

Chitin is the second most abundant natural polysaccharide in nature after cellulose and is widely distributed in marine invertebrates, insects, fungi and yeast (Kamble *et al.*, 2007). It is often used in the pharmaceutical, cosmetic, environmental and agricultural industries for applications that include wound dressings, lotions, contacts, pesticides, package film coatings and wastewater treatment. The chemical structure of chitin is composed of linear repeating beta-1,4-linked Nacetyl-D-glucosamine monomer units that are linked by (1-4)-β bonds, as shown in Figure 3.8.

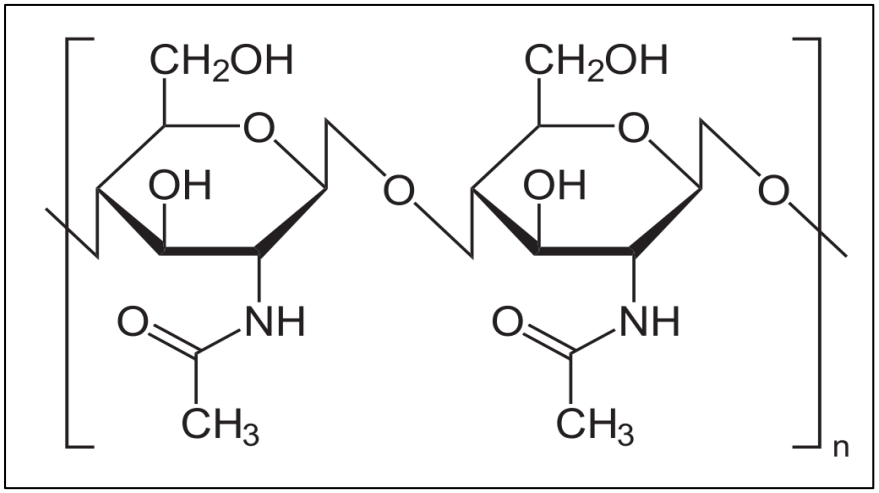

Figure 3.8: The chemical structure of chitin

Source: Tang *et al.,* 2015

Studies on the chemical properties of purified chitin have revealed it to be insoluble in water, but with the ability to dilute acids, organic solvents and concentrated alkali solutions. However, chitin is reported to be soluble in anhydrous formic acid, hypochlorite solutions and concentrated mineral acids. Both pure and cross-linked chitin have been widely used as ion exchangers and as an adsorbent in the purification of wastewater. Research by Nada *et al*. (2006) and Giles and Hassan (1958) on the adsorption properties of pure chitin using various metal ions and using ionic species of sulfonated azo dyes showed a high chelating ability of chitin in the removal of trace metal ions such as mercury, copper, zinc, chromium, cadmium, nickel and lead from contaminated wastewater

A study by Mohamed *et al.* (2015) demonstrated the effectiveness of cross-linked chitin in the isolation of heavy metals (Ni, Mg, Zn and Pb) using alkali and acid pre-treated chitin (Figure 3.9). Their results showed that acid pre-treated chitin derivatives that were phosphorylated were more efficient in removing heavy metals compared to the use of pure chitin. Their results also showed that phosphorylated cross-linked chitin treated with acid had the highest heavy metal ion removal ability compared to those in the alkali solutions. The high capacity of chitin derivatives for absorbing metal ions was attributed to a combination of unique properties such as its ionic nature, its affinity for water, and its porous polymer structure (Yoshida *et al*., 1993).

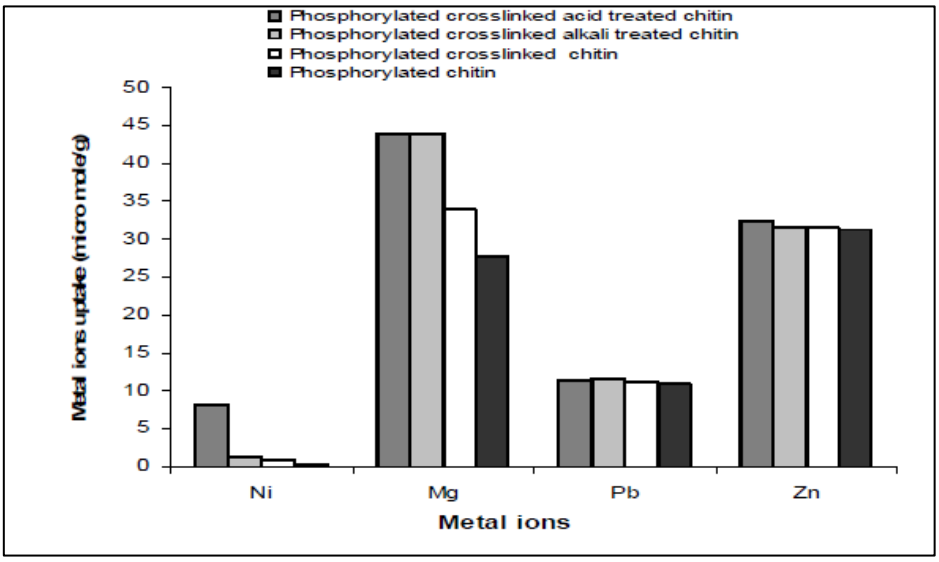

Figure 3.9: Effects of cross-linking of phosphorylated chitin on metal ion uptake capacity

Source: Mohamed *et al*., 2015

3.3.1 Uses of chitin derivatives (chitosan) in the isolation of heavy metals

Chitin usage in the purification wastewater has been reported to be enhanced from N-deacetylation of chitin to form chitosan (Figure 3.10). Both these polysaccharides are copolymers of β (1-4) linked N-acetyl-D-glucosamine and D-glucosamine units. The degree of acetylation (DA) represents the proportion of N-acetyl-D-glucosamine units with respect to the total number of units. The degree of acetylation is often used to distinguish between chitin and chitosan (a chitin derivative) with the former being below 50% (Tokura & Nishi, 1995). The poor solubility of chitin in acid solutions makes it more complicated to work with compared to chitosan, which is chemically soluble and more versatile than chitin or cellulose, hence its preference as a method of choice.

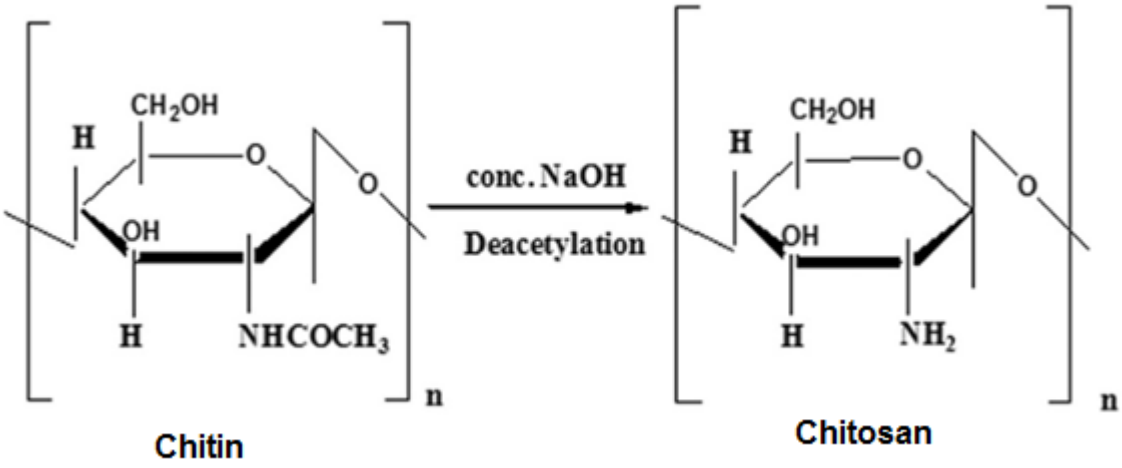

Figure 3.10: Conversion of chitin to chitosan through deacetylation using concentrated sodium hydroxide

Source: Devi *et al.*, 2016

During the past several years, chitosan has received increased attention for its commercial applications in wastewater treatment due to its biocompatibility, biodegradability, bioactivity and its ability to act as a polycationic electrolyte in acidic solutions (Chen & Chen, 1998). Chemically modified chitosan such as N-carboxymethyl and N-benzyl sulphonated are extensively used as adsorbents in the removal of heavy metals in wastewater. These modifications are reported to enhance the polymer's metal removal properties and to improve polymer stability in acidic environments (Muzzarelli *et al.,* 1985). Chen et al. (2009), reporting on the adsorption of Cu(II), Zn(II), and Pb(II) ions using glutaraldehyde cross-linked chitosan, found that maximum adsorption of the metal ions occurred at pH 5 as shown in Figures 3.11 and 3.12.

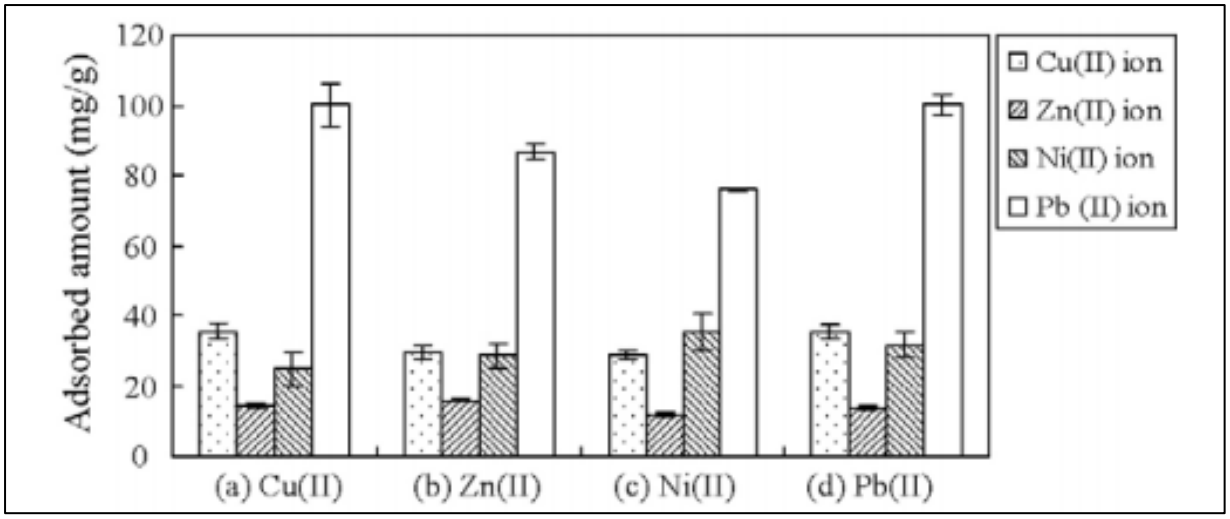

Figure 3.11: Adsorption of Cu(II), Zn(II), Ni(II) and Pb(II) ions on the glutaraldehyde cross-linked chitosan in 50 mg/ℓ aqueous solution of metal ions

Source: Chen *et al*., 2009

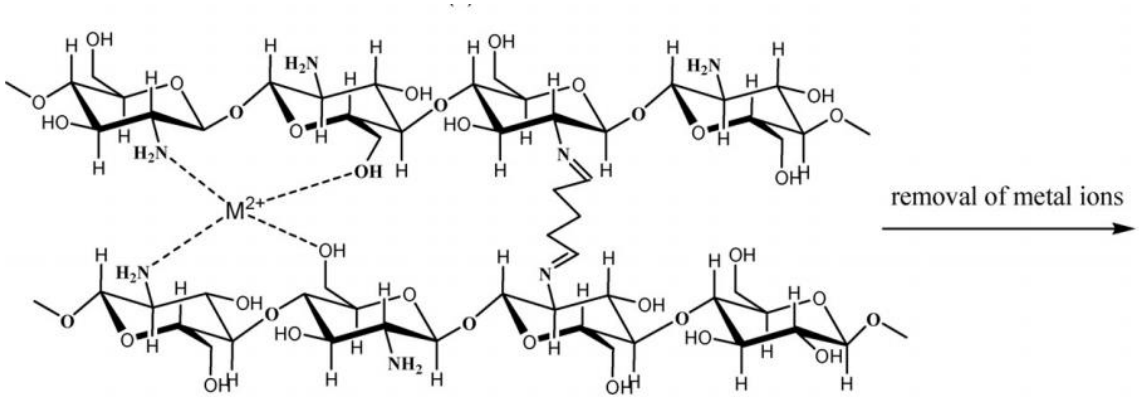

Figure 3.12: Adsorption mechanism of the metal ions (M^{2+} = Cu, Zn, Ni and Pb using cross-linked chitosan

Source: Chen *et al*., 2009

The use of chitosan as an adsorbent is also enhanced by its ability to be moulded into various shapes such as beads or fibres. This moulding is achieved by neutralizing the acidified chitosan in sodium hydroxide (Arora *et al*., 2010). These modified forms of chitosan have the potential to be used as materials for ion exchange due to their increased affinity for heavy metals.

3.4 Conclusion

The use of adsorption material such as chitosan for the removal of heavy metals from wastewater was shown to have several advantages compared to other commonly used methods such as gravimetric and ionic exchange techniques. Although the gravimetric technique was shown to be an effective method for removing heavy metals in wastewater, its demand for large quantities of chemicals (precipitants) to reduce metals to an acceptable level, coupled with its poor selectivity, was noted as a significant drawback. The biggest challenges in using the ionic exchange technique were shown to be its concentration limitation in the separation of heavy metals and the unavailability of resins for selective metals. On the other hand, the use of chitosan products was shown to have the advantage of being affordable and locally available. Furthermore, the use of chitosan products was also shown to be versatile as they have the ability to be modified to any shape and chemical structure through cross-linking in order to meet the required conditions.

4 SYNTHESIS AND CHARACTERIZATION OF CHITOSAN DERIVATIVE PRODUCTS

4.1 Introduction

It was argued in Chapter 3 Section 3.4 that the use of chitin and chitosan derivatives is a promising technique for the removal of heavy metals from wastewater. Chemically modified chitosan products such as N-carboxymethyl and N-benzyl sulphonate have been used extensively in the selective isolation of heavy metals in wastewater. Structural modifications of chitosan through cross-linking have also been shown to enhance the polymer's metal removal properties and improve polymer stability in acidic environments. With this information as background, this study attempted to synthesize different cross-linked chitosan products in the quest to improve the purification of wastewater from poultry and red meat abattoirs. An objective was also to characterize the synthesized chitin and chitosan products using various spectrometric and spectrophotometric techniques as summarized in Flow chart, 4.1.

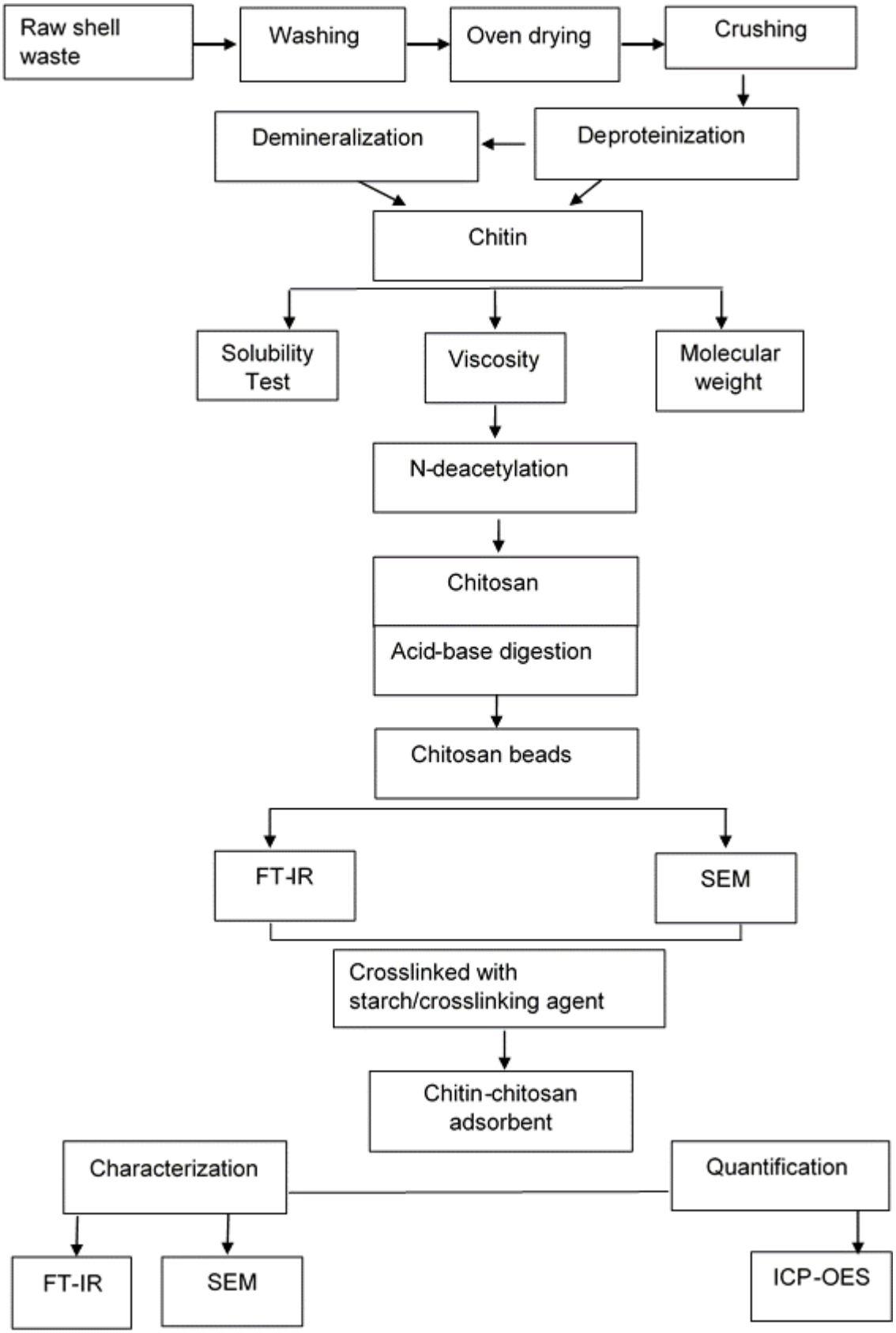

Figure 4.1: Flow diagram of the synthesis and characterization processes of chitosan derivative products

4.2 Materials

4.2.1 Reagents and raw materials

All chemicals and reagents used in this study were obtained commercially from different suppliers and were used without further purification (Table 4.1). The water was prepared from the Thermo Scientific Barnstead Nanopure Water Purification System as analytically supplied by the Sepsi company. The conductivity of the purified water was determined to be 0.00 µS/cm.

Table 4.1: List of chemicals and reagents used in this research study

Raw materials	Amount (g)		Supplier
Mussel, prawns, crab, oyster and fish scales	1000		Ocean Basket, Loch Logan, Bloemfontein, South Africa
Chitin powder (shrimp and crab shell)	500		Kapikapa International Tuticorin, India
Chemicals	**Formula**	**Purity (%)**	**Supplier**
Glutaraldehyde solution	$C_5H_8O_2$	25	Sigma-Aldrich
Formaldehyde solution	CH_2O	96	Sigma-Aldrich
1-vinyl-2-pyrrolidone	C_6H_9NO	98	Sigma-Aldrich
p-benzoquinone	C_6H_4O	98	Sigma-Aldrich
Acrylic acid stabilized with hydroquinone monomethyl ether	$C_3H_4O_2$	99	Sigma-Aldrich
Maleic Anhydride	$C_4H_2O_3$	98	Sigma-Aldrich
1,3 Dichloroacetone	$C_3H_4Cl_2O$	99	Sigma-Aldrich
(s)-(-)(α) Methylbenzylamine	$C_6H_5CH(CH_3)NH_2$	95	Sigma-Aldrich
(±)-Epichlorohydrine	C_3H_5ClO	98	Sigma-Aldrich
Poly ethylene glycol digylcidyl ether	$(C_8H_{14}O_4)_n$	95	Sigma-Aldrich
Mineral acids			
Hydrochloric acid (AR*)	HCl	32	Merck
Nitric acid (AR)	HNO_3	65	Merck
Acetic acid (AR)	CH_3COOH	100	Merck
Absolute ethanol (AR)	C_2H_6O	96	Merck
Acetone (AR)	C_3H_6O	100	Merck
Base			
Sodium hydroxide pellets	NaOH	≥98	Merck

*AR - Analytical reagent grade

As the starting material, mussel, oyster, crab and prawn shells and silver and pang fish scales (Figure 4.2) were supplied by Ocean Basket, a local restaurant in the Loch Logan Mall in Bloemfontein.

Mussel shells

Oyster shells

Crab shells

Prawn shells

Silver scale

Pang scale

Figure 4.2: Graphical presentation of the locally sourced starting material

4.2.2 Glassware and general house keeping

Grade A-type Schott Duran beakers and round bottom flasks were used in all the experimental procedures. Glass and plastic Pasteur pipettes with high accuracy values (±0.01 mℓ) were used to dispense accurate volumes of reagents. Appropriate handling regimens of chemicals, reagents, standards and solutions were strictly adhered to in order to avoid cross contamination and to ensure quality assurance of all analytical results. Contamination of glassware was avoided by soaking them in freshly prepared 10% v/v HNO_3 for at least 48 hours and finally washing them with deionised water prior to use.

4.3 Instrumentation

4.3.1 Viscometer and centrifuge

Suspended chitin and chitosan products in solution were separated using Eppendorf centrifuge equipment whilst a Brookfield viscometer from the Department of Food science (UFS) (Figure 4.3), Model DV-II supplied by Brookfield Engineering Laboratories Inc., Stonghton, was used to measure the viscosity of all the chitin and chitosan products.

Figure 4.3: Eppendorf centrifuge (A) and Brookfield viscometer (B)

4.3.2 Fourier-transform infrared spectroscopy (FTIR)

Characterization of the chitin and chitosan products was done using a Thermo Scientific Nicolet (6700 FTIR) spectrometer from the Physics department (UFS) (Figure 4.4). The dried samples were pressed into pellets with powdered potassium bromide (KBr) in the ratio 1:100 respectively and analysed. The FTIR was first calibrated by running a background scan (10 scans) before analysing the samples. The pellet sample for analysis was mounted on a crystal plate using an adjustable pressure clamp. Sample spectrums were collected from 64 repetition scans; the resultant scans were base line corrected and the final peaks labelled. All the infrared spectrums were plotted on all specimens over the frequency range 4000-400 cm^{-1}.

Figure 4.4: A Thermo Scientific Nicolet (6700 FTIR) spectrometer

4.3.3 Scanning electron microscope (SEM)

A scanning electron microscope (model JSM-7800F) from the Center of Microscopy (UFS) (Figure 4.5) was used to determine the physical morphology of the newly synthesized chitosan products. Samples were mounted on stubs slides at 35ºC (Cambridge pin type, 10 mm) using double sided carbon-carbon tape and gold coated (± 60 nm) with a Bio-Rad sputter coater (United Kingdom). Pictures of the specimens were taken at different magnifications depending on the sample.

Figure 4.5: SEM instrument showing the electron column, sample chamber, Energy-dispersive X-ray spectroscopy (EDX) detector, electronics console and visual display monitors

4.3.4 Weighing balance and magnetic hot plate

All the samples were accurately weighed using a Shimadzu (AW320) electronic balance, calibrated under ISO 9001. All experimental samples and reagents used in the study were weighed by adding a sample in a pre-weighed plastic petri dish or filter paper. A digital magnetic stirrer/hotplate (H3760-HS) purchased from Lasec was used for stirring and heating of the chemical reactions

4.4 Experimental processes and discussion of results

4.4.1 Chitin extraction

The preliminary procedure in the synthesis of chitosan was the extraction of chitin from the raw materials. The raw material was first washed, dried and then crushed into a powder and stored in opaque glass/plastic containers before use. The raw materials were the shells from molluscs (mussels and oysters), crustaceans (crabs and prawns) and fish scales (silver and pang). A two-step procedure was used to isolate chitin from the raw materials: thus deproteinization was used for the removal of proteins and demineralization was used for the removal of minerals. Chitosan was formed from deacetylation of the newly isolated chitin products.

4.4.1.1 Deproteinization

A sodium hydroxide (10%) solution was added to the dried, powdered crustacean (oyster) (100 g) sample and the resultant mixture was stirred until a colourless solution was formed (ca.18 to 24 hours). The colourless solution that formed was a confirmation of the complete removal of proteins (Abdulkarim *et al.*, 2013). The resultant white solid residue was filtered with a glass funnel and washed with copious amounts of water (Abdulkarim et al. 2013).

The residue was dried at room temperature and a white solid powder product (68.85 g, 69.65%) was obtained. The same procedure was used for mussel, oyster, prawn and crab shells and silver and pang scales. The results are presented in Table 4.2**.**

Table 4.2: Percentage yields of chitin isolated from mussel, oyster, prawn and crab shells and silver and pang scales

Raw materials	% Chitin
Oyster shells	69.65
Mussel shells	35.03
Crab shells	60.00
Prawn shells	40.16
Pang scales	35.53
Silver scales	31.30

4.4.1.2 Demineralization

The samples of the deproteinized chitin (0.20 g) derived from mussel, oyster, prawn and crab shells and silver and pang scales were stirred in hydrochloric acid (10%) for 16 to 72 hours to remove calcium salts ($CaCl_2$ and $CaSO_4$) and other water-soluble impurities. The mixtures were filtered and washed with copious quantities of deionised water and the resultant white solid precipitate was collected and dried before use in the synthesis of chitosan products (Abdulkarim et al. 2013).

4.4.1.3 Determination of the degree of acetylation (DA) of the chitin products at different temperatures

Chitin samples (0.20 g) were dissolved in HCl (30 mℓ; 0.1 mol/ℓ) in separate beakers and stirred at different temperatures (50 – 100^{o}C) until they were completely dissolved (ca. 50 mins). The resultant solutions were cooled at room temperature and a methyl orange indicator (5 − 6 drops) was added. The resultant solutions were titrated with NaOH (0.1 mol/ℓ) to a yellow colour (Domard & Rinaudo, 1983). The obtained titrant values were used to calculate the degree of acetylation measured at different temperatures using Equation 4.1 as described by Czechowska-Biskup *et al*. (2012). The results of the analyses were tabulated and are presented in Table 4.3.

$$DA = \frac{2.03 \cdot (V_2 - V_1)}{m + 0.0042 \cdot (V_2 - V_1)}$$

where: m – is the weight of the sample used,

V_1 and V_2 are the volumes of 0.1 mol·dm^{-3} sodium hydroxide solution corresponding to the deflection points,

2.03 – is the coefficient resulting from the molecular weight of chitin monomer unit, 0.0042 – coefficient resulting from the difference between molecular weights of chitin and chitosan monomer units.

Table 4.3: Degree of acetylation (DA) of chitin obtained at different temperatures

Temperature (ºC)	50	60	70	80	90	100
Mussel shells	77.2	83.3	85.8	91.0	93.2	96.5
Oyster shells	69.7	74.0	80.0	85.6	90.4	93.3
Prawn shells	40.2	45.8	48.6	51.6	54.2	60.6
Crab shells	54.1	56.5	63.7	69.4	74.2	74.6
Pang scales	50.1	52.6	56.9	62.4	65.8	69.1
Silver scales	47.6	49.2	52.2	56.1	60.1	65.9

The influence of temperature on the degree of acetylation of chitin was investigated using the refined chitin as described in Section 4.4.1.2. Figure 4.6 shows how increase in temperature influenced the degree of acetylation of the chitin products. The degree of acetylation for all the chitin products was found to increase with an increase in temperature (50 – 100ºC). A linear correlation between the temperature and the degree of acetylation was observed and a maximum degree of acetylation for all the chitin products was obtained at 100ºC whereas the lowest was recorded at 50ºC. The degree of acetylation of all the chitin products was in the order mussel < oyster < crab < pang< silver< prawn shells/scales.

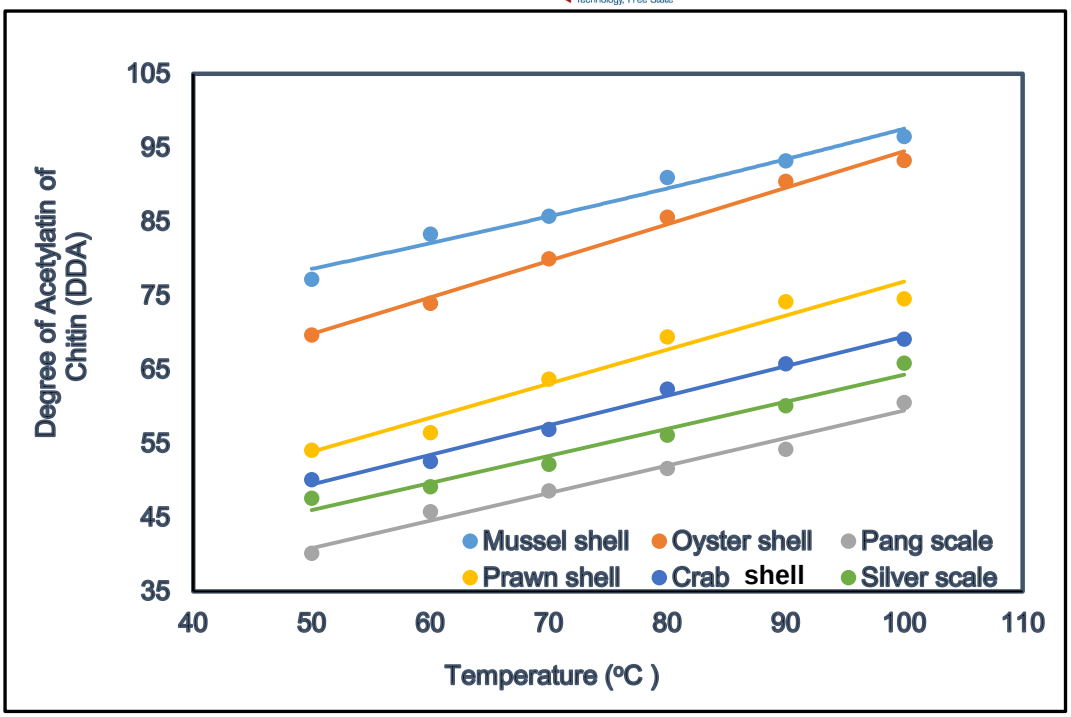

Figure 4.6: Determination of the degree of acetylation of chitin at various temperatures at 50, 60, 70, 80, 90 and 100ºC

4.4.1.4 Determination of the intrinsic viscosity, molecular weight and solubility of the isolated chitin

Determination of the intrinsic viscosity, molecular weight and solubility of the chitin samples, methods were modified from (Brine and Austin,1981; Wang *et al*., 1991; Terbojevidh and A. Cosani,1997).This procedure was performed using a Brookfield viscometer (see Figure 4.4). The samples of chitin were dissolved in 1% acetic acid and measurements were done in duplicate using a spindle at 50 rpm at a temperature range of 5 − 80ºC. The results are presented in Table 4.4. The highest solubility was achieved for mussel chitin at 86%, followed by oyster chitin at 78%. The prawn chitin recorded the least solubility up to 68%. The poor solubility of prawn shell and silver and pang fish scale chitin samples possibly occurred as a result of the close packing of chains and the strong inter- and intramolecular bonds among the hydroxyl and acetamide groups (Urbariczyk *et al*., 1997).

Table 4.4: Determination of the intrinsic viscosity, molecular weight and solubility of the isolated chitin at 25ºC

Sample of chitin (shell and scale waste)	Average intrinsic viscosity η (Cps)	Average intrinsic viscosity (%)	Molecular weight (Mw) (Da)	Solubility in acetic acid (%)
Mussel shells	4500	30	7.5×10^6	85.7
Oyster shells	3500	18	5.8×10^6	77.8
Prawn shells	2300	15	3.7×10^6	58.3
Crab shells	1500	11	2.3×10^6	70.7
Pang scales	1000	5	1.5×10^6	68.0
Silver scales	600	4	0.9×10^6	67.7

Tests to determine the intrinsic viscosity, molecular weight and solubility of the samples revealed a variation in both chemical and physical properties of the chitin products. The mussel chitin product had the highest intrinsic viscosity value (4500 Cps) compared to the other chitin products. Chitin with the least intrinsic viscosity value was procured from the Silver scale sample that recorded 600 Cps. It was determined that a direct correlation existed between intrinsic viscosity and molecular weight; i.e., an increase in molecular weight resulted in higher intrinsic viscosity. Analysis of the chitin intrinsic viscosity at different temperatures showed lower readings at higher temperatures (80ºC) compared to lower temperatures (5ºC) (Figure 4.7).

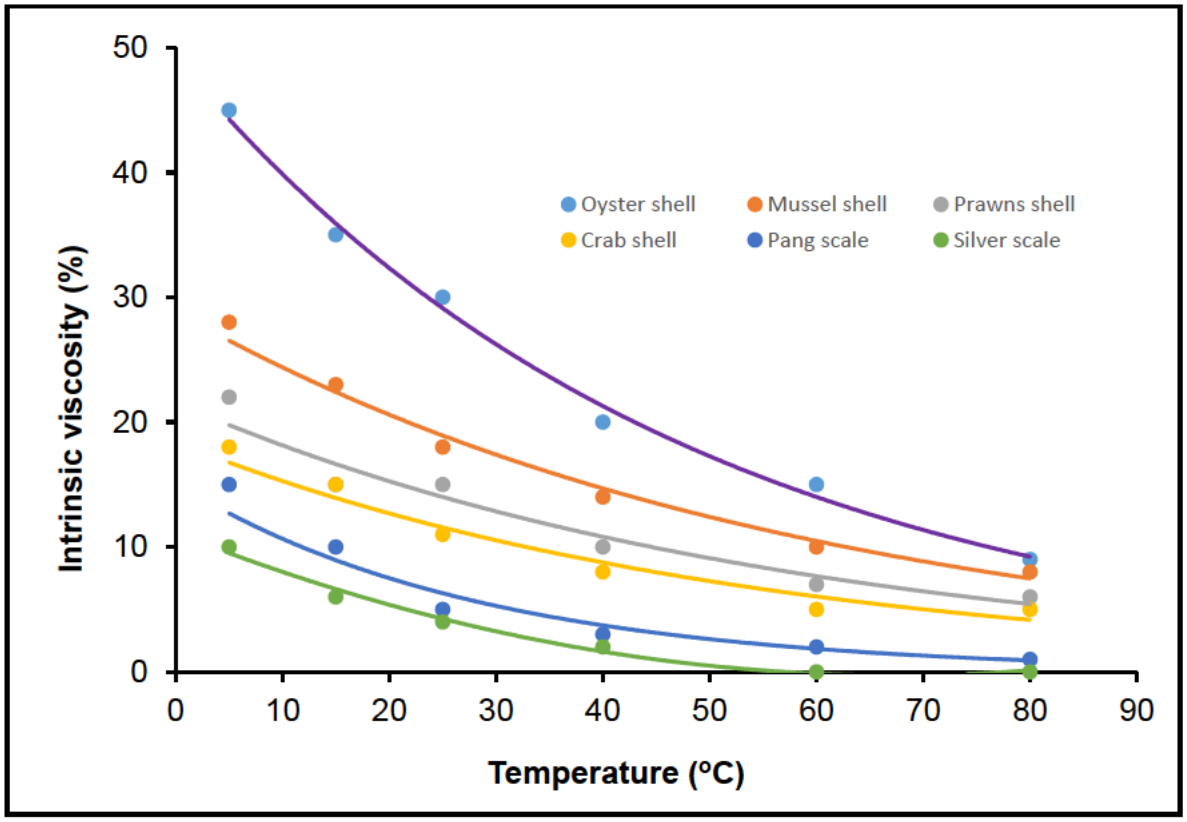

Figure 4.7: Changes in intrinsic viscosity of chitin at different temperatures (5 – 80°C)

4.4.2 Synthesis of the crab and shrimp chitosan through deacetylation

Chitin samples from crab and shrimp shells (2 g; 0.131 mmol) were placed in separate round bottom flasks (250 mℓ) and were transferred to and dissolved in acetic acid (200 mℓ) using a magnetic stirrer. The mixtures were stirred at ambient temperature for 24 hours until highly viscous solutions were obtained. A solution of NaOH (2%) was added drop-wise to neutralize the acidity of the solution and the resultant mixtures were filtered and the white precipitate was washed with copious quantities of distilled water. The white precipitate product was dried at room temperature and yields of 98% for chitosan crab and 88% for chitosan shrimp were obtained. Both products were characterized using SEM and FTIR spectroscopy. The results are presented in Figure 4.8. (Domard and Rinaudo,1983).

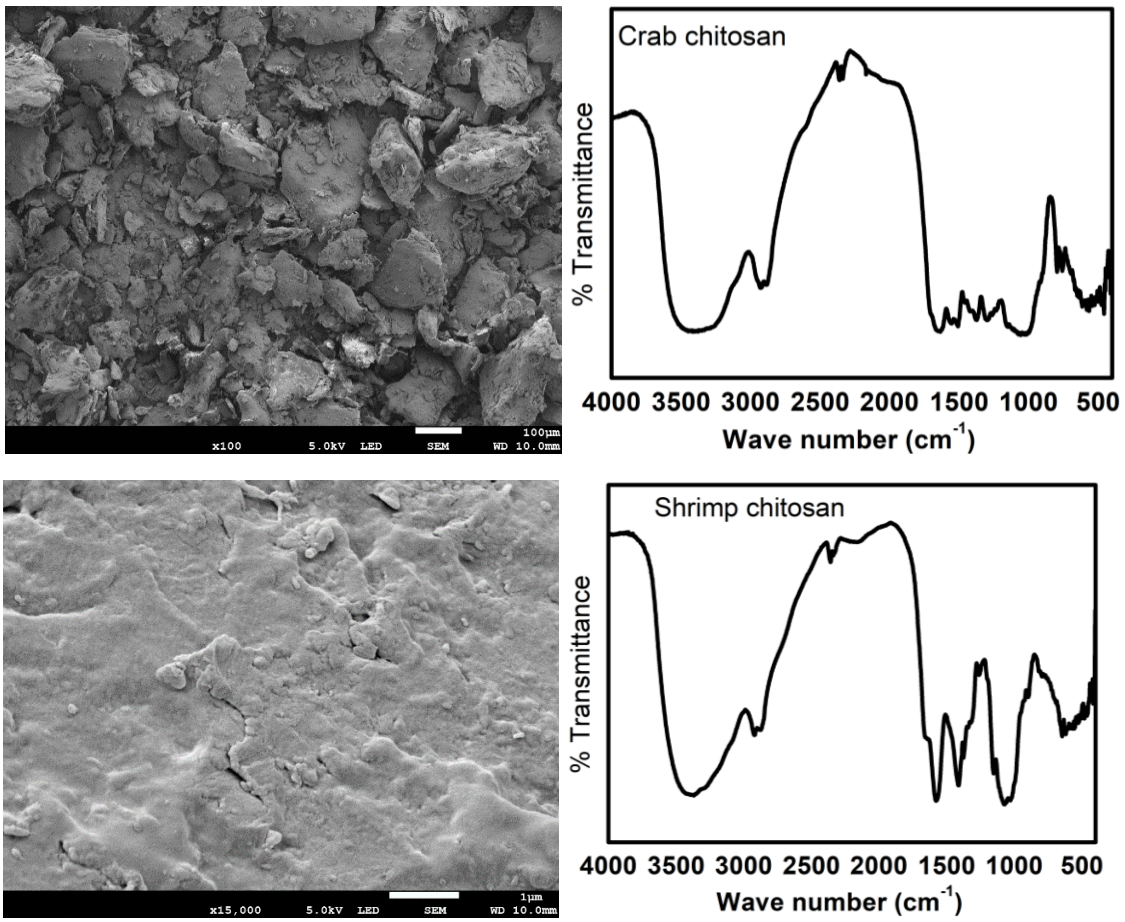

Figure 4.8: Scanning electron microscope images and FTIR spectrums of crab and shrimp chitosan products

Synthesis of crab and shrimp chitosan was achieved through deacetylation of the respective chitin products. Comparatively, a higher percentage yield was achieved for chitosan crab (98%) than for chitosan shrimp (88%). The SEM images of crab chitosan revealed a mixture of small and large spherical, cube-like structures that appeared amorphous while the shrimp chitosan appeared flaky with small particles appearing closely-packed at higher magnification (x15000). FTIR analysis of the crab chitosan powdered products showed a prominent peak at 3375 cm^{-1} which corresponded to OH stretching. The presence of the methyl group in $NHCOCH_3$, the methylene group in CH_2OH and the methylene group in the pyranose ring was shown by the corresponding peaks in the range 2923 − 2870 cm^{-1} respectively. The band at 1630 cm^{-1} was due to CO stretching of the amide group, and the band at 1500 cm^{-1} corresponded to the NH bending vibration in the amide group, which suggested the effective deacetylation of chitin. A small band observed at 1310 and 1280 cm^{-1} was

due to the CH_3 in the $NHCOCH_3$ group and CH in the pyranose ring complex vibrations of the NHCO group and the band at 1050 cm^{-1} was due to CO stretching vibration. The bending at vibration CO in the ring CH at 762 cm^{-1} represented a β-linked chitosan molecule (Zvezdova, 2010).

Characterization of chitosan shrimp using FTIR revealed a strong band which was observed ranging from 3200 − 3700 cm^{-1} and this was due to the NH_2 and OH associated in the primary amine group stretching vibrations. The presence of a methyl group in $NHCOCH_3$, a methylene group in CH_2OH and a methylene group in the pyranose ring was demonstrated by the corresponding stretching vibrations range 2870 and 2340 cm^{-1} respectively. The bands between the ranges of 1651 − 1558 cm^{-1} describe vibrations of CO bonds of the amide group RNHCO (secondary amide at 1657 cm^{-1}). The bending vibrational stretch of the CH_2 groups was attributed to the bands formed at 1421, 1379 and 1389 cm^{-1}. The absorption bands in the range 1160 − 1000 cm^{-1} were related to the stretching vibrations of the CO groups. The small peaks occurring at 647 and 610 cm^{-1} as a result of the bending vibration of NH and OH related to the wagging of the polysaccharide morphology of chitosan. These were observed out of the chitosan plane (Zvezdova, 2010).

Zvezdova (2010) confirms that the presence of crab chitosan has prominent peaks occurring in the region of 3425 cm^{-1} which he suggests corresponds to OH stretching, while the band in the current study at 2921 cm^{-1} corresponded to a methylene group in CH_2OH. However, the band at 1630 cm^{-1} was present because of the CO stretching of the amide group while, on the other hand, the band occurring between 1656 and 1628 cm^{-1} corresponded to NH bending vibration in the amide group. The occurrence of small bands around 1257 − 1380 cm^{-1} corresponded to CH_3 in the $NHCOCH_3$ group and CH in the pyranose ring complex vibrations of the NHCO group. The COC glycosidic linkage was represented by bands at 1158 and 1154 cm^{-1} which corresponded to the COC glycosidic linkage. The band of 1099 cm^{-1} (CO) was present there because of the secondary OH group while 1027 was in the primary OH group. The bending occurred at vibration CO in the ring CH at 894 cm^{-1} pyranose ring skeletal vibrations while 665 and 603 cm^{-1} were out of the plane.

The shrimp chitosan product revealed a strong peak in the region of 3424 cm^{-1} which corresponded to the OH group. The presence of a methylene group in CH_2OH was

confirmed by the corresponding stretching vibration in the region of 2879 cm^{-1}. The shoulder band in the region of 1667−1597 cm^{-1} was due to the presence of the CO in $NHCOCH_3$ group. Small bands around 1257 − 1380 cm^{-1} corresponded to CH_3 in the $NHCOCH_3$ group and CH in pyranose ring complex vibrations of the NHCO group. The bands at 1152 cm^{-1} corresponded to the COC glycosidic linkage. The band 1093 cm^{-1} (CO) was present there because of the secondary OH group while the 1035 cm^{-1} was in the primary OH group. The bending occurred at vibration CO in the ring CH at 897 cm^{-1} pyranose ring skeletal vibrations while 664 and 614 cm^{-1} were out of the plane.

4.4.3 Synthesis and characterization of cross-linked crab and shrimp chitosan compounds

Using separate glass vessels, two sets of solutions of glutaraldehyde, formaldehyde, epichlorohydrine, acrylic acid, 1-vinyl-2-pyrrolidone, glutaraldehyde, poly (ethylene) glycol diglycidyl ether, s-methyl-benzylamine, *p*-benzoquinone, 1,3-dichloroacetone and maleic anhydride (8 mℓ) were added to an acetic acid solution (100 mℓ; 1%) and stirred for 15 minutes until a homogeneous solution was obtained. Powdered crab chitosan and starch and shrimp chitosan and starch (2 g; 0.131 mmol; 1%) were added to the respective solutions. The resultant mixtures were stirred at ambient temperature for 24 – 48 hours until a viscous colour solution had formed (Table 4.2). Drops of NaOH solution (2%) were added to neutralize the acidity and the mixtures were filtered and the respective brown products were collected as a precipitate and dried at room temperature (Li and Bai, 2006). The percentage yields are presented in Table 4.5. Characterization of the chitosan cross-linked products was conducted using SEM and FTIR. These results are presented in Figures 4.9 to 4.18.

Table 4.5: Percentage yields of the cross-linked chitosan products obtained from crab and shrimp shells

Cross-linked polymer	Chitosan	Colour of products	Yield (%)
Glutaraldehyde	Crab shrimp	Brown	98 72
Formaldehyde	Crab shrimp	White	69 65
Epichlorohydrine	Crab shrimp	White	55 72
Maleic anhydride	Crab shrimp	White	26 30
p-Benzoquinone	Crab shrimp	Black	62 59
Poly (ethylene) glycol diglycidyl ether (PEG diglycidyl ether)	Crab shrimp	White	58 59
1-vinyl-2-pyrrolidone	Crab shrimp	Yellow Orange	53 55
1,3-dichloroaceone	Crab shrimp	White	92 71
Acrylic acid	Crab shrimp	White	57 57
S-methyl-benzylamine	Crab shrimp	White	59 63

4.4.3.1 Crab and shrimp chitosan starch (CT-ST) cross-linked with glutaraldehyde

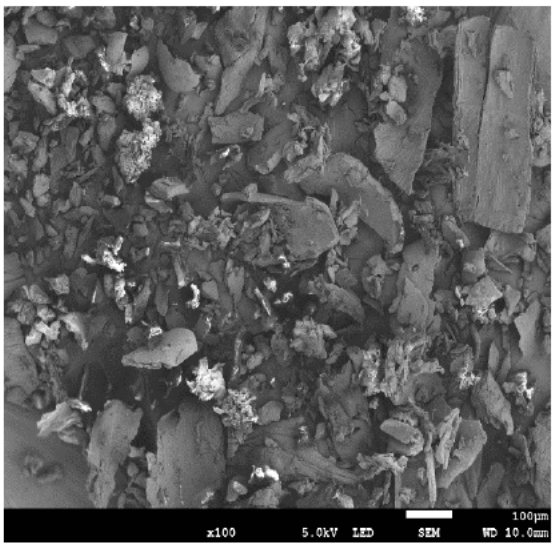

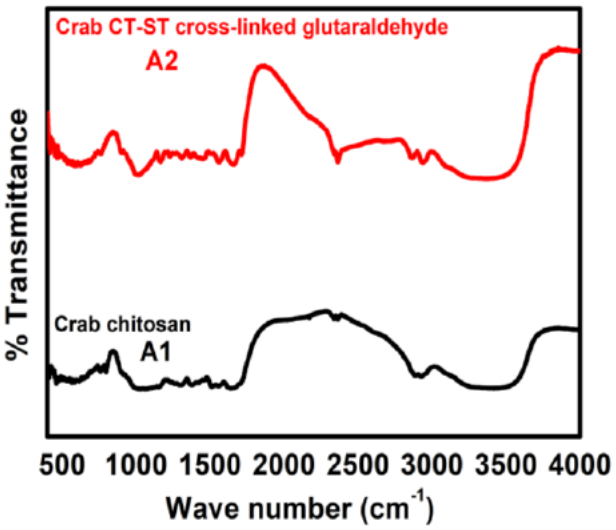

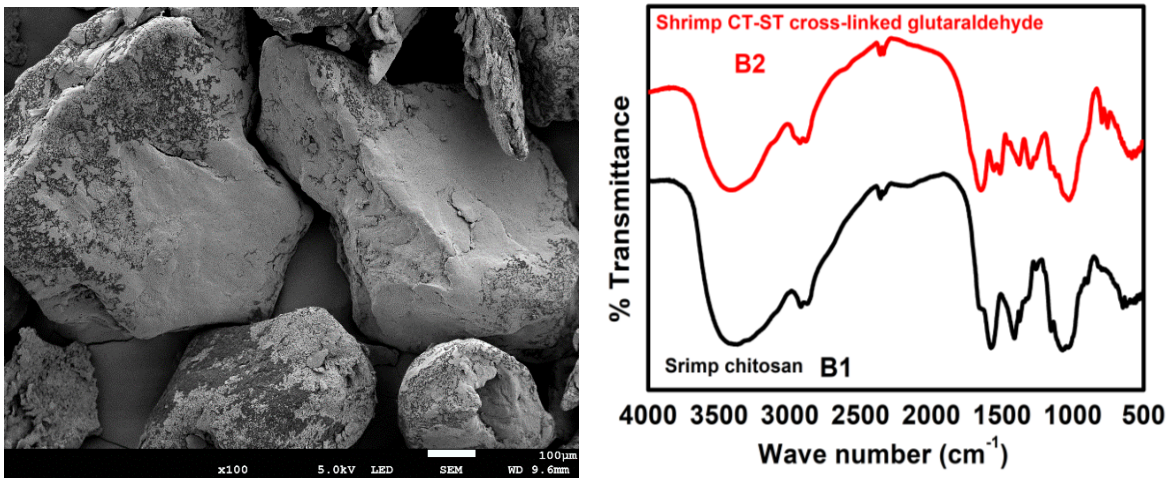

Figure 4.9: Scanning electron microscope images and FTIR spectrums of crab and shrimp chitosan starch cross-linked with glutaraldehyde

The crab and shrimp chitosan starch samples that were cross-linked with glutaraldehyde yielded 98 and 72% respectively. SEM analysis of the products showed an irregular shape of both products. The FTIR analysis of crab chitosan starch that was cross-linked with glutaraldehyde showed that the OH stretching peak of chitosan (A1) and the chitosan product (A2) were diminished from 3375 to 3360 cm^{-1}, whereas the CH_2 group shifted upwards from 2870 to 2860 cm^{-1}. A symmetrical peak was obtained at 2930 cm^{-1}, which was an indication of the CH_2 group that was not present in the starting crab chitosan material. The absence of peaks within the region 1740 − 1720 cm^{-1} showed that the addition of an amount of glutaraldehyde to the bead solution reacted completely with the chitosan and starch. The observed change obtained in bond cleavage was assessed for comparative augmentation and a decrease in the intensity of the band, linked to the functional groups present in beads, was found. The corresponding band to the amino group shifted from cross-linked crab chitosan to normal crab chitosan and shifted from 1630 to 1640 cm^{-1}. This was an indication of interaction between the hydroxyl group of starch and the amino group of chitosan.

It was observed that the intensity of wave number 1133 cm^{-1} reduced when chitosan starch beads were cross-linked with glutaraldehyde. The reduction of intensity showed a bond cleavage in the reaction, even though a precise and accurate confirmation of the chitosan starch product could not be established by this process. When shrimp chitosan was blended with starch in the presence of glutaraldehyde as the cross-linking agent, the corresponding band to the amino group of chitosan shifted from 1651

to 1655 cm^{-1}, indicate the presence of interaction between the hydroxyl group of starch and the amino group of chitosan.

When the chitosan and starch were cross-linked with glutaraldehyde (B2), the OH stretching peak shifted from 3414 to 3345 cm^{-1} while the CH_2 group shifted from 2889 to 2879 cm^{-1} and from 2338 to 2335 cm^{-1} respectively. The amino peak of chitosan shifted from 1571 to 1639 cm^{-1} with the addition of starch. These analyses shows that the interactions occurred between the hydroxyl groups of starch and the amino groups of chitosan. There was an absence of peaks in the region 1740 − 1720 cm^{-1}, indicating that the addition of a small quantity of glutaraldehyde to the bead solution reacted completely with the chitosan and starch. The observed change in bond cleavage was estimated to have occurred from the relative augmentation or reduction in the intensity of the band corresponding to the functional groups present in the beads.

When the chitosan starch beads were cross-linked with glutaraldehyde, there was a reduction of the intensity of the wavenumber to 1110 cm^{-1}. The reduction of intensity indicated a cleavage in the reaction, even if a precise and accurate confirmation of the chitosan starch product could not be established (spectrum B2). Based on a direct comparison of the chitosan cross-linked spectrum and the conventional chitosan spectrum of shrimp (B1), the following differences may be singled out: A broad and strong band was observed ranging from 3200 − 3700 cm^{-1} (i.e., stretching vibration of OH and stretching vibration of NH). The peak located at 1651 cm^{-1} was characteristic of CO in the amine group, and the band at 1514 and 1558 cm^{-1} corresponded to the NH bending vibration in the amide group.

4.4.3.2 Crab and shrimp chitosan starch (CT-ST) cross-linked with formaldehyde

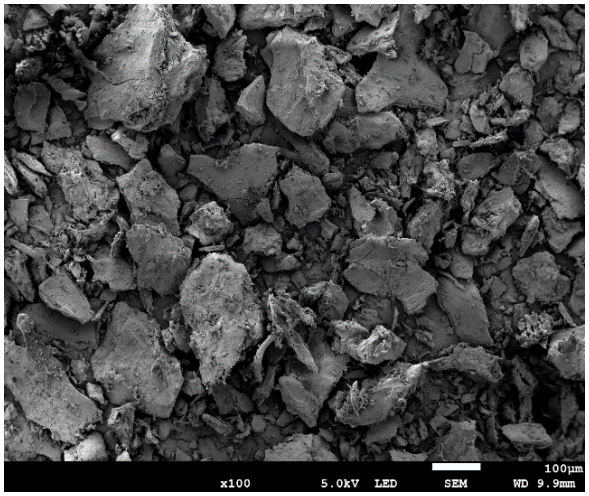

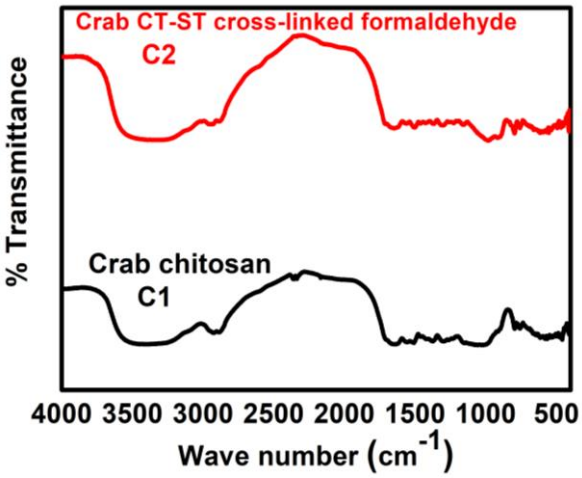

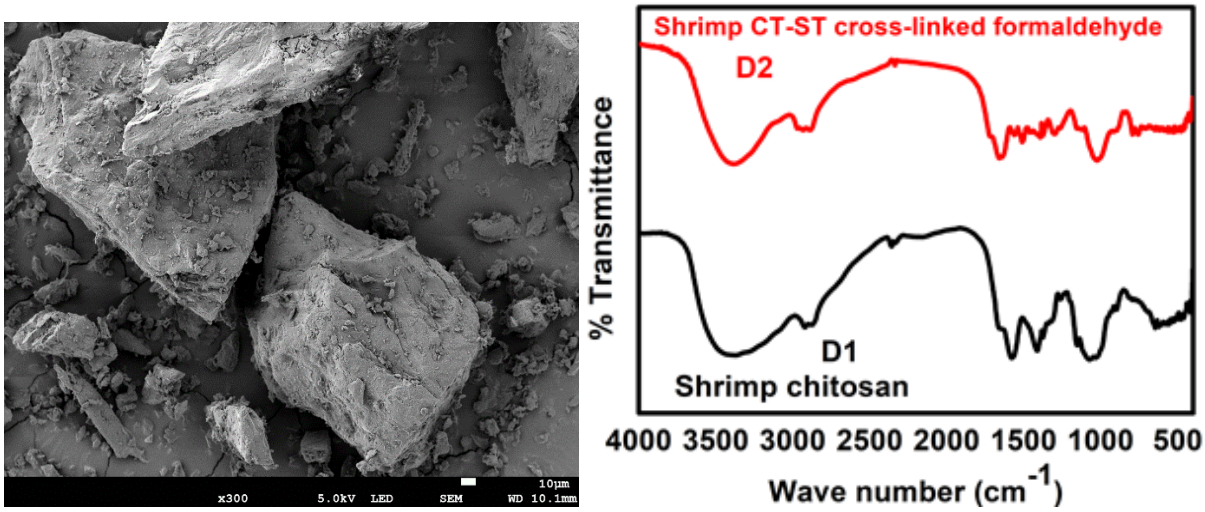

Figure 4.10: Scanning electron microscope images and FTIR spectrums of crab and shrimp chitosan starch cross-linked with formaldehyde

When cross-linked with formaldehyde, the results of the yield for crab chitosan starch was 69%, which was higher than the conventional shrimp chitosan starch when cross-linked with formaldehyde, which was 65%. The scanning electron microscope image of crab chitosan starch that was cross-linked with formaldehyde under low magnification (x100) showed a crystalline structure with small blocks of filament that are closely packed together. When shrimp chitosan starch was cross-linked with formaldehyde at lower magnification (x300), a micro-structure with a similar shape of large globular cube-like structures with small and low surfaces was observed. Nonetheless, slightly different particles sizes without any significant differences in homogeneity were observed.

The FTIR spectrum of a crab cross-linked bead (C2) was slightly similar to that of the initial crab chitosan (C1). The corresponding band to the amino group of chitosan shifted from 1630 − 1668 cm^{-1}, which was an indication of the presence of interaction between the hydroxyl group of starch and the amino group of chitosan. In the process of cross-linking with formaldehyde, a peak was observed at 1668 cm^{-1} because of the carbonyl stretching vibration. A prominent peak was visible at 1502 cm^{-1} (Figure 4.10 [C2]) which was due to the imine bonds (CN) that formed due to a cross-linking reaction between the amino groups in the chitosan and the aldehyde group in the formaldehyde. The characteristic peak assured the formation of a Schiff base after the reaction of the formaldehyde with the chitosan. The peak of the ether group (C2)

became stronger and shifted slightly from chitosan to cross-linked chitosan, in which case 1058 − 979 cm^{-1} (C2) indicated the formation of a new opened chain of ether linkage in the bead after reaction to cross-linking. A comparison of this spectrum with the chitosan beads (C1) from crab shell indicated the following differences: The characteristic peaks were situated at 337 cm^{-1}, indicating the stretching of OH and NH; the absorption bands at 2340 and 2870 cm^{-1} were represented by the CH_2 group stretching vibration; the peak situated at 1630 cm^{-1} was due to the CO stretching of the amide group; while the band at 1500 cm^{-1} corresponded to the NH bending vibration in the amide group.

The FTIR spectrum resulting from cross-linking (D2) showed some similarities with that of the initial shrimp chitosan (D1). The corresponding band to the amino group of the chitosan shifted from 1651 to 1658 cm^{-1}, which was an indication of the presence of interaction between the OH group of starch and the NH_2 group of chitosan. When cross-linked with formaldehyde, the peak obtained at 1658 cm^{-1} was due to the stretching of carbonyl vibration of the remaining acetamide group in chitosan, while the peaks at 1514 and 1511 cm^{-1} were due to imine bonds (CN) constructed via a cross-linking reaction between the amino groups in the chitosan and aldehyde groups in the formaldehyde. The occurrence of a Shiff base after the reaction of formaldehyde with chitosan was confirmed by its characteristic peaks. The peak of the ether group (D2) became stronger and shifted slightly from 1029 – 1027 cm^{-1}, which suggested that a new open chain ether linkage was formed in the bead due to a cross-linking reaction. The following differences were observed when comparing the cross-linked chitosan spectrum (D2) with the chitosan beads from the shrimp shell (D1) sample: A broad and strong band was observed ranging from 3200 − 3700 cm^{-1} (stretching vibration of OH and stretching vibration of NH); the peak located at 1651 cm^{-1} was the result of CO in the amine group; and the band at 1514 and 1558 cm^{-1} indicated an NH bending vibration in the amide group (see spectrum D1).

4.4.3.3 *Crab and shrimp chitosan starch (CT-ST) cross-linked with epichlorohydrine*

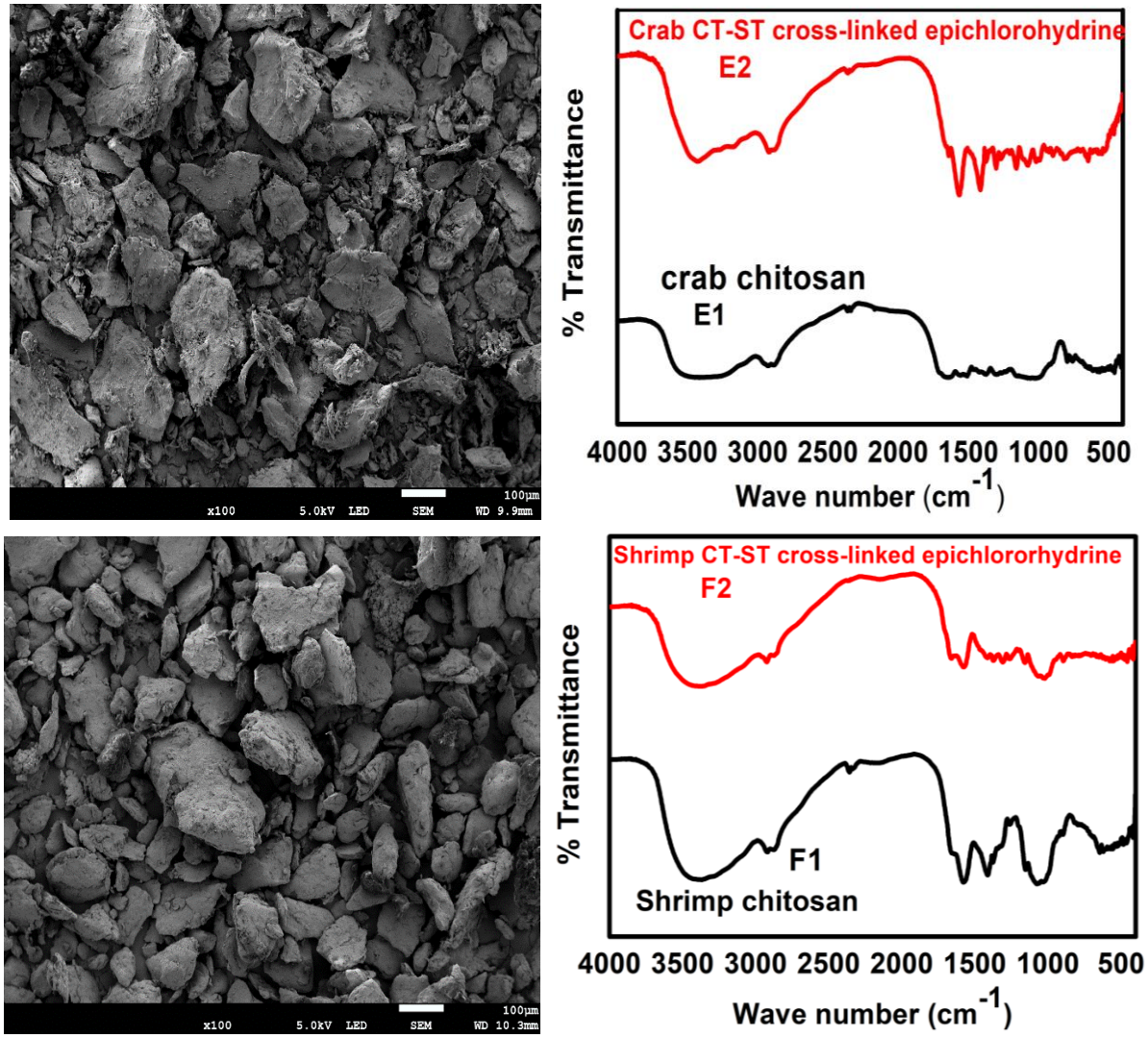

Figure 4.11: Scanning electron microscope images and FTIR spectrums of crab and shrimp chitosan starch cross-linked with epichlorohydrine

When crab chitosan was cross-linked with epichlorohydrine, the yield was 55%, which was considerably lower than the 72% yield when conventional shrimp chitosan starch was cross-linked with formaldehyde. The scanning electron microscope image of crab chitosan starch that was cross-linked with epichlorohydrine under low magnification (x100) showed a crystalline structure with small blocks of filament which were closely packed together. The shrimp chitosan starch that was cross-linked with epichlorohydrine to the same magnification showed that the microstructure possessed

tiny stone-like shapes similar to structures with small and low surfaces, but with slightly different particles sizes, without any significant changes in homogeneity.

The infrared spectrum of crab chitosan starch that was cross-linked with epichlorohydrine (E2) showed some similarity to the chitosan from wave number 4000 − 1500 nm and from 1400 − 400 nm, but a big variety of differences with relative intensities was observed. The representative band of the amino group of chitosan shifted from 1630 to 1606 cm^{-1}, which was an indication of interaction between the hydroxyl group of starch and the amino group of chitosan. The absorption intensity of the NH_2 group and the OH group (peak value from 3200 to 3700 cm^{-1}) of the cross-linked chitosan was obviously lower than that of the NH_2 and OH groups of chitosan. This indicated that a cross-linked reaction occurred between chitosan and epichlorohydrine. Additionally, the reduction in the intensities at 1488 cm^{-1} peak (in the NH_2 amino group) showed that most of the main amino groups were involved in the

cross-linking process. It is worth noting in this case that a comparison of the spectrum with the crab chitosan shell beads (E1) showed that the characteristic peaks were located at 3375 cm^{-1}, which indicated OH and NH stretching. However, the absorption bands at 2340 and 2870 cm^{-1} were represented by the CH_2 group stretching vibration while the peak located at 1630 cm^{-1} was an indication of the CO stretching of the amide group. The band at 1500 cm^{-1} corresponded to the NH bending vibration in the amide group (E1).

The results obtained from the infrared spectrum of shrimp chitosan starch that was cross-linked with epichlorohydrine adsorbent (F2) presented some similarities to that of shrimp chitosan. Nonetheless, with the presence of functional groups of epichlorohydrine in chitosan (F1), the same vibrations were observed but with different relative intensities. An analysis of the obtained results showed in this case that the absorption intensity of the NH_2 and OH groups (peak 3200 − 3700 cm^{-1}) of cross-linked chitosan (F2) was obviously lower than that of the NH_2 and OH groups of chitosan. This interpretation is an indication that a cross-linked reaction occurred between chitosan and epichlorohydrine. Thus the reduction in the intensities at 1488 cm^{-1} peak (NH_2 in the amino group) indicated that most of the primary amino groups were involved in the cross-linking process.

When comparing the cross-linked shrimp chitosan spectrum (F2) with the chitosan beads of shrimp shell (F1), a broad and strong band was observed that ranged from 3200 to 3700 cm^{-1} (due to the stretching vibration of OH and NH), while the peak located at 1651 cm^{-1} was a representation of CO in the amine group. The representative band of the amino group of chitosan was also shifted from 1651 to 1664 cm^{-1}, which indicated interaction between the hydroxyl group of starch and the amino group of chitosan. Finally, the band at 1514 and 1558 cm^{-1} represented NH bending vibration in the amide group (see spectrum F1).

4.4.3.4 Crab and shrimp chitosan starch (CT-ST) cross-linked with acrylic acid

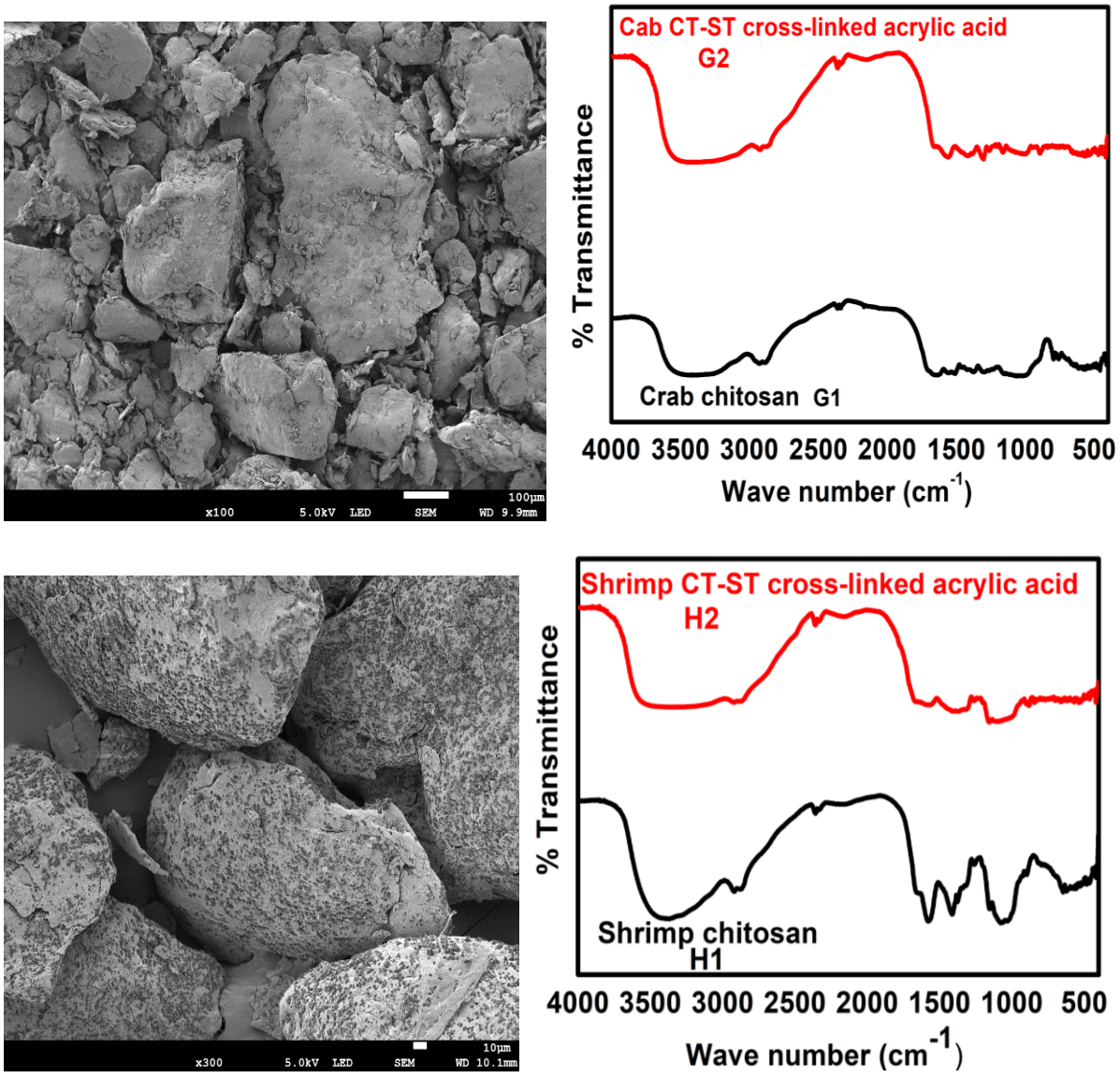

Figure 4.12: Scanning electron microscope images and FTIR spectrums of crab and shrimp chitosan starch cross-linked with acrylic acid

The results that were obtained experimentally yielded crab chitosan starch cross-linked with acrylic acid at 98% in contrast with the yield for shrimp chitosan starch cross-linked with glutaraldehyde at lower than 72%. The scanning electron microscope image of the crab chitosan starch that was cross-linked with acrylic acid can be seen at the top of Figure 4.12. This image was viewed under low magnification (x100). It was observed that its crystalline structure showed various shapes and sizes of scattered filament and that they were closely packed together. However, the shrimp chitosan starch that was cross-linked with acrylic acid under the same magnification (x100) displayed a filament that was scattered in a leaf-like arrangement of globular structures. The micro-structure of the shrimp chitosan starch that was cross-linked with acrylic acid at low magnification (x100) had a more distinct stone-like appearance with large particle surfaces. Nevertheless, different particle sizes were observed without any significant changes in homogeneity.

The results of the analysis of the spectrum of acrylic acid that was cross-linked with chitosan (G2) indicated a broad absorption potential with peaks ranging from 2973 to 3731 cm^{-1}. This result represents the OH bending vibration of the cross-linking agent, namely acrylic acid. The observation of peaks at 1550 and 1159 cm^{-1} suggests the stretching vibration of CO and CO of the carboxylic group. The peak at 1415 cm^{-1} is a representation of the OH bending vibration (G2), which thus suggests successful cross-linking of chitosan and starch with acrylic acid.

When comparing the cross-linked chitosan spectrum with the normal chitosan beads from crab shell (G1), it was noticed that the characteristic peaks were located at 3375 cm^{-1}, indicating both OH and NH stretching vibration. Absorption bands at 2340 and 2870 cm^{-1} were represented by the stretching vibration of the CH_2 group. The peak located at 1630 cm^{-1} was an indication of the CO stretching of the amide group, while the band at 1500 cm^{-1} corresponded to the NH bending vibration in the amide group (G2).

The results obtained from the analyses of the FTIR spectrum for normal shrimp chitosan beads and acrylic acid that was cross-linked with chitosan starch are depicted in Figure 4.12. These results indicate that the acrylic acid that was cross-linked with chitosan had broad absorption with peaks ranging from 2883 to 3588 cm^{-1}, which represented the OH bending vibration of the cross-linking agent, acrylic acid, while the

peaks appearing at 1558 and 1151 cm^{-1} explained the stretching vibration of CO of the carboxylic group. However, the peak at 1419 cm^{-1} was due to the OH bending vibration (see spectrum H2). This indicates that the cross-linking reaction between chitosan and starch was successful. The cross-linking of the chitosan spectrum (H2) with the chitosan beads from shrimp shell (H1) revealed a broad and strong band at 3200 − 3700 cm^{-1} because of the stretching vibration of OH and NH.

The peak located at 1651 cm^{-1} represented the CO in the amine group and the band at 1514 and 1558 cm^{-1} indicated NH bending vibration in the amide group (see spectrum H1).

4.4.3.5 Crab and shrimp chitosan starch (CT-ST) cross-linked with 1-vinyl-2-pyrrolidone

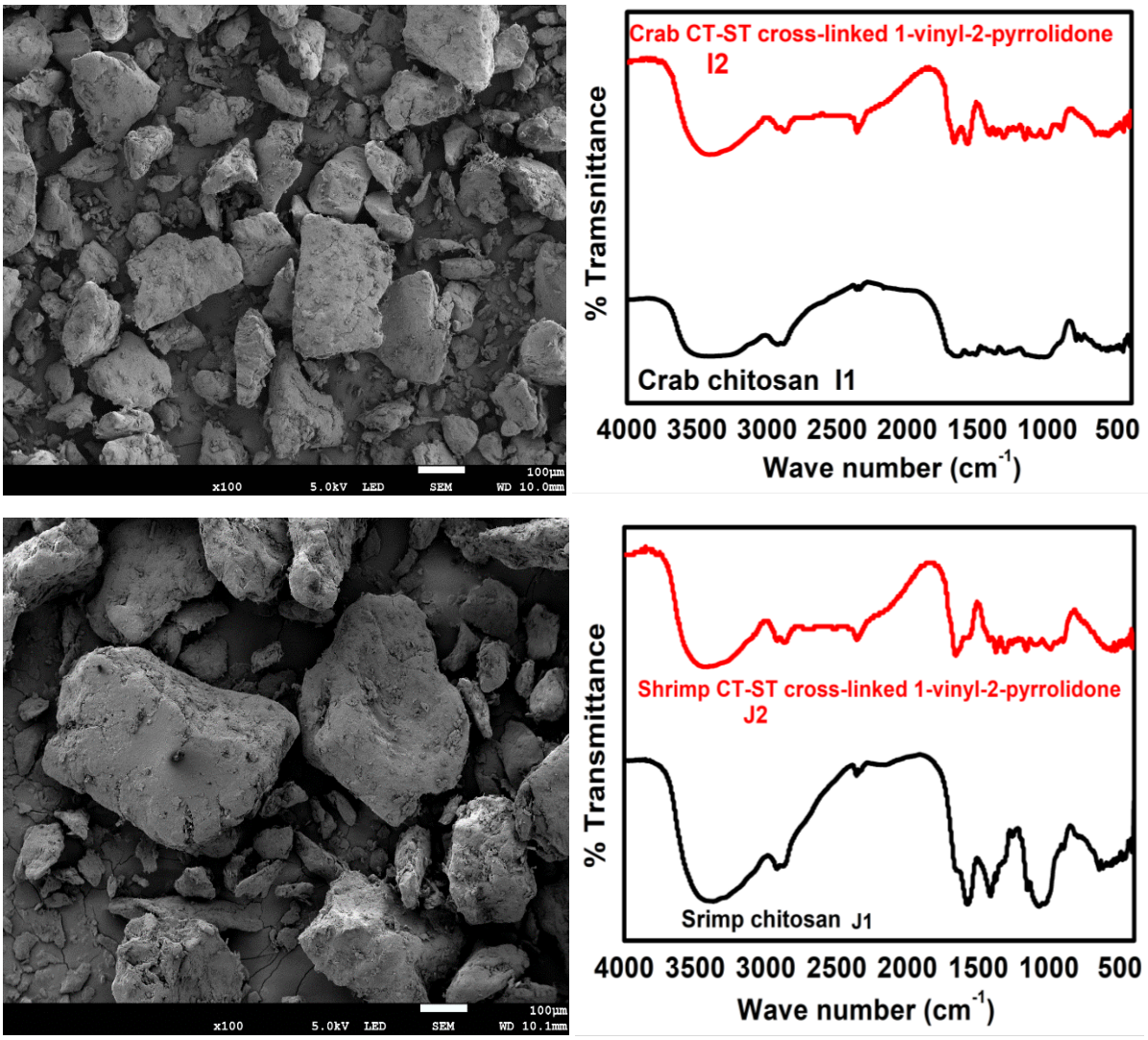

Figure 4.13: Scanning electron microscope images and FTIR spectrums of crab and shrimp chitosan starch cross-linked with 1-vinyl-2-pyrroidone

The empirical results of the characterization of crab chitosan starch that was cross-linked with 1-vinyl-2-pyrrolidone resulted in a 53% yield, which in this case was slightly lower in comparison to that of the shrimp chitosan starch that was cross-linked with 1-vinyl-2-pyrrolidone that yielded 55%. The corresponding scanning electron microscope image for crab chitosan starch that was cross-linked with epichlorohydrine under low magnification (x100) showed a crystalline structure with small filaments

closely packed together. When comparing this image to the shrimp chitosan starch that was cross-linked with epichlorohydrine under similar magnification, the micro-structure seemed to be retained in tiny and large block-shaped structures with small and low surfaces and different particle sizes, and with significant changes in homogeneity.

The FTIR spectrum of chitosan starch that was cross-linked with 1-vinyl-2-pyrrolidone (I2) showed strong peaks at 3418 cm^{-1} which was ascribed to the OH and NH stretching of CO (amide), thus indicating the presence of 1-vinyl-2-pyrrolidone on the cross-linked chitosan beads. A change in intensity at 1660 cm^{-1} for the stretching of CO (amide 1) revealed the presence of 1-vinyl-2-pyrroliodne on the beads. This suggests that the cross-linking reaction between chitosan and starch was successful. More so, the observed peaks at 1570, 1421,1309, 1376 and 1261 cm^{-1} were due to the characteristics of the amide II tertiary amine group and the bending of CN and CO respectively.

This spectrum differed from that of normal chitosan from crab shell (I1) in that it showed a broad peak at 3375 cm^{-1} due to the OH and NH stretching vibrations of the saccharide structure. The peak at 1630 cm^{-1} was attributed to the presence of the acetamide group with CO stretching. The peaks at 1370 and 1515 cm^{-1} corresponded to the CN bond stretching and the deformation of CH. The IR spectrum of chitosan starch − OH and NH stretching of CO (amide) − testified to the presence of 1-vinyl-2-pyrrolidone on the cross-linked chitosan beads. A little change in intensity at peak 1659 cm^{-1} for stretching of CO (amide I) also indicated the presence of 1-vinyl-2-pyrrolidone on the beads. Furthermore, peaks at 1421, 1376 and 1260 cm^{-1} were observed because of the characteristics of amide II, the tertiary amine group, and the bending of the CN bond respectively.

Comparative results of the spectrum for J2 and normal chitosan from shrimp shell (J1) showed a broad peak at 3375 cm^{-1} because of the OH and NH stretching vibrations of the saccharide structure. The peak at 1630 cm^{-1} was attributed to the presence of the acetamide group with CO stretching. The peaks at 1370 and 1515 cm^{-1} were analogous to the CN bond stretching and the deformation of the CH. In this case, the result was an indication of the successful cross-linking reaction between chitosan starch and 1-vinyl-2-pyrrolidone.

4.4.3.6 Crab and shrimp chitosan starch (CT-ST) cross-linked with polyethylene glycoldicglycider ether (PEG diglycider ether)

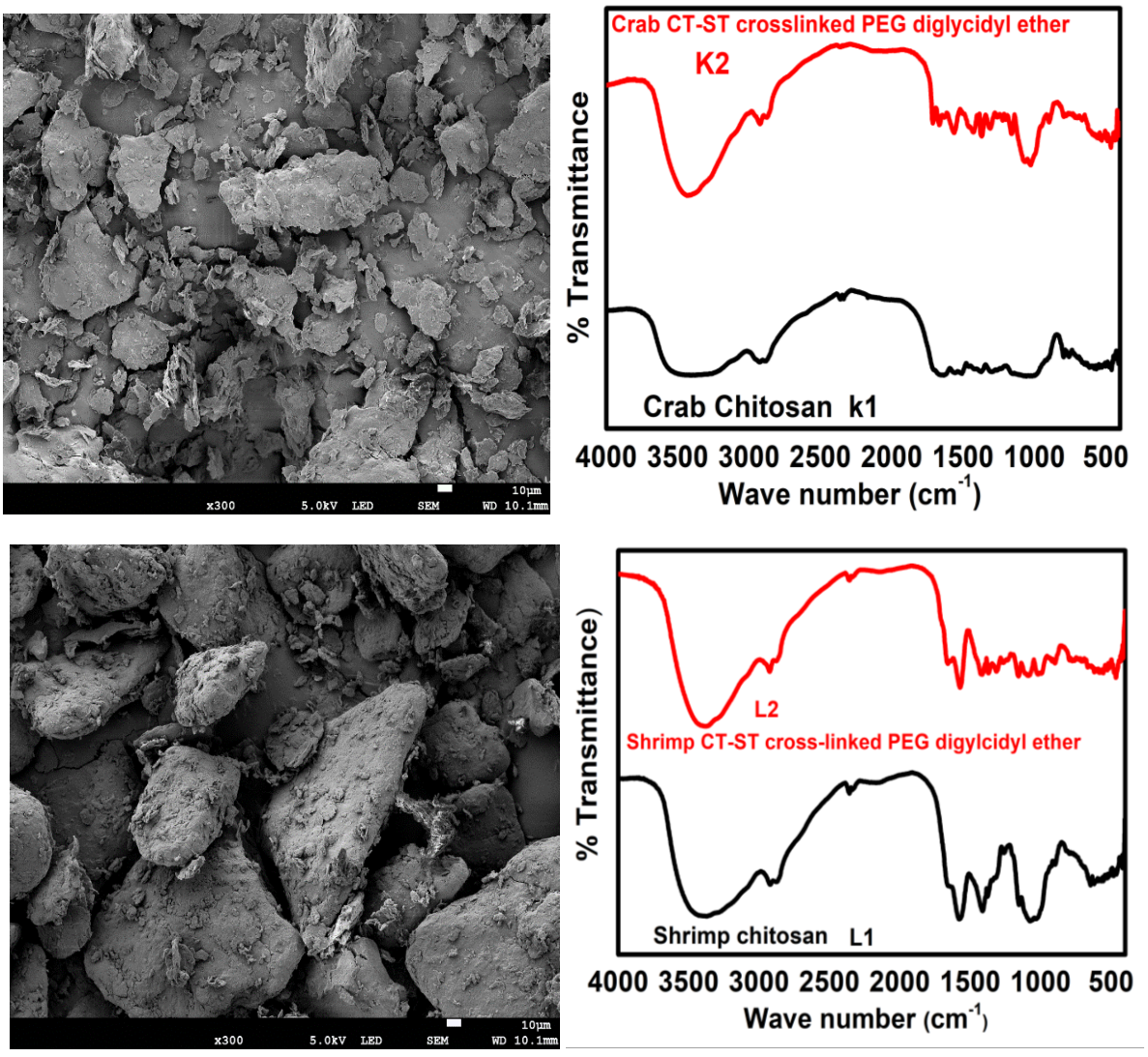

Figure 4.14: Scanning electron microscope images and FTIR spectrums of crab and shrimp chitosan starch cross-linked with poly ethylene glycol dicglycidyl ether (PEG digylcidyl ether)

The empirical yields for the crab and shrimp chitosan starch samples that were cross-linked with PEG diglycidyl ether were 58 and 72% respectively. The products were viewed under low magnification (x100) using a scanning electron microscope. The crab images revealed a small, scattered leafy filament with particles closely packed together. The shrimp images under same magnification showed a micro-structure with large and small block-shaped structures with small and low surfaces with no significant changes in homogeneity.

The infrared stretching frequencies of PEG diglycidyl ether cross-linked with crab chitosan starch adsorbent (K2) were similar to those of crab chitosan from 4000 - 1500 cm^{-1} but different in the region of 1400 - 400 cm^{-1}. The band corresponding to the amino group of chitosan shifted from 1660 to 1623 cm^{-1}, which was an indication of interaction between the hydroxyl group of starch and the amino group of chitosan. The absorption intensity of the NH_2 and OH groups (peak values ranged from 3200 − 3700 cm^{-1}) showed that the cross-linked characteristics of chitosan were lower than those of the NH_2 and OH groups from chitosan, which indicated that a cross-linked reaction occurred between chitosan and epichlorohydrine. In addition, the reduction in intensity at 1488 cm^{-1} peak (NH_2 in the amino group) showed that most of the primary amino groups were involved in the cross-linking process.

A difference was observed between this spectrum (K2) and the chitosan beads that were obtained from crab shell (K1), as the peaks that were located at 3375 cm^{-1} represented OH and NH stretching. Moreover, the absorption bands at 2389 and 2808 cm^{-1} were representative of the stretching vibration of the CH_2 group. The peak located at 1630 cm^{-1} was due to CO stretching of the amide group while the band that was noted at 1500 cm^{-1} corresponded to the NH bending vibration in the amide group (K1).

The infrared spectrum of shrimp chitosan starch that was cross-linked with PEG diglycidyl ether adsorbent (L2) was compared to that of normal crab chitosan beads and was found to be similar to that of shrimp chitosan beads (L1). However, with the presence of functional groups of PEG diglycidyl ether in chitosan, the same vibrations were observed but with different relative intensities. The absorption intensities of the NH_2 and OH groups respectively peaked at 3283 and 3485 cm^{-1}, while those of the cross-linked chitosan were lower than those of the NH_2 and OH groups of chitosan.

This result confirmed a cross-linking reaction between chitosan and poly ethylene glycol diglycidyl ether. The reduction in the intensities at 1663 cm^{-1} peak (NH_2 in the amino group) showed that most of the primary amino groups were involved in the cross-linking process. Comparison of the cross-linked chitosan spectrum (L2) with the chitosan beads from shrimp shell (L1) showed a broad and strong band in the range 3100 − 3700 cm^{-1} due to the stretching vibration of OH and NH in both spectrums. The

band in the region of 1535 − 1575 cm^{-1} could be ascribed to the stretching frequency of the NH bending vibration in the amide group (L1).

Crab and shrimp chitosan starch (CT-ST) cross-linked with polyethylene s-methylbenzylamine

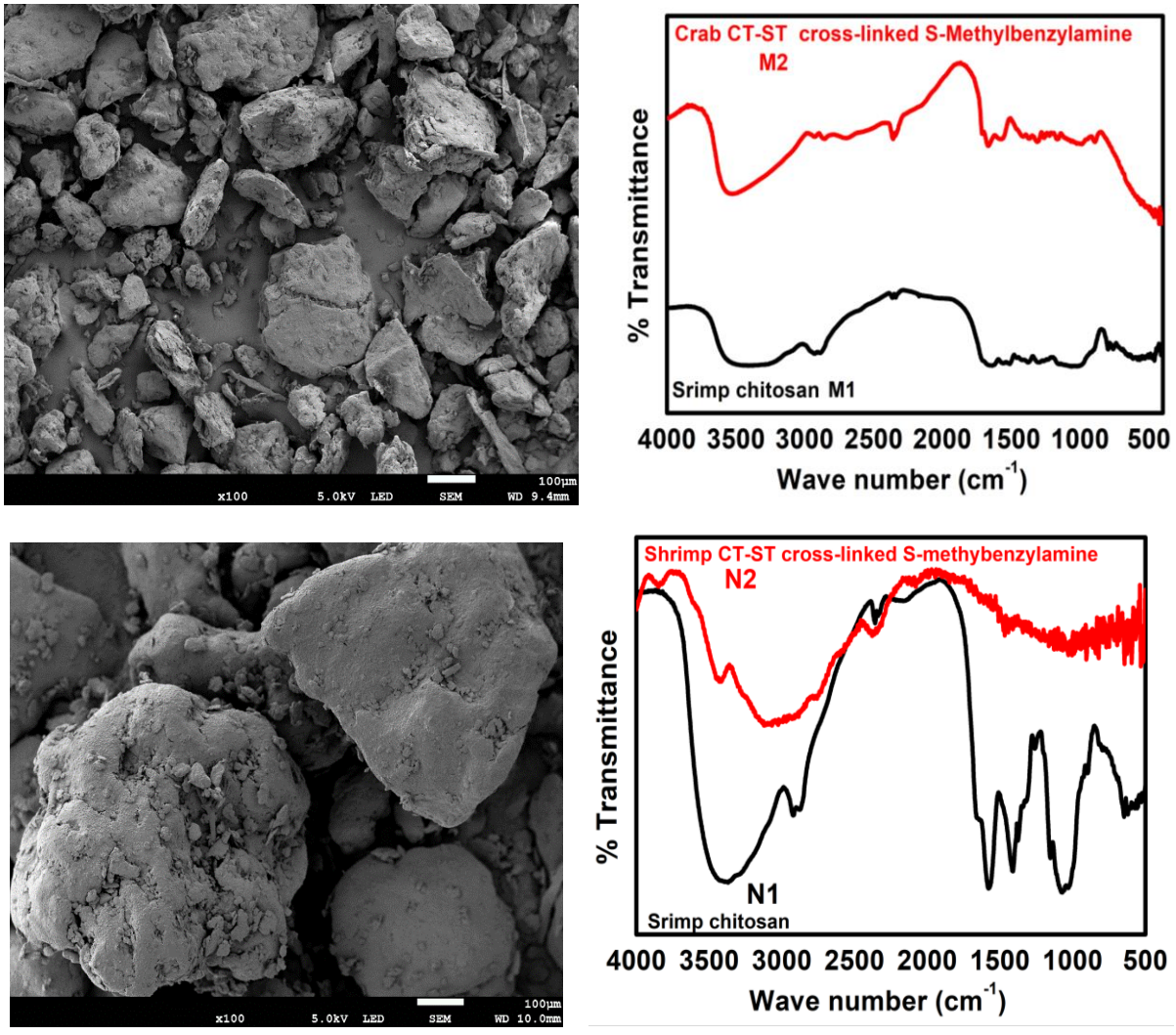

Figure 4.15: Scanning electron microscope images and FTIR spectrums of crab and shrimp chitosan starch cross-linked with s-methylbenzylamine

The reaction of crab and shrimp chitosan starches that were cross-linked with s-methylbenzylamine yielded 59 and 63% respectively. The crab and shrimp cross-linked products' structures as seen in images generated by the scanning electron microscope under low magnification (x100) revealed an amorphous spherical appearance with tiny and large stone-like structures with small and low surfaces. The s-methylbenzylamine cross-linked chitosan (M2) showed broad absorption peaks in the range of 2961 − 3654 cm^{-1}. The peaks appearing at 1559 and 1156 cm^{-1} were deemed depictions of the stretching vibration of CO of the carboxylic group, while the peak at 1478 cm^{-1} was due to the OH bending vibration which confirmed that successful cross-linking of chitosan and starch occurred. The presence of the characteristic peaks of normal chitosan beads from crab shell (M1) was observed at 1630 and 1567 cm^{-1} and this was ascribed to the CO and the NH groups (M2). The s-methylbenzylamine that was cross-linked with chitosan (M2) showed broad absorption with peaks ranging from 2771 − 3350 cm^{-1}, representing the OH bending vibration of the cross-linking agent (s-methylbenzylamine). The peaks appearing at 1502 and 1055 cm^{-1} depicted the stretching vibration of CO of the carboxylic group. The characteristic peak at 1431 cm^{-1} for the OH bending vibration (see N2) was a confirmation of a cross-linking reaction between chitosan and starch. The cross-linked chitosan product (N2) and the shrimp chitosan beads from shrimp shell (N1) resulted in a broad and strong band ranging from 3200 − 3700 cm^{-1}. The stretching frequencies ranging from 1504 − 1580 cm^{-1} represented the presence of NH bending vibration in the shrimp chitosan starch (CT-ST) cross-linked with *p*-benzoquinone.

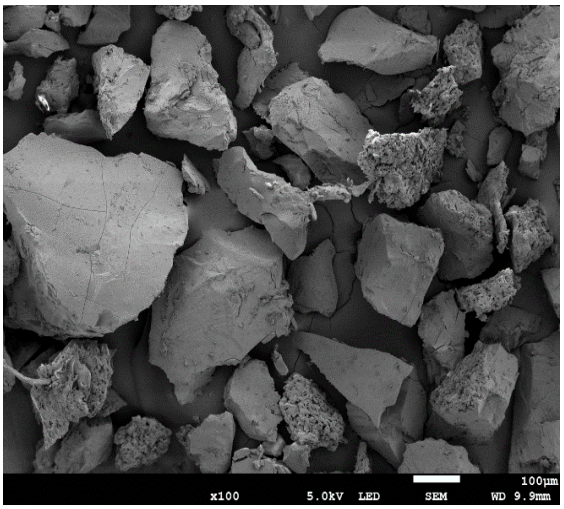

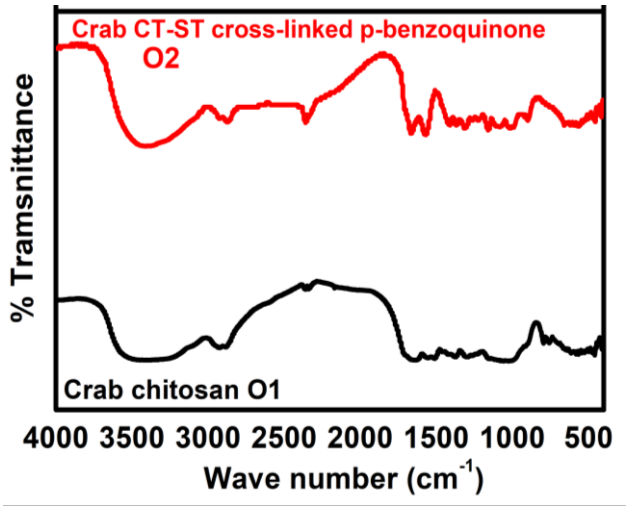

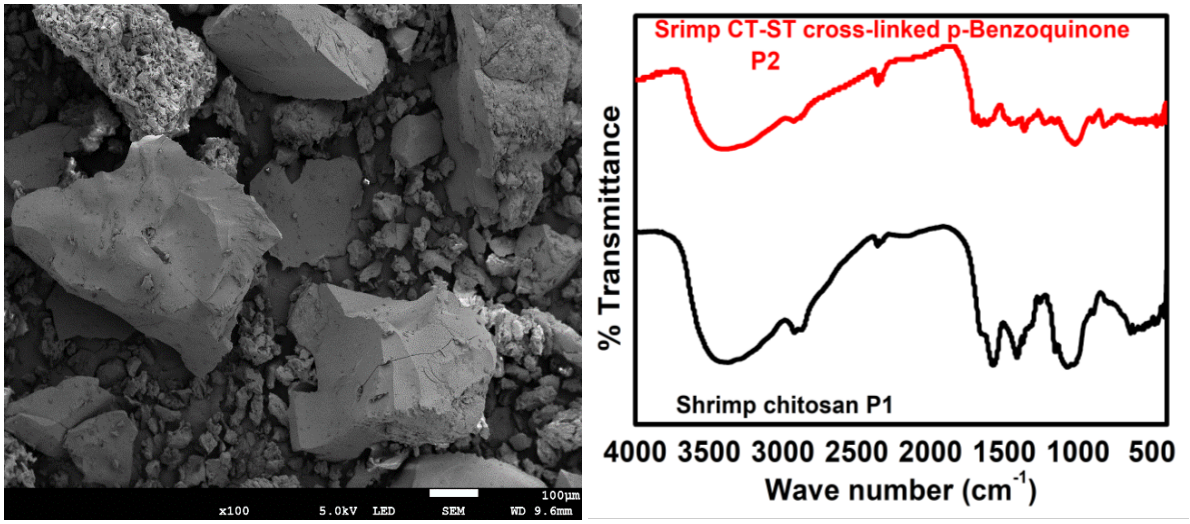

Figure 4.16: Scanning electron microscope images and FTIR spectrums of crab and shrimpchitosan starch cross-linked with *p*-benzoquinone

Crab and shrimp chitosan starch that was cross-linked with *p*-Benzoquinone yielded 62 and 59% respectively. The crab cross-linked product under low magnification (x100) was revealed to be composed of a tiny block structure with particles slightly spaced out, whilst the shrimp cross-linked product at similar magnification showed microfibrillar structures that were also slightly spaced out. The infrared spectrum of crab chitosan starch that was cross-linked with benzoquinone adsorbent (O2) was similar to that of the chitosan beads composed of crab shell. Similar stretching frequencies occurred but different relative intensities were noted. The adsorption intensity of the NH_2 and OH groups from cross-linked chitosan (O2) was visible in the range 3200 − 3700 cm^{-1} and it was weaker than that of the NH_2 and OH groups of normal chitosan from crab shell. This indicated a successful reaction. The reduction in intensity that peaked at 1488 cm^{-1} (NH_2 in the amino group) showed that most of the primary amino groups were involved in the cross-linking process. The spectrum (O2) had a broad and strong band that ranged between 3200 − 3700 cm^{-1} (stretching vibration of OH and NH) compared to the spectrum of (O1). The characteristic peak that occurred in the region of 1651 cm^{-1} of the same spectrum confirmed the presence of CO in the carboxylic group. The shift in the stretching frequencies in spectrum O1 from 1651 − 1618 cm^{-1} suggested the interaction between the hydroxyl group of starch and the amino group of chitosan. Moreover, the presence of the peak in the region of 1575 cm^{-1} revealed the presence of NH bending vibration in the amide group (see spectrum O1).

4.4.3.7 Crab and shrimp chitosan starch (CT-ST) cross-linked with 1,3-dichloroacetone

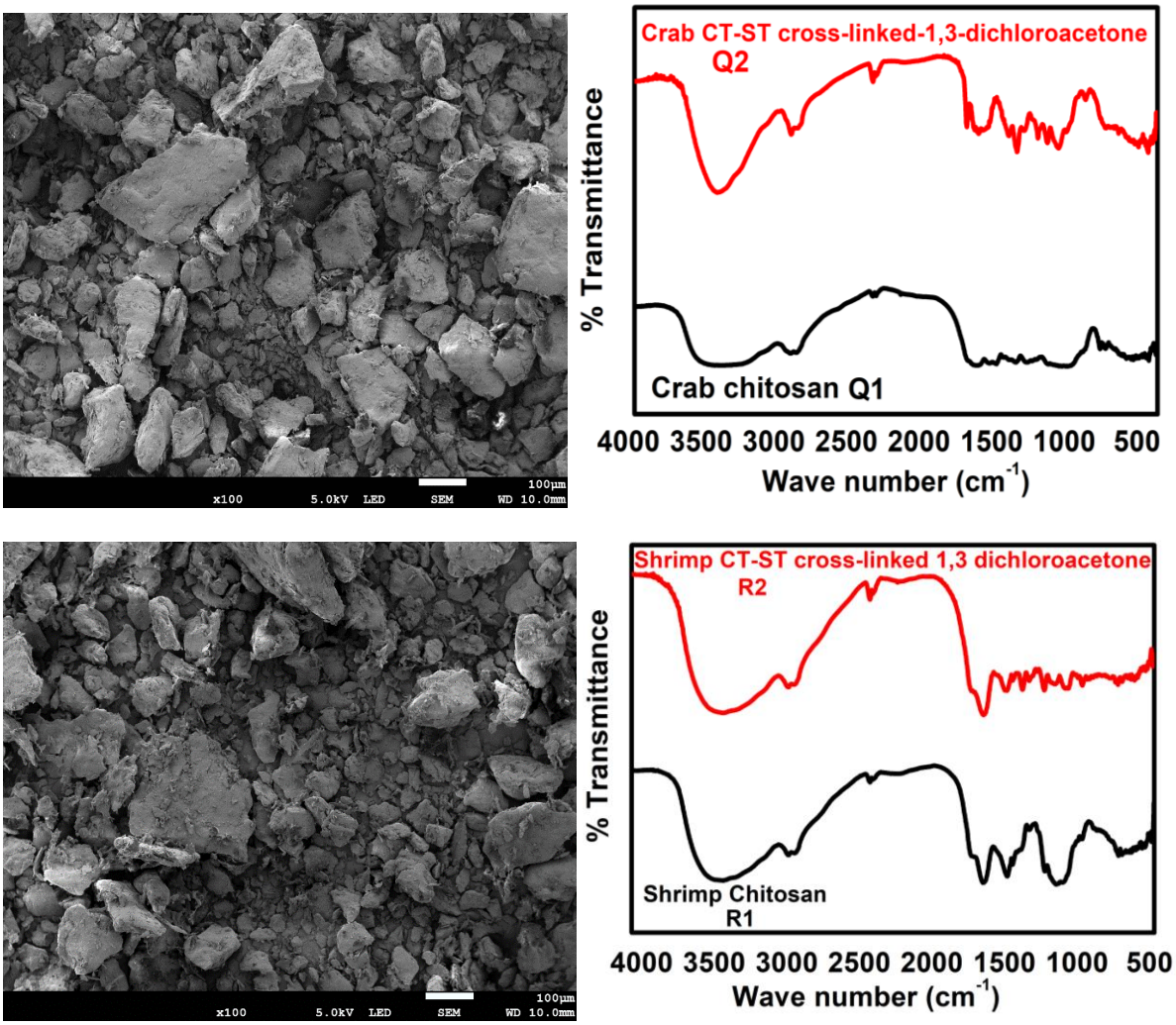

Figure 4.17: Scanning electron microscope images and FTIR spectrums of crab and shrimp chitosan starch cross-linked with 1,3-dichloroacetone

The crab chitosan starch and the shrimp chitosan starch that were cross-linked with 1,3 dichloroacetone yielded 71 and 92% respectively. Scanning electron microscope images for the crab chitosan starch that was cross-linked with 1,3 dichloroacetone under low magnification (x100) revealed scattered tiny pieces of filament packed close to one another, whilst the shrimp particles of chitosan starch that were cross-linked with 1,3 dichloroacetone under similar magnification appeared micro-fibrillar in structure. Both products showed some similarity at wave number 4000 − 1500 cm^{-1} and from 1400 − 400 cm^{-1} a large variety of differences with relative intensities could be observed. The presence of the amino group in the spectrum R2 was clearly visible in the 1630 − 1659 cm^{-1} range. The weaker absorption intensity of the NH_2 and OH

groups in R2 (peak values from 3200 − 3700 cm^{-1}) compared to R1 further confirmed that cross-linked reaction occurred between the chitosan and 1,3-dichloroacetone.

Differences were noted between the obtained spectrum of crab cross-linked chitosan starch (Q2) and the chitosan beads from crab shell (Q1). These differences were: the characteristic peaks at 3375 cm^{-1} represented OH and NH stretching; the absorption bands at 2340 and 2870 cm^{-1} depicted the CH_2 group stretching vibration; the peak located at 1630 cm^{-1} represented the CO stretching of the amide group; and the band at 1500 cm^{-1} corresponded to the NH bending vibration in the amide group (Q1). The infrared spectrum of shrimp chitosan starch that was cross-linked with 1,3-dicloroacetone (Q2) revealed similar stretching frequencies in the region of 3200 − 3700 cm^{-1}. The NH group peak was visible in the region of 1488 cm^{-1} which was consistent with the previous results and served as confirmation of the success of the cross-linked product.

4.4.3.8 Crab and shrimp chitosan starch (CT-ST) cross-linked with maleic anhydride

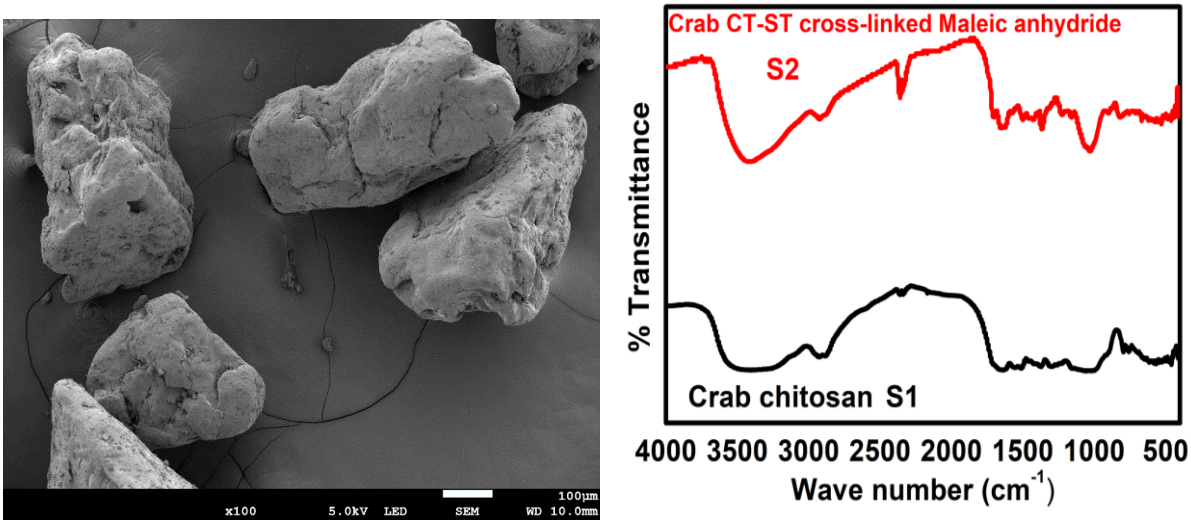

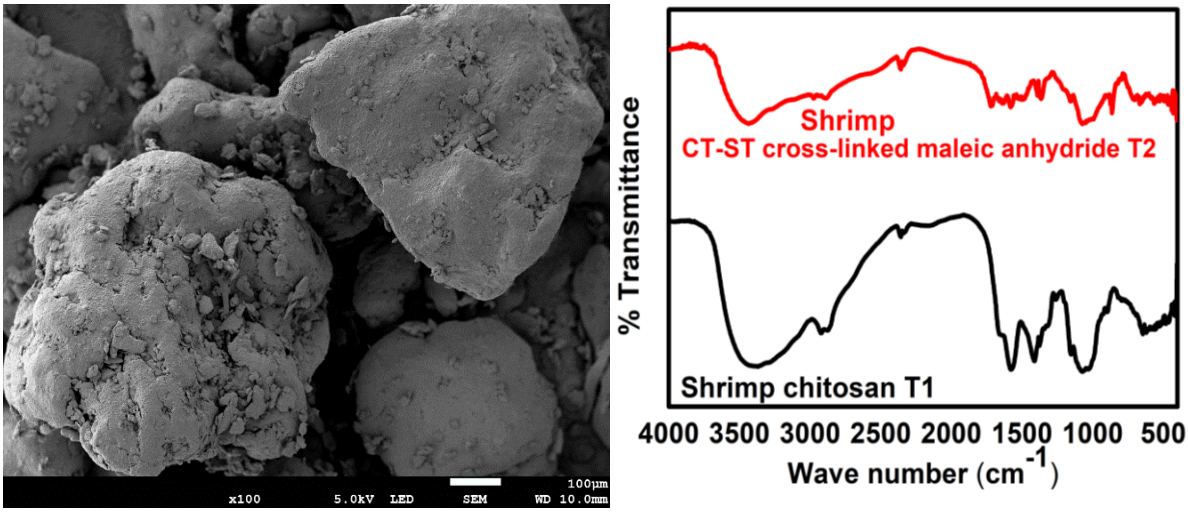

Figure 4.18: Scanning electron microscope images and FTIR spectrums of crab and shrimp chitosan starch cross-linked with maleic anhydride

The crab and the shrimp chitosan starch samples that were cross-linked with maleic anhydride yielded 30 and 26% respectively. The scanning electron microscope analysis of crab chitosan starch that was cross-linked with maleic anhydride under low magnification (x100) revealed a crystalline structure with large, compact blocks of granules that had settled adjacent to one another, while the shrimp chitosan starch that was cross-linked with maleic anhydride under similar magnification appeared as large, microfibrillar blocks of granular particles.

The characteristic stretching frequencies (NH_2 and OH groups) of the cross-linked products (S2) were observed in the region of 3200 − 3700 cm^{-1}. The strong peak observed in the region of 1714 cm^{-1} in the crab chitosan starch that was cross-linked with maleic anhydride was ascribed to the carboxyl stretching vibration of the carboxylic acid. Absorption bands in the region of 2340 − 2870 cm^{-1} for the crab chitosan starch corresponded to the stretching frequencies of the CH_2 group, whilst the peaks (S1) in the region of 1630 − 1500 cm^{-1} were ascribed to the CO and the NH groups. IR characterization of the shrimp chitosan starch that was cross-linked with maleic anhydride (T2) showed similar stretching frequencies in the NH_2 and OH groups that were in the region of 3200 − 3700 cm^{-1}. The CO peak was observed at 1641 cm^{-1}, which was slightly different from that of the shrimp (T1) product. The peaks located at 1714 and 1651 cm^{-1} represented the CO in the amine group while the band at 1514 and 1558 cm^{-1} occurred as a result of the NH bending vibration in the amide group (see spectrum T1).

4.5 Conclusion

The isolation of chitin was achieved through extraction using mussel, oyster, shrimp and crab shells and silver and pang fish scales (starting material). Satisfactory yields were obtained from oyster and crab samples (60 - 70%) whilst lower yields were obtained from the mussel, shrimp, pang and silver fish samples (31 – 40%). Successful conversion of the chitin to chitosan was achieved through cross-linkage with glutaraldehyde, formaldehyde, epichlorohydrine, maleic anhydride, *p*-benzoquinone, poly ethylene glycol (PEG) diglycidyl ether, 1-vinyl-2-pyrrolidone, 1,3-dichloroaceone, acrylic acid and s-methylbenzylamine chitosan products.

Characterization of these cross-linked chitosan products was performed using FTIR, SEM and viscometer applications. The FTIR results of the isolated cross-linked chitosan products showed a good correlation of the stretching frequencies to those cited in the literature, which confirmed the presence of the desirable product. Analyses using SEM spectroscopy revealed different morphological structures of the products and revealed how the particles were orientated in space. Determination of the physiochemical properties such as molecular weight, intrinsic viscosity and solubility revealed a direct correlation between the molecular weight and the intrinsic viscosity of the cross-linked chitosan products.

5 ISOLATION OF HEAVY METALS FROM WASTEWATER USING CROSS-LINKED CHITOSAN PRODUCTS

5.1 Introduction

The need to purify wastewater using chitosan derivatives was discussed in Chapter 3, while Section 3.4.1 demonstrated a promising technique to isolate heavy metals from wastewater. Therefore, a series of chitosan cross-linked products was synthesized and characterized as was discussed in the previous chapter. The differences in the morphological appearances and functional groups in the chitosan cross-linked products revealed features that have the potential to be used in the adsorption of metals from wastewater. The objective of this chapter is to determine the effectiveness of these modified chitosan derivatives in purifying wastewater from red meat and poultry abattoirs. Some of the common elements that affect animals and aquatic life such as Fe, Cu, Zn, Pb, Ni, Sn, Hg, Cr, As, Al and Cd as were identified in Chapter 2, Section 2.3.1 will be determined for their presence in purified water. The effectiveness of each cross-linked chitosan product will be assessed based on the number of elements adsorbed; i.e., the fewer elements retained the more efficient the chitosan product is, and vice versa.

5.2 Equipment

5.2.1 Instrumentation

A computer controlled Prodigy 7, ICP-OES sequential plasma spectrometer from the Institute for Groundwater Studies (UFS) (Figure 5.1) was used for the determination of the presence of heavy metals in abattoir effluent that was obtained from poultry and red meat abattoirs. The standard operating conditions of the ICP-OES are listed in Table 5.1.

Figure 5.1: Prodigy 7, ICP-OES used in the determination of heavy metals in abattoir wastewater

Table 5.1: ICP-OES selected operating conditions for the determination of heavy metals in wastewater from abattoirs

Parameter	Condition
RF power	1.2 kW
Coolant gas flow rate	14.0 ℓ/min
Plasma gas flow rate	1.2 m ℓ/min
Carrier gas flow rate	0.7 L/min
Sample uptake method	Peristaltic pump tube
Rinsing time	2.3 min
Type of spray chamber	Glass cyclonic with baffle
Type of nebulizer	Concentric
Injection tube diameter	3.0 mm

5.2.2 Materials, reagents and glassware

The chitosan products (see Chapter 4, Section 4.4.3) that were cross-linked with glutaraldehyde, formaldehyde, epichlorohydrine, maleic anhydride, *p*-benzoquinone, poly (ethylene) glycol diglycidyl ether, 1-vinyl-2-pyrrolidone, 1,3-dichloroaceone, acrylic acid and s-methyl-benzylamine were used as adsorbents in the isolation of heavy metals from the wastewater samples. The wastewater was collected and supplied to us in clean polyethylene containers (5 ℓ) and kept in a refrigerator. Other chemicals used included acids and solvents that were mentioned in Chapter 4, Section 4.2. Grade A-type Schott Duran beakers and Erlenmeyer flasks were used for all the wet chemical analyses. Glass burettes (50 mℓ) and plastic Pasteur pipettes of high accuracy and precision (±0.01 mℓ) were used to dispense accurate volumes during the chemical analyses.

5.2.3 Description of the water samples

Samples of the wastewater used in this research study were obtained from local poultry and red meat abattoirs situated in the outskirts of Bloemfontein in the Free State Province, South Africa. Samples were collected from effluent pipes and supplied to us in large 5ℓ containers. Strict regulation of equipment and adherence to confidentiality agreements were of high priority in securing the samples as most of the abattoirs did not want their identities revealed.

5.3 Experimental procedure

5.3.1 Preparation of ICP-OES calibration standards

ICP-OES multi-element standard (1000.00 µg/ℓ) stabilized in HNO_3 (7% v/v) was purchased from Merck and was used in the preparation of calibration standards. Standards in the concentrations of 5, 10, 20, 30 and 40 ug/ℓ were prepared using the “Transferpette” micro-pipette. Nitric acid (5.0 mℓ; 65%) was added to all the standards before the flasks were filled up to the mark using deionised water. The solutions were homogenized before use.

5.3.2 Preliminary treatment of the wastewater

Stock solutions of the red meat and poultry abattoir effluent/wastewater (2 x 5 ℓ) were first shaken to ensure homogeneity before filtered. The filtrates that contained most of the heavy metals were collected (2 x 2 ℓ) in separate beakers for ICP-OES analysis as shown in Scheme 5.1. The solid residues which included organic and inorganic wastes were removed from both solutions and discarded. ICP-OES qualitative analysis results of both filtrates (control) are reported in Table 5.2.

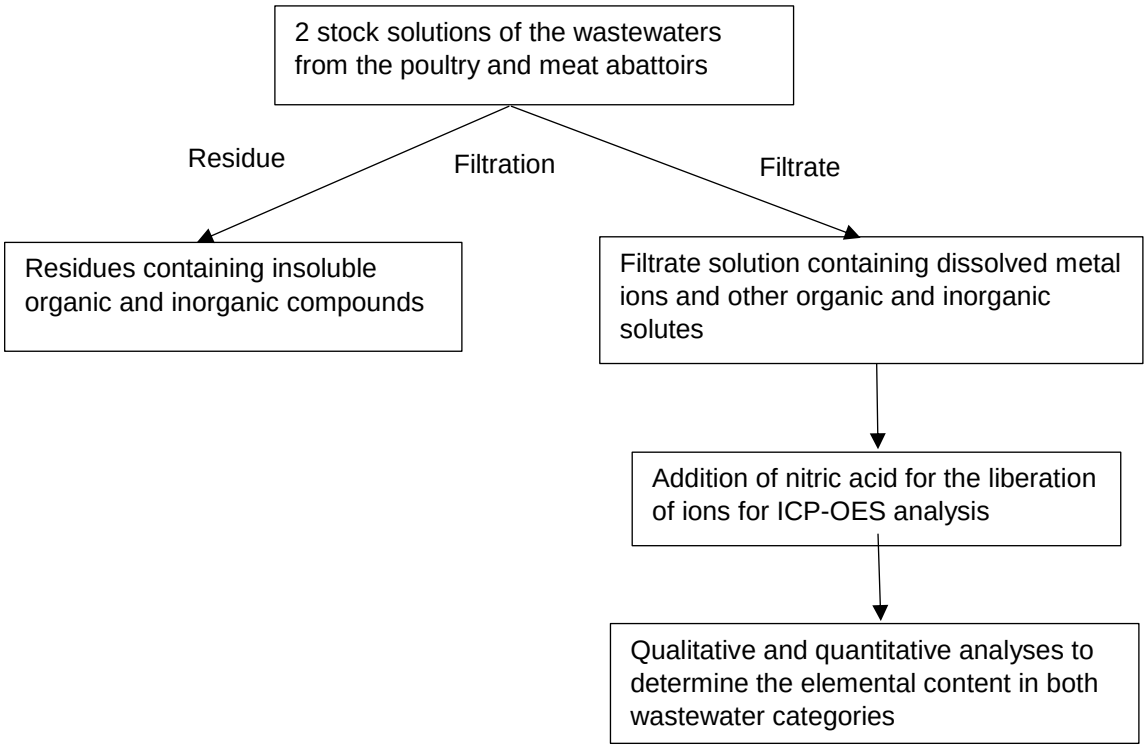

Scheme 5.1: Wastewater treatment before elemental analyses using ICP-OES

5.3.3 Preparation of the control solutions for ICP-OES analyses

Two control samples from both red meat and poultry wastewater were prepared from the original stock solutions by filtering the solution to remove insoluble particles. Aliquots (10 mℓ) of each solution (poultry and red meat) were transferred to volumetric flasks. Nitric acid (5.0 mℓ, 65%) was added and the solutions were homogenized before analyzed using ICP-OES. The qualitative results of the elements present in both samples are reported in Table 5.2.

Table 5.2: Determination of the elemental composition of wastewater from poultry and red meat abattoirs

Poultry wastewater (elements identified)	Estimated concentration range (mg/ℓ)	Red meat wastewater (elements identified)
Ca, Na and K	>100	Ca, Mg, Na, Si and K
-	>50	-
Mg	>10	Fe
Fe, Si and Al	>1	-
As, Co, Cr, Cu, Mn, Mo, Pb, Sr and Zn	<1	Al, As, Co, Cr, Cu, Mn, Mo, Pb, Sr and Zn

- No elements present

5.3.4 Chromatographic separation of elements in the wastewater from poultry and red meat abattoirs

Two sets of column chromatography were prepared for determining the capabilities of the previously synthesized chitosan products to adsorb heavy metals from the wastewater. The first chromatography column set was used to separate the heavy metals from the red meat wastewater and the second set was used for the poultry wastewater. Both sets of columns were loaded with different types of cross-linked chitosan products (150 mm length; 3.7 mm width). In each column, 15 mℓ of the wastewater was added and deionized water was used as an eluent. The effluent (ca. 70 – 80 mℓ) was collected at a rate of 1 drop per second in separate beakers for ICP-OES analyses and the results are shown in the Appendix.

5.3.5 *Abbreviation list of chitosan products used in the separation of elements in poultry and red meat wastewater*

X and Y - shrimp and crab chitosan beads

A2 and B2 - shrimp and crab chitosan starch cross-linked with glutaraldehyde

C2 and D2 - shrimp and crab chitosan starch cross-linked with formaldehyde

F2 and E2 - shrimp and crab chitosan starch cross-linked with epichlorohydrine

G2 and H2 - shrimp and crab chitosan starch cross-linked with acrylic acid

I2 and J2 - shrimp and crab chitosan starch cross-linked with 1-vinyl-2-pyrrolidone

K2 and L2 - shrimp and crab chitosan starch cross-linked with poly-ethylene diglycider ether

M2 and N2 – shrimp and chitosan starch cross-linked with s-methylbutylamine

O2 and P2 - shrimp and crab chitosan starch cross-linked with benzoquinone

Q2 and R2 – shrimp and crab chitosan starch cross-linked with 1,3 dichloroacetone

S2 and T2 - shrimp and crab chitosan starch cross-linked with maleic anhydride

5.3.6 *Quantitative analyses of the eluted solutions from poultry and red meat wastewater using ICP-OES*

The collected eluent solutions (poultry and the red meat) from the chromatography process were transferred to separate volumetric flasks (100.0 mℓ) and Nitric acid (5.0 mℓ, 65 %) was added to both sets of solutions. The solutions were homogenized and sent to the University of the Free State (Institute for Ground Water Studies (IGS), for analysis using ICP-OES. Table 5.3 contains selected wavelengths used for the elemental analysis using ICP-OES.

Table 5.3: Selected wavelengths for elemental analyses using ICP-OES

Element	Wavelength (nm)
Al	396.15
As	189.04
Cd	214.44
Co	228.61
Cr	205.55
Cu	324.75
Fe	239.56
Mn	257.61
Mo	202.03
Ni	221.64
Pb	220.35
Sb	217.58
Si	251.61
Sr	407.77

5.4 Results and Discussion

5.4.1 Qualitative analyses of red meat and poultry wastewater samples

Qualitative analyses of the wastewater samples (poultry and red meat) were done to determine which elements were present in the wastewater. The experimental results revealed the presence of different elements in each sample see Table 5.2. A total of 16 and 18 elements were present in the poultry and red meat wastewater samples respectively. Estimates indicated high concentrations (above 100 mg/ℓ) of Ca, Na and K in the poultry wastewater samples, whereas Ca, Mg, Na, K and Si (above 100 mg/ℓ) were present in the red meat wastewater samples. The high number of elements that were detected in both categories clearly revealed that high quantities of elements were deposited as effluent in the meat industry. It could be concluded that the high concentrations of alkali and alkaline earth metals present in the effluent would have a hardening effect on the fresh water bodies they were deposited in, if not removed.

5.4.2 Quantitative analyses of the poultry and red meat wastewater samples

5.4.2.1 Poultry samples

Quantitative analyses of the elements revealed high concentrations of Na (207.7 mg/ℓ), K (120.2 mg/ℓ) and Ca (258.5 mg/ℓ) in the poultry wastewater samples. The presence of these alkali and alkaline earth metals in high concentrations presented a challenge in quantification. The analysis of these elements using flame techniques has been reported to result in false high percentage recoveries and the effects of alkali and alkaline earth metals, sometimes referred to as easily ionized elements (EIE), are well documented (Brenner *et al*., 1997). According to the literature, when these elements are present in high concentrations (exceeding 400 mg/ℓ), they can alter the flame properties due to the ionization and atomization ratios of the analyte, which will then result in false findings of high concentrations. In the current study, a slight yellowing of the flame was observed during ICP-OES analyses, which was a positive indication of the presence of EIE. According to Brenner *et al.* (1997), the presence of high concentrations of EIE (Li, Na and K) in the analyte solution often results in red, yellow and pink/purple/lilac flames respectively, all of which are not ideal

for ICP-OES analyses. The effects caused by the presence of a high sodium concentration (as was first confirmed by the yellow colour in the qualitative analysis process) were circumvented by diluting the samples to concentrations under 100 mg/ℓ and using a horizontally oriented torch (Figure 5.2). The presence of high concentrations of sodium in the wastewater was attributed to the use of chemicals such as $NaHCO_3$ and NaCl, which are used to marinate and preserve meat.

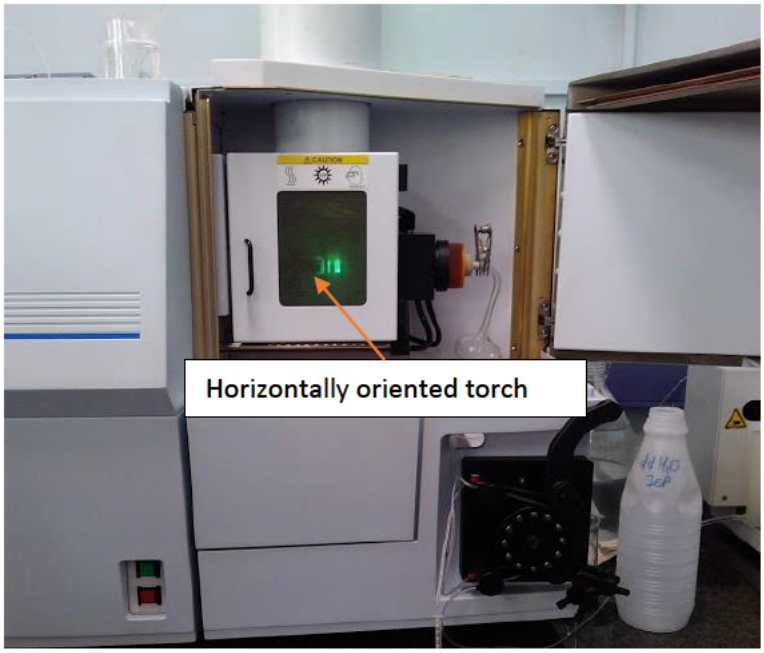

Figure 5.2: Prodigy 7, ICP-OES showing a horizontally oriented torch

Results of other elements in the poultry wastewater revealed low concentrations of As, Co, Mo, Ni, Sb (0.1 mg/ℓ) and Cr, Pb, Sr, Zn (0.2 mg/ℓ). The presence of As, Cr, Ni, Pb and Zn even at trace levels (mg/ℓ) was a matter of concern as these elements have the potential to accumulate in dams or rivers where they cause serious environmental problems. The slightly higher concentration of Fe in the wastewater occurred undoubtedly due to the presence of blood which contains hemoglobin. Iron is an essential component in blood and is used in the production of red blood cells. Other elements such as Mn (0.6 mg/ℓ), Al (1.4 mg/ℓ) and Si (7.5 mg/ℓ) were also present in appreciable concentrations and will inarguably also contribute to water pollution if their presence is not curbed.

5.4.2.2 Red meat samples

Quantitative analyses of the red meat wastewater samples showed the presence of high concentrations of alkali and alkali earth metals such as Ca (193.8 mg/ℓ), Mg (117.8 mg/ℓ), Na (987.3 mg/ℓ), and K (295.8 mg/ℓ). The abundance of the alkali and alkaline earth metals in the wastewater suggested the high usage of chemicals such as NaOH, KOH, $Mg(OH)_2$ and $Ca(ClO)_2$ in the abattoir for disinfection purposes. The presence of these elements in excessive concentrations undoubtedly contributes to the hardening of water which in turn affects aquatic life negatively. It is noteworthy that no apparent sources of Si from the abattoirs could attribute for the high concentrations of Si (130.1 mg/ℓ) found in the red meat wastewater. Silicon often exists as silica (silicon dioxide) and is commonly found in nature as quartz. Its presence in the wastewater could therefore be attributed to dissolved soil particles. The presence of other elements such as As, Co, Cu, Mo, Pb (0.1 mg/ℓ), Cr, Mn (0.2 mg/ℓ) and Sr, Zn (0.3 mg/ℓ) that were detected in lower concentrations was indicative of unsafe and poor abattoir practices that resulted in the indiscriminate disposal of waste in the environment.

5.4.2.3 Comparison of poultry and red meat results

A comparison of the results obtained from the poultry and red meat wastewater samples (Table 5.4) shows that the red meat processing industry contributes more extensively to water pollution compared to the poultry industry. The higher concentration levels of the detected elements disposed of in drains revealed a significant water pollution contribution by both abattoir categories, but more specifically by red meat abattoirs. The Mg and K contents in the red meat waste were approximately three times higher than those in the poultry waste, while the Na content was five times higher in the poultry wastewater samples. The concentrations of Ca were slightly higher in the poultry (259 mg/ℓ) wastewater than in the red meat wastewater samples (194 mg/ℓ). However, it is undeniable that the accumulation of these alkali and alkaline earth metals in the fresh water bodies that they reach consistently increase the alkalinity and hardness of the water.

Table 5.4: Comparison of the concentrations of some of the major elements present in poultry and red meat wastewater

Elements	Concentration (poultry) (mg/ℓ)	Concentration (red meat) (mg/ℓ)
Ca	258.5	193.8
Mg	43.8	117.8
Na	207.7	987.3
K	120.2	295.0
Si	7.5	130.1
Fe	5.7	11.3

5.4.3 *Determination of the elements present in poultry and red meat wastewater using various cross-linked chitosan products*

The objective of this phase of the study was to determine the effectiveness of the synthesized chitosan products in adsorbing heavy metals from the wastewater. The results of the analyses of eluted solutions of poultry and red meat wastewater using different chitosan products (stationery phases) in the chromatographic technique varied among the chitosan products. The presence of alkaline and alkali earth metals (Ca, Mg, Na and K) was predominant in the eluted solutions of all the chitosan products. However, lower percentages of Mg (18%) and K (20%) were recorded compared to the original red meat wastewater samples. Almost half of the concentrations of Ca (43%) and Na (46%) were eluted from the same wastewater solution. The eluted solutions from the poultry wastewater showed low average percentage concentrations of Ca (12%) and Mg (24%) and higher percentages for K (35%) and Na (55%) concentrations. Low retention rates of Mg in poultry (18%) and red meat (24%) were obtained, revealing the efficiency of these products to adsorb the Mg element. Further comparison of the poultry and red meat results showed the lowest concentrations of Mg eluted to be 5 and 12 mg/ℓ respectively (Figure 5.3).

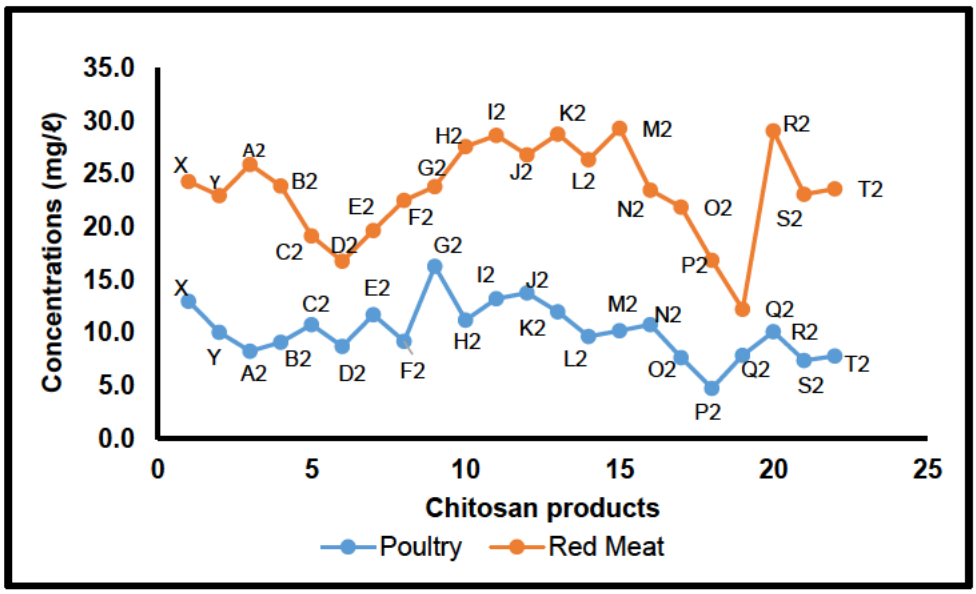

Figure 5.3: Concentrations of magnesium in poultry and red meat wastewater eluted from the columns prepared using different chitosan products

Although good results for magnesium adsorption were recorded using most of the chitosan products, exceptional absorbance levels for Mg, Ca and K were achieved using chitosan shrimp starch that was cross-linked with maleic anhydride (S2), crab chitosan starch that was cross-linked with acrylic acid (H2), and shrimp and crab chitosan starch that was cross-linked with formaldehyde (C2 and D2). Due to the low recovery rates of the alkali and alkaline earth metals, the immediate application of these chitosan products occurs in the separation of these elements in the lithium industry.

The variations in the experimental results and the performance of the shrimp (S2) and crab chitosan starch (T2) products that were cross-linked with maleic anhydride suggests the existence of chemical composition differences between the two products. The differences between these two products were evidenced by the sharp margins between their results; e.g., Ca, K and Mg in S2 using the red meat wastewater recorded 45.1, 37.5 and 12.2 mg/ℓ respectively, against 121.0, 71.9 and 29.1 mg/ℓ respectively using the poultry wastewater. These results revealed the high affinity of the shrimp chitosan cross-linked with maleic anhydride for adsorption. Other chitosan products that demonstrated good adsorption potential for Ca and K from the red meat wastewater included shrimp and crab chitosan starch that was cross-linked with formaldehyde (C2 and D2), shrimp chitosan that was cross-linked with

epichlorohydrine (F2), and crab chitosan starch that was cross-linked with acrylic-acid (H2) (Figures 5.4 and 5.5).

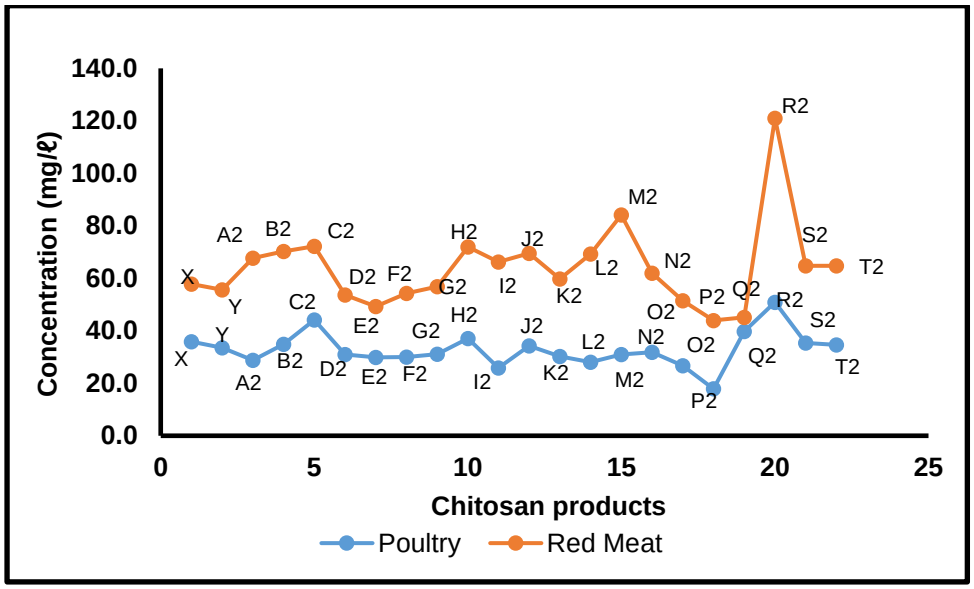

Figure 5.4: Concentrations of calcium in poultry and red meat wastewater eluted from the columns prepared using different chitosan products

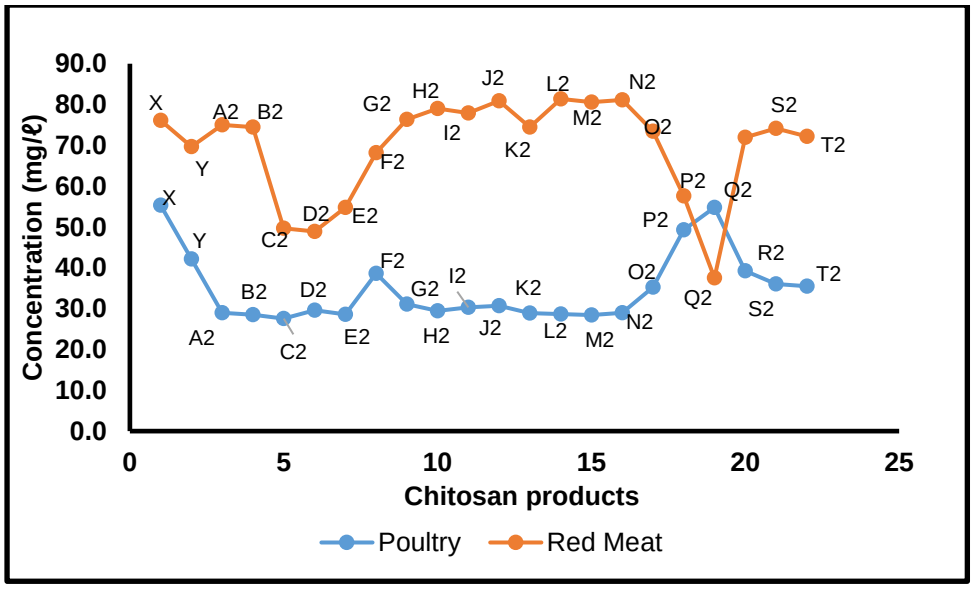

Figure 5.5: Concentrations of potassium in poultry and red meat wastewater eluted from the columns prepared using different chitosan products

The results also showed fluctuating recoveries of the eluted sodium concentrations from the poultry and red meat (control samples) whose initial concentrations were 207.7 and 987.3 mg/ℓ respectively. Low sodium concentrations (30 – 70 mg/ℓ) were eluted from the poultry wastewater using A2, B2, C2, D2, F2, L2, I2, J2, Q2, R2, S2, T2, O2 and P2 chitosan products, and this result indicated good separation or adsorbance potential of sodium from wastewater (Figure 5.6). However, higher sodium concentrations than the initial concentrations (above 207.7 mg/ℓ) were obtained using X, G2 and H2 (218 − 544 mg/ℓ), which might have been due to errors in the measurement (see Section 5.4.2 above). Analysis results of the sodium content in the eluted solutions from the red meat wastewater using the same chitosan products showed a similar trend as the poultry results. Reduced sodium concentrations (120 – 361 mg/ℓ) were obtained using A2, E2, B2, C2, D2, L2, M2, N2, I2, J2, Q2, R2, S2, T2, O2 and P2 chitosan products. However, higher concentrations (440 – 967 mg/ℓ) of sodium were obtained using X, Y, K2, G2 and H2 chitosan products. These results were consistent with the results obtained from the poultry wastewater analyses, which suggests the inability of the X, Y, K2, G2 and H2 chitosan products to effectively adsorb sodium ions. The exceedingly high sodium content (1781 mg/ℓ) reported using F2 might also have occurred as a result of the false high measurement error discussed in Section 5.4.2 above.

The results of the analyses to determine the removal potential of alkali and alkaline earth metals from wastewater using modified chitosan products were generally not encouraging, as it was clear that not all the modified chitosan products were capable of completely removing these elements. However, a few chitosan products were shown to adsorb appreciable quantities of alkali and alkaline earth metals from the wastewater samples, which significantly contributed to the reduction of these elements in the water samples. This finding is encouraging and thus needs further exploration.

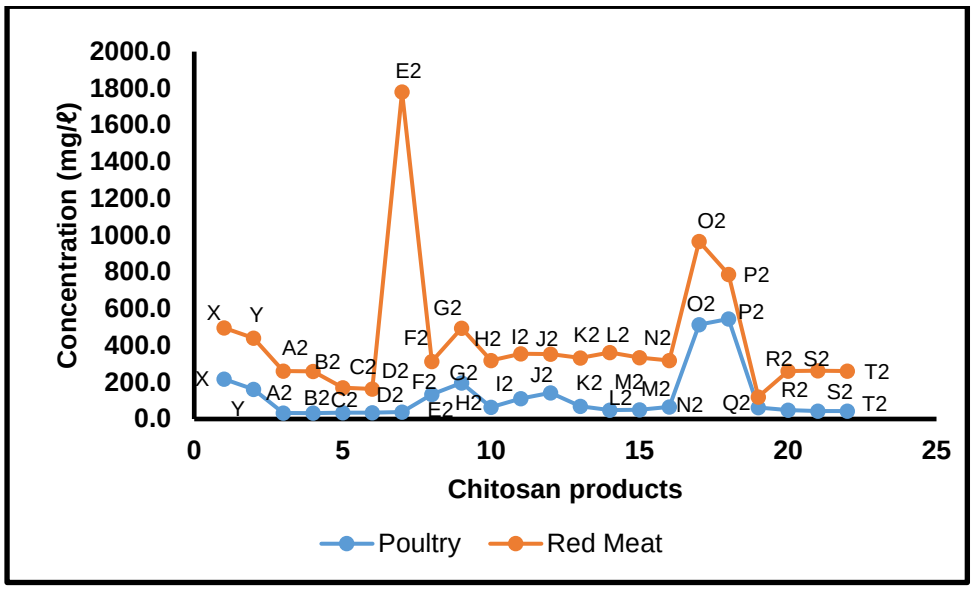

Figure 5.6: Concentrations of sodium in poultry and red meat wastewater eluted from the columns prepared using different chitosan products

5.4.3.1 Analyses of the content of other elements in poultry and red meat wastewater

Quantitative analyses to determine the presence of elements (Cu, Zn, Pb, Ni, Sn, Hg, Cr, As, Al and Cd) in waste water were conducted. As was described in Chapter 2 Section 2.3.1, these elements often cause health issues affecting animal and aquatic life, and their presence was thus assessed in the eluted solutions. Although not very high concentration levels of these elements were detected in the wastewater solutions (control samples), the results indicated the ability of the chitosan products to adsorb these elements. Trace amounts of Fe and Si (less than 0.1 mg/ℓ) and ultra-trace amounts of As, Cd, Cr and Pb were detected in both categories of wastewater samples using the chitosan products. The presence of these metals, even at ultra-trace levels, was enough to signal long-term effects and persistent water pollution. The continual deposition of these elements in rivers, lakes and dams will eventually lead to an intolerable increase in their concentrations (pre-concentration) due to water evaporation.

Concentrations of Si and Fe were detected in appreciable quantities in both poultry (5.7 and 7.5 mg/ℓ) and red meat (11.3 and 130.1 mg/ℓ) respectively. As was mentioned in Section 5.4.1.2, the most probable source of Si was the dissolved particles of the

soil which contains quartz, a major source of silica in nature. Figure 5.7 clearly illustrates that chitosan products C2, D2, F2, S2 and H2 were good adsorbers of Si in both wastewater categories. The results also showed that significant reduction of less than 10.0 mg/ℓ of Si concentrations were obtained in samples eluted using the above chitosan products. Exceptional reduction in Fe concentrations of up 0.14 mg/ℓ in the eluted samples using both categories of wastewater were obtained using H2 and O2 chitosan products (Figure 5.8).

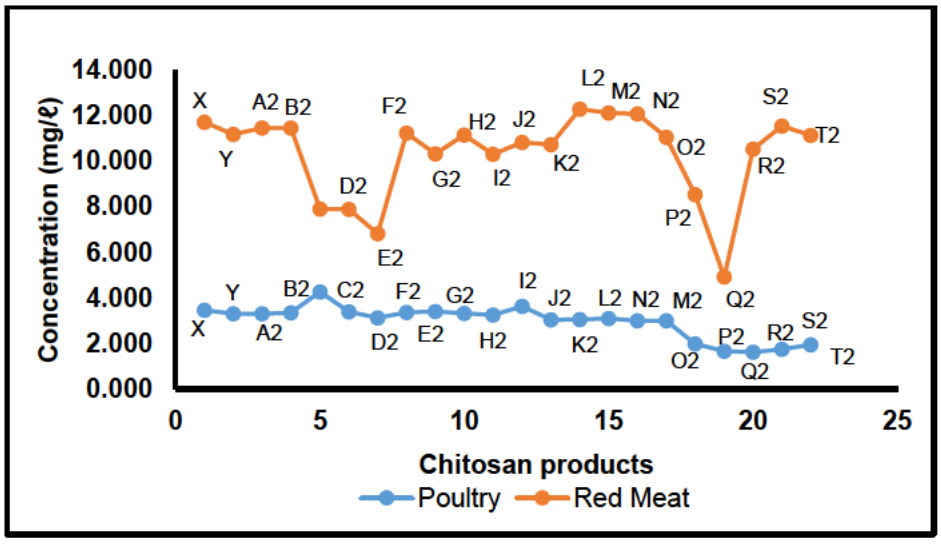

Figure 5.7: Concentrations of silicon in poultry and red meat wastewater eluted from the columns prepared using different chitosan products

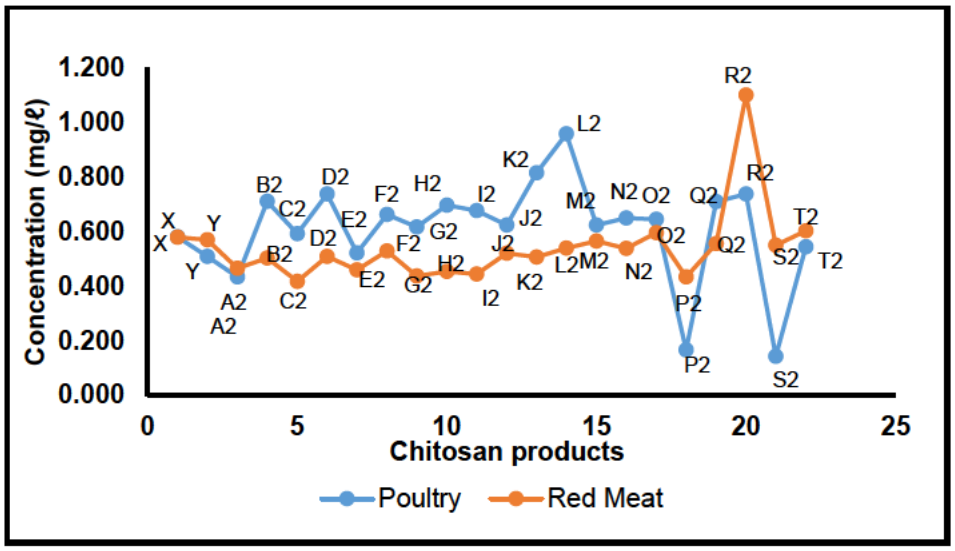

Figure 5.8: Concentrations of iron in poultry and red meat wastewater eluted from the columns prepared using different chitosan products

.

5.4.3.2 Analyses of the eluted solutions for the determination of ultra-trace elements

Analyses of both wastewater categories (poultry and red meat) indicated the presence of ultra-trace amounts of Cr, Ni, Cu and Pb, which are all categorized as heavy metals. Analyses of the original wastewater solutions detected a negligible proportion (0.05 – 0.2 mg/ℓ) of these metals in the effluent. However, the presence of these metals confirmed reports of water pollution due to the presence of heavy metals (Nkansah, and Ansah, 2014). The presence of Cr and Pb is of great concern as these elements have great toxicity potential when released indiscriminately in nature. The effects of chromium in the hexavalent state are most devastating compared to chromium in the trivalent state. However, the analyses using ICP-OES did not distinguish between Cr^{6+} and Cr^{3+} and therefore, because the Cr concentrations were in ultra-trace amounts, the oxidation state of this element was not determined. It is noteworthy that the initial concentration of Cr in both industries' wastewater was almost the same (0.16 – 0.2 mg/ℓ) and, according to the results, E2, N2, R2, S2 and T2 chitosan products were able to retain/adsorb this element (Figure 5.9). Nearly all the Cr was absorbed by the above listed chitosan products which suggests their possible application in adsorbing chromium ions. The chitosan products with the best adsorption potential of Cr, Ni, Cu and Pb were S2 (Cr), H2 (Ni), Y and C2 (Cu) and G2 and N2 (Pb), as shown in Figures 5.9 – 5.12.

Series 1: Poultry wastewater
Series 2: Red meat wastewater

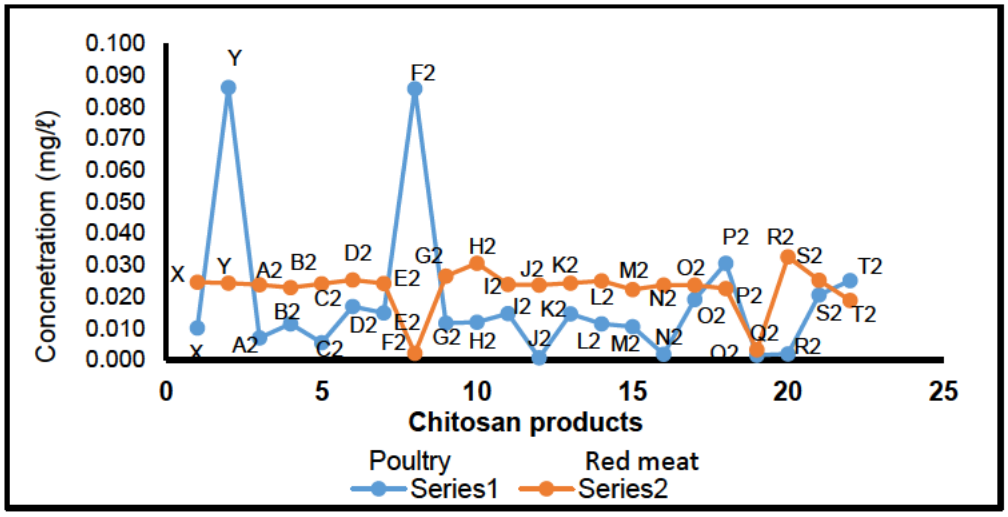

Figure 5.9: Concentrations of chromium in poultry and red meat wastewater eluted from the columns prepared using different chitosan products

Series 1: Poultry wastewater
Series 2: Red meat wastewater

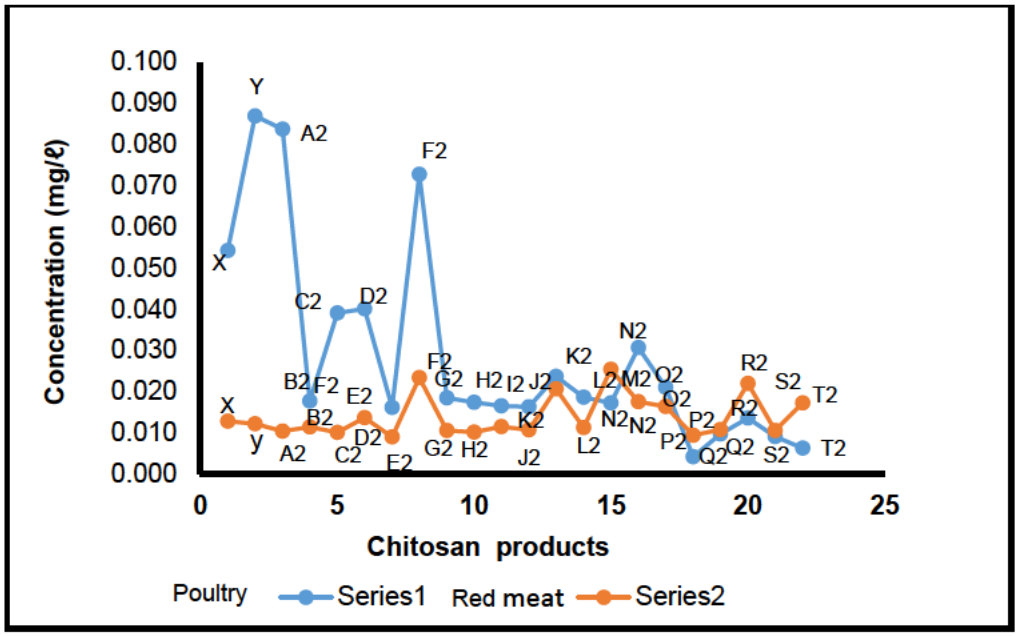

Figure 5.10: Concentrations of nickel in poultry and red meat wastewater eluted from the columns prepared using different chitosan products

Series 1: Poultry wastewater
Series 2: Red meat wastewater

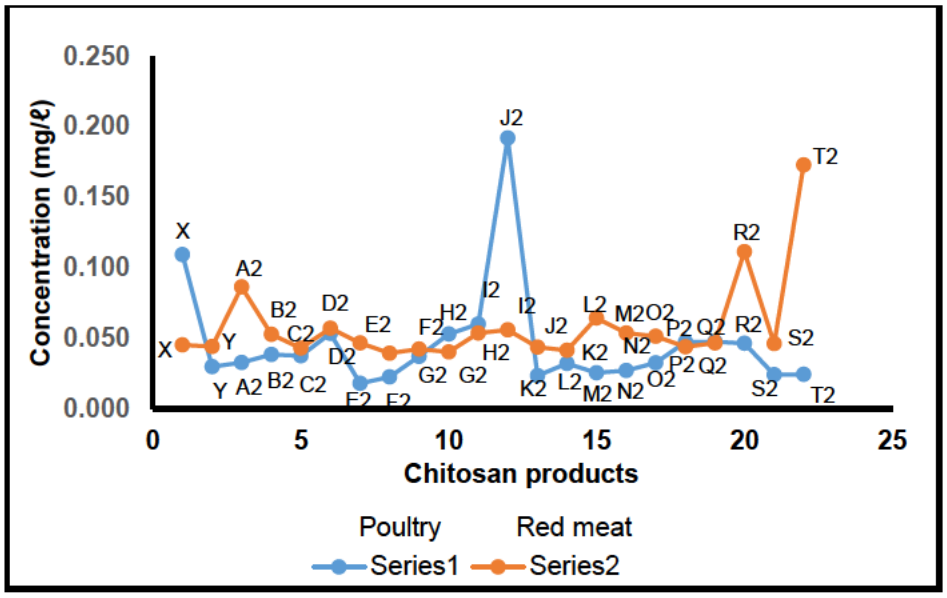

Figure 5.11: Concentrations of copper in poultry and red meat wastewater eluted from the columns prepared using different chitosan products

Series 1: Poultry wastewater
Series 2: Red meat wastewater

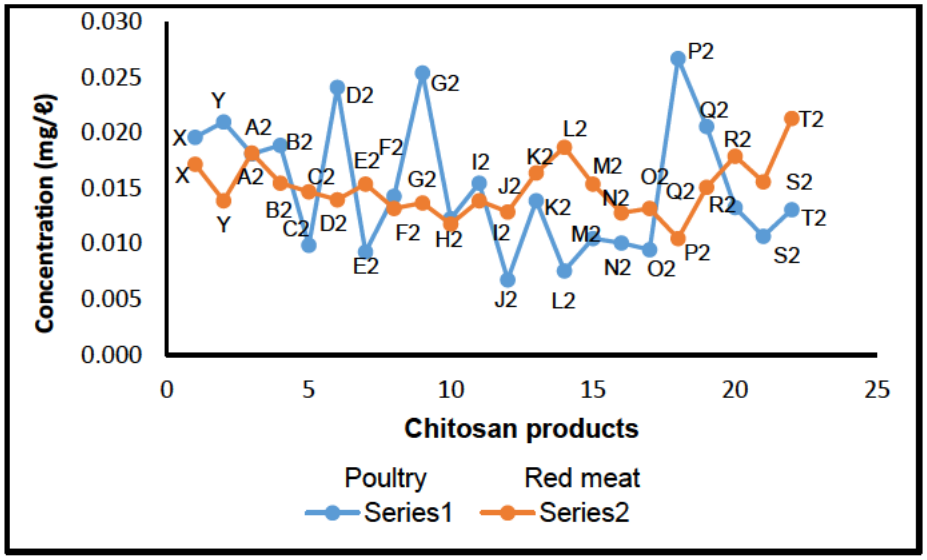

Figure 5.12: Concentrations of lead in poultry and red meat wastewater eluted from the columns prepared using different chitosan products

5.5 Conclusion

Quantitative analyses of poultry and red meat wastewater using ICP-OES revealed the presence of 18 and 16 elements in the sampled wastewater respectively. These elements were present in different concentrations. Alkali and alkaline earth group metals (Ca, Mg, Na and K) were predominantly present in the effluent as waste. Quantitative analyses of these elements required that the samples be diluted to avoid interference. Shrimp chitosan that was cross-linked with maleic anhydride (S2) and shrimp chitosan that was cross-linked with acrylic acid (H2) were found to possess the highest adsorbance potential amongst all the analysed chitosan products. Low concentrations of heavy metals were recovered (0.05 - 0.2 mg/ℓ) for Cr, Ni, Cu and Pb using the prepared chitosan products. Although no complete adsorption of any of the elements was achieved, the results showed a substantial reduction in the quantities of the elements present in the wastewater samples using the chitosan products, and this reduction included heavy metals.

6 EVALUATION OF THE FINDINGS AND RECOMMENDATIONS FOR FUTURE STUDIES

6.1 Introduction

The main purpose of this chapter is to evaluate the outcomes of this study with reference to the objectives.

The aim of the study was to assess the presence of heavy metals in abattoir wastewater and thus optimize and establish alternative methods of purifying wastewater from Bloemfontein abattoirs in the quest to reduce water pollution.

The objectives were to:

- Identify raw materials (domestic waste) such as fish scales (silver and pang), crustacean shells (crab, shrimp and prawn), and mollusc shells (oyster and mussel) for preparation of chitin and chitosan products to be used for wastewater treatment;

- Synthesize a variety of adsorbents from chitins and chitosan biopolymers obtained from fish scales and prawn, shrimp, crab, oyster, and mussel shells that can be used for wastewater purification;

- Characterize these adsorbents using spectroscopy techniques such as solubility tests, viscometer, degree of acetylation, SEM and FTIR spectroscopy; and

- Sample abattoir wastewater and investigate the effectiveness of the modified product(s) in purifying abattoir wastewater/effluent by means of comparative tests using commercially available adsorbents such as chitosan beads, chitins, natural polysaccharides, and Amberlite resins.

This study was successful in achieving the above-mentioned objectives. Different chitosan products were synthesized and cross-linked with various compounds in an attempt to determine the adsorption abilities of these products for use in wastewater purification. The analyses of wastewater samples from poultry and meat abattoirs

detected high concentrations of alkali and alkaline earth metals (Ca, Mg, K and Na) exceeding 100 mg/ℓ in each sample. Other elements that were detected in both wastewater categories were Cr, Ni, Cu and Pb, which have all been reported to be contributing to water pollution. Characterization of the synthesized chitosan products using the FTIR and the SEM was aimed at identifying different functional groups within these compounds that might be active in the adsorption of the elements – particularly heavy metals that could be detected in the wastewater. The results of the investigation using FTIR and SEM analyses showed the presence of amorphous products with different functional groups.

The results clearly revealed a disconcerting high potential for persistent water pollution by effluent from both the poultry and red meat industries. The presence of Cr, Ni, Cu and Pb in the wastewater was enough evidence to reveal the indiscriminate disposal of heavy metals by these meat industries in the environment. It is a matter of grave concern that the ICP-OES analyses revealed the presence of ultra-trace concentrations of Cr, Ni, Cu and Pb in the wastewater. However, the technique did not distinguish between Cr^{3+} and Cr^{6+} (the latter is considered to be toxic to both animals and the environment), and this suggests that future studies should explore the presence of this element in wastewater as a matter of urgency. The products that were derived from shrimp chitosan that was cross-linked with maleic anhydride (S2) and shrimp chitosan that was cross-linked with acrylic acid (G2) (Figure 6.1) were found to yield exceptional results, which rendered these findings encouraging for future application. Using these chitosan products to purify the poultry and red meat wastewater samples, a significant reduction of the alkali and alkali earth metals (Ca, Mg, K and Na) and other elements that are considered as toxic to the environment (Cr, Ni, Cu and Pb) was obtained.

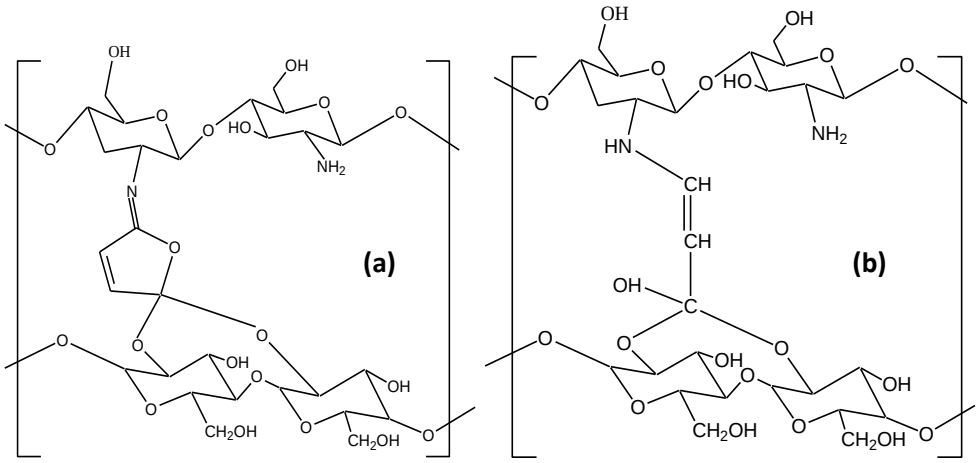

Figure 6.1: (a) Shrimp chitosan cross-linked with maleic anhydride (S2); and (b) shrimp chitosan cross-linked with acrylic acid (G2).

6.2 Recommendations for future studies

The results obtained from the shrimp chitosan that was cross-linked with maleic anhydride (S2) and acrylic acid (G2) and some other chitosan products showed excellent results for alkali and alkali earth metals. The significant differences that were observed between the original samples (wastewater) and the eluted solutions using S2 and G2 suggest that these adsorbents can be used in the separation of alkali and alkaline earth metals in, for example, the lithium industry. These chitosan products can also be applied in the water industry where they can be used for softening water and the removal of for example Ca and Cr in the wastewater of the abattoir industry. However, the exploration of the application of these products is in its infancy and future studies are required to explore the potential of these products on a larger scale.

The detection of heavy metals in the wastewater of the meat industry, albeit in ultra-low concentrations, was a disconcerting finding which suggests that future studies should explore this phenomenon and its eradication in the poultry and red meat industries as a matter of urgency.

REFERENCES

Abdulkarim, A. Y., Isa, M. T. Muhammed, A.J. M., Ameh, A.O.(2013). Extraction and characterisation of chitin and chitosan from mussel shell. Civil and Enviromental Research, 3:2222-2863.

Adeniji, A.O., Okoh, O. O. and Okoh, A. I. (2017). Analytical Methods for the Determination of the Distribution of Total Petroleum Hydrocarbons in the Water and Sediment of Aquatic Systems: A Review, Journal of Chemistry, 13.

Adeyemo, O.K. (2002). Unhygienic operation of a city abattoir in south western Nigeria: environment implication. *AJEAM/RAGEE*, 491:23-28.

Akpor, O.B. & Muchie, M. (2011). Environmental and public health implications of wastewater quality. *African Journal of Biotechnology*, 10:2379-2387.

Aksu, Z. (2005). Application of biosorption for the removal of organic pollutants: a review. *Process Biochem*, 40:997-1026.

Alayash, A.I. (2004). Uncontrolled autoxidation of haemoglobin leads to changes in haem geometry and subsequent degradation. *Nature Reviews Drug Discovery*, 3:152-159.

Ali, I., Asim, M., & Khan, T.A. (2012). Low cost adsorbents for the removal of organic pollutants from wastewater. *Journal of Environmental Management*, 113, 170-183.

Al-Qahtani, K.M.A. (2017). Extraction of heavy metals from contaminated, water using chelating agents. *Oriental Journal of Chemistry*, 33:1698-1704.

Álvarez-Ayuso, E., García-Sánchez, A., & Querol, X. (2003). Purification of metal electroplating wastewater using zeolites. *Water Research,* 37:4855-4862.

Aniebo, A.O., Wekhe, S.N., & Okoli, I.C. (2009). Abattoir blood waste generation in Rivers State and its environmental implications in the Niger Delta. *Toxicology Environmental Chemistry*, 91:619-625.

Anthony, R.G., & Kozlowski, R. (1982). Heavy metals in tissues of small mammals inhabiting wastewater-irrigated habitats. *Journal of Environmental Quality,* 11:20-22.

Arora, M., Eddy, N.K., Mumford, K.A., Baba, Y., Pereira, J.M., & Stevens, G.W. (2010). Surface modification of natural zeolite by chitosan and its use for nitrate removal in cold regions. *Cold Regions Science and Technology*, 62:92-97.

Attla, A.A., Girgis, B.S., & Fathy, N.A. (2008). Removal of methylene blue by carbons derived from peach stones by H_3PO_4 activation: batch and column studies. *Dye Pigments*, 76:282-289.

Aziz, H.A., Adlan, M.N., & Ariffin, K.S. (2008). Heavy metals (Cd, Pb, Zn, Ni, Cu and Cr [III]) removal from water in Malaysia: post treatment by high quality limestone. *Bioresource Technology*, 99:1578-1583.

Ayandiran T, P.A., & Hutchings, G.P. (1987). Chitosan, a natural, cationic biopolymer: commercial applications. In: M. Yalpani (Ed.). *Industrial polysaccharides: genetic engineering, structure/property relations and applications*. Elsevier, Amsterdam, 363–376.

Badawy, M.I., Gohary, F.El., Ghaly, M.Y., Ali, M.E.M. (2009) Enhancement of olive mill wastewater biodegradation by homogeneous and heterogeneous photocatalytic oxidation, *Journal of Hazardous Materials* 169: 673-679.

Li, N., Bai, R.B. (2006) Highly enhanced adsorption of lead ions on chitosan granules Functionalized with Poly(acrylic acid). *Industrial & Engineering Chemistry Research,* 45 (23): 7897 – 7904.

Badmus, K.O. Tijani, J. O. Massima, E. and Petrik, L. (2018). Treatment of persistent organic pollutants in wastewater using hydrodynamic cavitation in synergy with advanced oxidation process. Environmental Science and Pollution Research 25(7): 299–7314.

Benotti, M.J., Trenholm, B.A., Vanderford, B.J., Holady, J. C., Stanford, B.D., & Snyder, S.A. (2009). Pharmaceuticals and endocrine disrupting compounds in U.S. drinking water.*Journal of Environnemental Science and Technology*. 43, 597-603.

Brenner, I.B.; Zander, A.; Cole, M.; & Wiseman, A.J. (1997). Anal. At. *Spectrom*., 12, 897.

Brine, C.J. and Austin, P.R. (1981). Chitin variability with species and method of preparation. *Comparative Biochemistry and Physiology*. 69B: 283286 (1981).

Brostow, W., HaggLobland, H.E., Pal, S., & Singh, R.P. (2009). Polymeric flocculants for wastewater and industrial effluent treatment. *J. Mater Educ*. 31, 157-166.

Carro, Leticia, Barriada, J. L. Herrero, R. Sastre de Vicente,M. E. (2015). Interaction of heavy metals with Ca-pretreated Sargassum muticum algal biomass: Characterization as a cation exchange process. *Chemical Engineering Journal*, 264, 15 181-187

Carmen, Z., & Daniela, S. (2012). Textile organic dyes – characteristics: polluting effects and separation/elimination procedures from industrial effluents. *A critical overview*. 55-86.

Charerntanyarak, l. (1999). Heavy metal removal by chemical coagulation and precipitation. *Water Science and Technology*, 39:135-138.

Chen, A., Yang, C., Chen, C., & Chen, C.W. (2009). The chemically crosslinked metal-complexed chitosan for comparative adsorptions of Cu(II), Zn(II), Ni(II) and Pb(II) ions in [an] aqueous medium. *Journal of Hazardous Materials*, 163:1068-1075.

Chen, R.H. (1998). Manipulation and application of chain flexibility of chitosan. In: R.H. Chen, & H.C. Chen (Eds.). *Advances in Chitin Science Vol. III*: 39-46. Department of Food Science, National Taiwan Ocean University, Keelung, Taiwan, ROC.

Chukwu, O., Adeoye, P.A., & Chidiebere, I. (2011). Abattoir waste generation, management and the environment: a case of Minna, North Central Nigeria. *Int. J. Biosci*, 1(6):100-109.

Corin, N., Backlund, P., & Wiklund, T. (1998). Bacterial growth in humic waters exposed to UV-radiation and simulated sunlight. *Chemosphere*, 36:1947-1958.

Coleman, A. (2015). *Farmer's weekly magazine*, Free State Drought officially declared Thursday, September 10.

Crini, G. (2005). Recent developments in polysaccharide-based materials used as adsorbents in wastewater treatment. *Progress in Polymer Science*, 30:38-70.

Crini, G., & Badot, P.M. (2008). Application of chitosan, a natural Aminopolysaccharide for dye removal from aqueous solutions by adsorption processes using batch studies: a review of recent literature. *Progress in Polymer Science*, 33:399-447.

Cunningham, W.P., & Siago, B.W. (2001). Textile effluent impact persistent color to the receiving streams and interfere with photosynthesis of the phytoplankton. *Environmental Science Global Concern*. New York: Mc Graw Hill, 267-269.

Czechowska-Biskup, R., Jarosińska, D., Rokita, B., Ulański, P., & Rosiak, J.M. (2012). Determination of degree of deacetylation of chitosan-comparision of methods. *Progress on Chemistry and Application of Chitin and its derivatives* Volume XVII, 5-20.

Department of Water Affairs (DWA). (2011). WS/WR policies and strategies. Water Sector Policy Database. Available at: http://www.dwa.gov.za/dir_ws/waterpolicy (Accessed January 2011).

Devi, N., Sarmah, M., Khatun, B., & Maji, T.K. (2016). Encapsulation of active ingredients in polysaccharide–protein complex coacervates. *Advances in Colloid and Interface Science*, 293:136-145.

Domard, A., & Rinaudo, M. (1983). Preparation and characterization of fully deacetylated chitosan. *International Journal of Biological Macromolecules*, 5:49-52.

Dupare, D.B. (2015). Detection of heavy metal ions from water using conventional chelating agents (citric acid and EDTA) in and around Murtizapur Region. *International Journal of Chemical and Physical Sciences*, 4:30-37.

Esterhuizen, L.L. (2012*). A study of the South African tomato curly stunt virus patho-system: epidemiology, molecular diversity and resistance*. ETDs dissertation, University of Johannesburg.

Fenglian, F., & Wang, Q. (2011). Removal of heavy metal ions from wastewaters: a review. *Journal of Environmental Management,* 92:407-418.

Galadima, A., & Garba, Z.N. (2012). Heavy metals pollution in Nigeria: causes and consequences. *Pollution*, 45:7919-7922.

Gardea-Torresdey, J.L., Gonzalez, J.H., Tiemann, K.J., Rodriguez, O., & Gamez, G. (1998). Phytofiltration of hazardous cadmium, chromium, lead and zinc ions by biomass of medicago sativa (alfalfa). *Journal of Hazardous Materials*, 57:29-39.s

Otto, F. and Wolski, P. Global warming raised the risk of more severe droughts in Cape Town.https://www.moneyweb.co.za/news/south-africa/global-warming-raised-the-risk-of-more-severe-droughts-in-cape-town/, 2018.

Gauri, S.M. (2006). Treatment of wastewater from abattoirs before land application: a review *Bioresource Technology* 97, 1119-1135. Available at: http://www .filconfilters. co.za/blog/wastewater-treatment-in-south-Africa.

Giles, C.H., Hassan, A.S.A., Laidlaw, M., & Subramanian, R.V.R. (1958). Some observations on the constitution of chitin and on its adsorption of inorganic and organic acids from aqueous solutions. *Journal of the Society of Dyers and Colourists*, 74:846.

Gongwala, J., Djepang, S. A., Abba, P., Payom, G., Laminsi, S., Njopwouo, D. (2014). Treatment of Wastewater from a Slaughterhouse by Gliding Arc Humid Air Plasma: Chlorophyll Degradation. *International Journal of Environmental Protection and Policy*, 2:118-125.

Grozes, G., White, P. and Marshall, M. (1995). Enhanced coagulation: Its effect on NOM removal andchemical costs. *Journal American Water Works Association*, *87*:78-89.

Guala, S.D., Vega, F.A., & Covelo, E.F. (2010). The dynamics of heavy metals in plant-soil interactions. *Ecological Modelling*, 221:1148-1152.

Inoue, K. Baba, Y, Zeng, X., & Ruckenstein, E. (1993). 66W Weight of swollen beads (g) s. *Journal of Membrane Science*. Bulletin of the Chemical Society Japan, 2915.

Irshad, A. (2013). Treatment of abattoir effluents. *Indian Veterinary Research Institute*, 1-42.

Jabbar, A.Z., Hadi, A.G., & Sami, F. (2014). Removal of azo dye from aqueous solutions using chitosan. *Oriental Journal of Chemistry*, 30:571-575.

Järup, L. (2003). Hazards of heavy metal contamination. *British Medical Bulletin*, 68:167-182.

Kamble, S.P., Jagtap, S., Labhsetwar, N.K., Thakare, D., Godfrey, S., Devotta, S., & Rayalu, S. S. (2007). Defluoridation of drinking water using chitin, chitosan and lanthanum-modified chitosan". *Journal of Chemical Engineering,* 129: 173-180.

Kiepper, B. (2001). A survey of waste-water treatment practices in the broiler industry. The University of Georgia. Engineering Outreach Program, Driftmier Engineering Centre, Athens, Georgia.

Khan, A., Khan, S., Muhammad Amjad Khan, A., Qamar, Z., & Waqas, M. (2015). The uptake and bioaccumulation of heavy metals by food plants, their effects on plants nutrients, and associated health risk: a review. *Environmental Science and Pollution Research*, 22:13772-13799.

Khansari, F.E, Ghazi-Khansari, M., & Abdollahi, M. (2005). Heavy metals content of canned tuna fish. *Food Chemistry*, 93:293-296.

Knorr, D. (1984). Use of chitinous polymers in food: a challenge for food research and development. *Food Technol* 38(1):85–97.

Lee, I.H, Kuan, Yu-Chung and Chern, Jia-Ming (2007). Equilibrium and Kinetics of Heavy Metal Ion Exchange. *Journal of the Chinese Institute of Chemical Engineers* 38(1):71-84

Lower, S. (2007). Hard water and water softening. Available at: https://en. wikipedia.org/wiki/Water-softening#Methods (Accessed on 2007-10-08).

Lvovich, M.I. (1979). World water resources and their future (Translation by the American Geophysical Union). Chelsea: LithoCrafters Inc.

Massé, D.I., & Massé, L. (2000). Treatment of slaughterhouse wastewater in anaerobic sequencing batch reactors. *Can. Agric. Eng*. 42 (3), 131–137.

Mirbagheri, S.A., & Hosseini, S.N. (2004). Pilot plant investigation on petrochemical wastewater treatment for the removal of copper and chromium with the objective of reuse. *Desalination,* 171-193.

Mohamed, S.H., El-Gendy, A.A., Abdel-Kader, A.H., & El-Ashkar, E.A. (2015). Removal of heavy metals from water by adsorption on chitin derivatives. *Der Pharma Chemica*, 7:275:283.

Moorjani, M.N., Achutha, V., & Khasim, D.I. (1975). Parameters affecting the viscosity of chitosan from prawn waste. *J. Food Sci. Technol*. 12:187-189.

Mouzdahir, E.I.Y., Elmchaouri, A., Moahboub, A., Gil, R.A., & Korili, S.A. (2010). Equilibrium modelling for the adsorption of methylene blue from aqueous solution on activated clays minerals. *Desalination*, 250:335-338.

Muzzarelli, R.A.A. (1973). *Natural chelating polymers*. New York: Pergamon Press.

Muzzarelli, R.A.A. (1977). Human enzymatic activities related to the therapeutic administration of chitin derivatives. *Cell. Mol. Life Sci*., 53:131-140.

Muzzarelli, R.A.A, Tanfani, F., Emanuelli, M., & Bolognini, L. (1985). Aspartate glucan, glycine glucan, and serine glucan for the removal of cobalt and copper from solutions and brines. *Biotechnology and Bio-engineering*, 27:1115-1121.

Nada, A.M.A., El-Wakeal, N., Hassan, M.L., & Adel, A. (2006). Differential Adsorption of heavy metal ions by cotton stalk cation-exchangers containing multiple functional groups. *Journal of Applied Polymer Science*, 101:4124-4132.

Nkansah, M.A., & Ansah, J.K. (2014). Determination of Cd, Hg, As, Cr and Pb levels in meat from the Kumasi Central Abattoir. *International Journal of Scientific and Research Publications*, 4:1-4.

No, H.K., & Meyers, S.P. (1989). Recovery of amino acids from seafood processing wastewater with a dual chitosan-based ligand-exchange system. *J. Food Sci.* 54(1):60–62, 70.

No, H. K., Lee, K. S., & Meyers, S. P. (2000). Correlation between physicochemical Characteristics and binding capacities of chitosan products. *Journal of Food Science*, 65: 1134-1137.

Nolan, K.R. (1983). Copper toxicity syndrome. *Journal of Orthomolecular Psychiatry*, 12:270-282.

Oehmen, A., Viegas, R. Velizarov, S. Reis, MAM Crespo, J.G (2006). Removal of heavy metals from drinking water supplies through the ion exchange membrane bioreactor. *Desalination* 199 (1-3), 405-407.

Okegye, J.I., & Gajere J.N. (2015). Assessment of heavy metal contamination in surface and ground water resources around Udege Mbeki mining district, North-Central Nigeria. *Journal of Geology and Geophysics*, 4:1-7.

Owuli, M.A. (2003). Assessment of impact of sewage effluents on coastal water quality in Hafnarfjordur, Iceland. United Nations Fishery Training Program Final Report.

Pagga, U., & Brown, D. (1986). The degradation of dye stiffs Part II: behaviour of dyestuffs in aerobic biodegradation tests. *Chemosphere*, 15:479-491.

Peniston, Q.P, & Johnson, E.L. (1970). Method for treating an aqueous medium with chitosan and derivatives of chitin to remove an impurity. U.S. patent 3,533, 940.

Petracci, M., Laghi, L., Rocculi, P., Rimini, S., Panarese, V., Cremonini, M.A., & Cavani, C. (2012). The use of sodium bicarbonate for marination of broiler breast meat. *Poultry Science*, 91(2):526 – 534.

Rinaudo, M. (2014). Materials based on chitin and chitosan. In: S. Kabasci (Ed.). *Bio-based plastics*, 63-80. Chichester: Wiley.

Rio, S., & Delebarre A. (2003). Removal of mercury in aqueous solution by fluidized bed plant fly ash. *Fuel*, 82:153–9.

Saikia, S.K., Gupta, R., Pant, A., & Rakesh Pandey, R. (2014). Genetic revelation of hexavalent chromium toxicity using Caenorhabditis elegans as a biosensor. *Journal of Exposure Science and Environmental Epidemiology*, 24:180-184.

Salem, H.M., Eweida, E.A., & Farag, A. (2000), Heavy metals in drinking water and their environmental impact on human health. *The Institution of Chemical Engineers*, 542-556.

Sapari, N., Idris, A., & Hamid, N.H.A. (1996). Total removal of heavy metal from mixed plating rinse wastewater. *Desalination,* 106:419-422.

Senn, T.L., & Kingman, A.R.A. (1973). Review of humus and humic acids. *Research Series No. 145.* South Carolina, Clemson: Agricultural Experiment Station.

Shaidan, N.H., Eldemerdash, U., & Awad, S. (2012). Removal of Ni(II) ions from aqueous solutions using a fixed-bed ion exchange column technique. *Journal of the Taiwan Institute of Chemical Engineers*, 43:40-45.

Singh, R.P., Karmakar, G.P., Rath, S.K., Pandey, S.R., Tripathy, T., Panda, J., Kanan, K., Jain, S.K., & Lan, N.T. (2000). Novel biodegradable flocculants based on polysaccharides. *Current Science,* 78:798–803.

Steffen, Robertson, & Kirsten (1989). *Inc Consulting engineers, Water Research Commission (WRC) Project No. 145, 41/89*. Pretoria: WRC, December.

Stevenson, F.J. (1994). *Humus chemistry: genesis, composition, reactions*. 2nd ed. New York: Wiley.

Sun, B., Zhao, F.J., Lombi, E., & McGrath, S.P. (2001). Leaching of heavy metals from contaminated soils using EDTA. *Environmental Pollution*, 113:111-120.

Suponik, T. (2010). Ensuring permeable reactive barrier efficacy and longevity. *Archives of Environmental Protection*, 36:60-73.

Tang, W.J., Fernandez, J.G., Sohn, J.J., & Amemiya, C.T. (2015). Chitin is endogenously produced in vertebrates. *Current Biology***,** 25:897-900.

Thakare, Y.N and Jane, A.K. (2015). Performance of high density ion exchange resin (INDION225H) for removal of Cu(II) from waste water, J*ournal of Environmental Chemical Engineering* 3:1393-1398.

Terbojevidh, M. and Cosani, A. (1997). Molecular weight determination of chitin and chitosan. In Chitin Handbook (Muzzarelli, R. A. A. & Peter, M. G., eds). *European Chitin Society*, 87–101

Tokura, S., & Nishi, N. (1995). Specification and characterization of chitin and chitosan. In: M.B. Zakaria, W.M.W. Muda, & M.P. Abdullah (Eds.). *Chitin and chitosan: the versatile environmentally friendly modern materials*, 68-86. Bangi, Malaysia: University Kebangsaan.

Ubwa, S.T., Abah Ada, C.A., & Alechenu, E. (2013). Levels of some heavy metal contamination of street dust in the industrial and high traffic density areas of Jos Metropolis. *Journal of Biodiversity and Environmental Sciences*, 3:13-21.

United States Environmental Protection Agency. (2005). *Guidelines for carcinogen risk assessment.* Washington: Risk Assessment Forum, USEPA, DC.EPA/630/P-03/001F.

Urbariczyk, G.B., Lipp-Symonowicz, B., Jeziorny, A., Doran, K., Wrzosek, K., Urbaniak-Domagala, H., & Kowalska, W.S. (1997). Progress on chemistry and application of chitin and its derivatives. *Biomaterials,* 3:186-187.

Van der Oost, R., Beyer, J., & Vermeulen, P.E. (2003). Fish bioaccumulation and biomarkers in environmental risk assessment: a review*. Environmental. Toxicology Pharmacology,* 13:57-149.

Van Vuuren, A.J., Jordan, H., Van Der Walt, E., & Van Jaarsveld, S. (2003). Olifants Water Management Area: water resources situation assessment. *Report No. P/04000/00/0101*. Pretoria: Department of Water Affairs and Forestry.

Van Zyl, A.P. (1995). Manual for the abattoir industry. Red Meat Abattoir Association. Pretoria: Sentraaldruk, 31.

Verheijen, L.A.H.M., Wiersema, D.L.W., & Hulshoff Pol, L.W. (1996). Management of waste from animal product processing. In: J. De Wit. Wageningen, The Netherlands: International Agriculture Centre.

Vijayaraghavan, J., Basha, S.S.J., & Jegan, J. (2013). A review on efficacious methods to decolorize reactive azo dye. *Journal of Urban and Environmental Engineering*, 7:30-47.

Wang, S., & Shi, X. (2001). Molecular mechanisms of metal toxicity and carcinogenesis. *Molecular Cell Biochemistry*, 222:3–9.

Wang, W. Bo, S.Q., Li, S.Q., Qin, W. (1991) .International *Journal of Biological Macromolecules*, 13 (1991) 281-285.

Yoshida, H., Okamoto, A., Kataoka, T. (1993). Adsorption of acid dye on cross-linked chitosan fibers: equilibria. *Chemical engineering and Science Journal*, 48: 2267-2272.

Zewail, T.M, Yousef, N.S.(2015) Kinetic study of heavy metal ions removal by ion exchange in batch conical air spouted bed, *Alexandria Engineering Journal* 54 (1), 83-90.

Zvezdova, D. (2010). Synthesis and characterization of chitosan from marine sources in the Black Sea. *Scientific Work of the Russian University*, 49:65-69.

APPENDIX A

Abbreviation list of red meat wastewater samples

RM X and RM Y - shrimp and crab chitosan bead

RM A-2 and PB-2 - shrimp and crab chitosan starch cross-linked with glutaraldehyde

RM C-2 and RM D-2 - shrimp and crab chitosan starch cross-linked with formaldehyde

RM E-2 and RM F-2 - shrimp and crab chitosan starch cross-linked with epichlorohydrine

RM G-2 and RM H-2- shrimp and crab chitosan starch cross-linked with acrylic acid

RM H-2 and RM J-2 - shrimp and crab chitosan starch cross-linked with 1-vinyl-2-pyrrolidone

RM K-2 and RM L-2 - shrimp and crab chitosan starch cross-linked with poly-ethylene diglycider ether

RM M-2 and RM N-2 - shrimp and chitosan starch cross-linked with s-methylbutylamine

RM O-2 and RM P-2 - shrimp and crab chitosan starch cross-linked with benzoquinone

RM Q-2 and RM R-2 - shrimp and crab chitosan starch cross-linked with 1,3 dichloroacetone

RM S-2 and RM T-2 – shrimp and crab chitosan starch cross-linked with maleic anhydride

APPENDIX B

Quantitative analysis and detection limits results of the elements found in the poultry wastewater using ICP-OES
Quantitative analysis Results using ICP-OES

Red meat samples	Elements detected on ICP-OES, concentration (mg/ℓ)

Elements	Ca	Mg	Na	K	Al	As	Cd	Co	Cr	Cu	Fe	Mn	Mo	Ni	Pb	Sb	Si	Sr	Zn
Control	193,8	117,8	987,3	295,8	0,595	0.080	0.012	0.080	0,159	0,125	11,301	0,274	0,088	0,048	0,086	0,004	130,125	0,317	0,272
RM X-2	57,8	24,3	496,9	76,1	0,095	0.020	0.003	0.020	0,025	0,045	0,579	0,091	0,005	0,013	0,017	0,008	11,729	0,297	0,097
RM Y-2	55,7	23,0	440,3	69,7	0,106	0.020	0.003	0.020	0,024	0,044	0,570	0,096	0,005	0,012	0,014	0,014	11,186	0,290	0,059
RM A-2	70,2	23,9	258,6	74,4	0,133	0.020	0.003	0.020	0,023	0,053	0,503	0,071	0,006	0,011	0,016	0,012	11,470	0,344	0,114
RM B-2	67,6	25,9	261,6	75,1	0,143	0.020	0.003	0.020	0,024	0,086	0,465	0,089	0,015	0,010	0,018	0,004	11,469	0,362	0,131
RM C-2	53,7	16,8	164,2	48,9	0,174	0.020	0.003	0,024	0,025	0,057	0,509	0,088	0,005	0,014	0,014	0,014	7,905	0,262	0,130
RM D-2	72,1	19,2	170,5	49,7	0,119	0.020	0.003	0.020	0,024	0,043	0,418	0,095	0,004	0,010	0,015	0,015	7,911	0,273	0,134
RM E-2	54,3	22,5	313,3	68,2	0,077	0.020	0.003	0.020	0,002	0,039	0,529	0,109	0,005	0,023	0,013	0,010	11,250	0,310	0,071
RM F-2	49,3	19,7	1780,8	54,8	0,150	0.020	0.003	0.020	0,024	0,047	0,459	0,064	0,005	0,009	0,015	0,009	6,834	0,176	0,099
RM G-2	44,0	16,9	787,5	57,6	0,085	0.020	0.003	0.020	0,023	0,044	0,434	0,077	0,004	0,009	0,011	0,012	8,543	0,221	0,054
RM H-2	51,5	21,9	966,9	73,4	0,084	0.020	0.003	0.020	0,024	0,051	0,596	0,104	0,006	0,016	0,013	0,013	11,067	0,285	0,069
RM-I-2	69,3	26,4	361,6	81,4	0,099	0.020	0.003	0.020	0,025	0,041	0,540	0,104	0,004	0,011	0,019	0,015	12,303	0,359	0,082
RM J-2	59,8	28,8	332,3	74,5	0,096	0.020	0.003	0.020	0,024	0,044	0,507	0,061	0,005	0,021	0,016	0,012	10,740	0,282	0,108
RM K-2	71,9	27,6	318,5	79,0	0,080	0.020	0.003	0.020	0,031	0,040	0,454	0,084	0,004	0,010	0,012	0,011	11,157	0,339	0,096
RM L-2	56,9	23,8	495,0	76,4	0,076	0.020	0.003	0.020	0,027	0,042	0,438	0,041	0,004	0,011	0,014	0,018	10,328	0,258	0,095
RM M-2	69,5	26,8	352,9	80,9	0,099	0.020	0.003	0.020	0,024	0,056	0,520	0,076	0,005	0,011	0,013	0,015	10,836	0,362	0,124
RM N-2	66,2	28,7	355,7	77,9	0,089	0.020	0.003	0.020	0,024	0,054	0,444	0,058	0,004	0,012	0,014	0,012	10,313	0,322	0,094
RM O-2	64,8	23,6	260,7	72,2	0,156	0.020	0.003	0.020	0,019	0,173	0,603	0,121	0,005	0,017	0,021	0,015	11,146	0,330	0,115
RM P-2	64,7	23,1	263,2	74,2	0,108	0.020	0.003	0.020	0,025	0,046	0,551	0,102	0,005	0,011	0,016	0,018	11,554	0,330	0,092
RM Q-2	61,9	23,5	318,1	81,1	0,079	0,022	0.003	0.020	0,024	0,054	0,539	0,072	0,006	0,018	0,013	0,017	12,095	0,336	0,080
RM R-2	84,1	29,3	335,1	80,6	0,192	0.020	0.003	0.020	0,022	0,064	0,566	0,113	0,016	0,025	0,015	0,015	12,131	0,376	0,114
RM S-2	121,0	29,1	260,3	71,9	0,277	0.020	0.003	0.020	0,033	0,111	1,100	0,158	0,006	0,022	0,018	0,011	10,544	0,428	0,331
RM T-2	45,1	12,2	120,6	37,5	0,131	0.020	0.003	0.020	0,003	0,047	0,555	0,077	0,005	0,011	0,015	0,014	4,926	0,193	0,109

APPENDIX C

Elements below the detection limits of ICP-OES

As	Cd	Cr	Co	Sb	Se
189.042	214.441	-0.62	228.615	217.581	196.090
<0.080	<0.012	-0,010	<0.080	0,030	-0,106
<0.080	<0.012	0,086	<0.080	0,018	0,017
0,008	<0.003	-0,007	<0.020	0,007	<0.020
<0.020	<0.003	-0,011	<0.020	0,007	<0.020
<0.020	0,099	-0,005	<0.020	0,002	<0.020
<0.020	0,030	-0,017	<0.020	-0,005	<0.020
<0.020	<0.003	-0,015	<0.020	0,008	<0.020
<0.020	<0.003	0,086	<0.020	-0,001	<0.020
<0.020	<0.003	-0,012	0,048	0,008	<0.020
<0.020	<0.003	-0,012	<0.020	0,005	<0.020
<0.020	<0.003	-0,015	<0.020	0,001	<0.020
<0.020	<0.003	-0,001	<0.020	0,000	<0.020
<0.020	<0.003	-0,015	<0.020	0,003	<0.020
<0.020	<0.003	-0,011	<0.020	0,003	<0.020
<0.020	<0.003	-0,010	<0.020	0,002	<0.020
<0.020	<0.003	-0,002	<0.020	0,002	<0.020
<0.020	<0.003	-0,019	<0.020	0,003	<0.020
<0.020	<0.003	-0,031	<0.020	0,002	<0.020
<0.020	<0.003	-0,001	<0.020	-0,002	<0.020
<0.020	<0.003	0,002	<0.020	0,001	<0.020
<0.020	0,003	-0,021	<0.020	0,012	<0.020
<0.020	<0.003	-0,025	<0.020	0,011	<0.020
<0.020	<0.003		<0.020	0,012	<0.020
<0.020	<0.003		<0.020	0,007	<0.020
<0.020	<0.003		<0.020	0,008	<0.020

B

APPENDIX D

Abbreviation list of Poultry wastewater samples

P X and Y - shrimp and crab chitosan bead

P A-2 and P B-2 - shrimp and crab chitosan starch cross-linked with glutaraldehyde

P C-2 and P D-2 - shrimp and crab chitosan starch cross-linked with formaldehyde

P E-2 and P F-2 - shrimp and crab chitosan starch cross-linked with epichlorohydrine

P G-2 and P H-2- shrimp and crab chitosan starch cross-linked with acrylic acid

P H-2 and P-2 - shrimp and crab chitosan starch cross-linked with 1-vinyl-2-pyrrolidone

P K-2 and P L-2 - shrimp and crab chitosan starch cross-linked with poly-ethylene diglycider ether

P M-2 and P N-2- shrimp and crab chitosan starch cross-linked with s-methylbutylamine

P O-2 and P P-2 - shrimp and crab chitosan starch cross-linked with benzoquinone

P Q-2 and P R-2 - shrimpn and crab chitosan starch cross-linked with 1,3 dichloroacetone

P S-2 and P T-2 - shrimp and crab chitosan starch cross-linked with maleic anhydride

Quantitative analysis and detection limits results of the elements found in the poultry wastewater using ICP-OES

Quantitative analysis Results using ICP-OES

Poultry samples	Elements detected on ICP-OES, concentration (mg/ℓ)

Raw labels	Ca	Mg	Na	K	Al	AS	cd	co	cr	cu	Fe	Mn	Mo	Ni	Pb	Sb	Si	Sr	Zn
Control Poultry	258,5	43,8	207,7	120,2	1,443	0.080	0.012	0.080	0,190	0,504	5,693	0,584	0,093	0,109	0,219	0,120	7,542	0,164	0,172
X	35,9	13,0	217,9	55,3	0,237	0.020	0.003	0.020	0,010	0,109	0,580	0,108	0,026	0,054	0,020	0,007	3,473	0,121	0,190
Y	33,6	10,0	162,6	42,2	0,129	0.020	0,099	0.020	0,086	0,030	0,509	0,219	0,004	0,087	0,021	0,002	3,314	0,121	0,093
P A-2	34,9	9,1	32,0	28,5	0,148	0.020	0.003	0.020	0,011	0,038	0,711	0,204	0,005	0,018	0,019	0,008	3,350	0,124	0,097
P B-2	28,7	8,3	32,5	29,0	0,127	0.020	0,030	0.020	0,007	0,033	0,433	0,201	0,013	0,084	0,018	-0,005	3,309	0,109	0,094
P C-2	31,0	8,7	34,9	29,6	0,111	0.020	0.003	0,048	0,017	0,053	0,738	0,205	0,003	0,040	0,024	0,008	3,402	0,118	0,074
P D-2	44,2	10,8	35,1	27,6	0,174	0.020	0.003	0.020	0,005	0,038	0,592	0,187	0,004	0,039	0,010	-0,001	4,275	0,159	0,104
P E-2	30,0	9,2	134,6	38,6	0,145	0.020	0.003	0.020	0,086	0,022	0,663	0,210	0,002	0,073	0,014	0,001	3,367	0,114	0,059
P F-2	29,9	11,7	38,4	28,6	0,107	0.020	0.003	0.020	0,015	0,018	0,522	0,147	0,004	0,016	0,009	0,005	3,135	0,114	0,034
P G-2	17,9	4,8	544,5	49,3	0,046	0.020	0,003	0.020	0,031	0,047	0,166	0,024	0,005	0,004	0,027	0,012	1,993	0,057	0,033
P H-2	26,8	7,6	513,5	35,2	0,080	0.020	0.003	0.020	0,019	0,033	0,645	0,110	0,005	0,021	0,010	0,001	2,998	0,081	0,041
P I-2	28,1	9,7	49,0	28,6	0,134	0.020	0.003	0.020	0,011	0,032	0,958	0,156	0,003	0,019	0,008	0,003	3,067	0,106	0,048
P J-2	30,2	12,0	69,3	28,9	0,115	0.020	0.003	0.020	0,015	0,024	0,815	0,140	0,003	0,024	0,014	0,002	3,053	0,109	0,041
P K-2	37,1	11,2	63,8	29,5	0,150	0.020	0.003	0.020	0,012	0,053	0,696	0,152	0,004	0,017	0,012	0,003	3,324	0,124	0,052
P L-2	31,1	16,3	196,7	31,1	0,143	0.020	0.003	0.020	0,012	0,037	0,617	0,085	0,003	0,019	0,025	0,000	3,413	0,105	0,046
P M-2	34,2	13,8	142,8	30,7	0,197	0.020	0.003	0.020	0,001	0,192	0,625	0,096	0,003	0,016	0,007	0,002	3,644	0,119	0,070
P N-2	25,9	13,2	111,5	30,3	0,120	0.020	0.003	0.020	0,015	0,060	0,677	0,072	0,004	0,017	0,016	0,003	3,263	0,101	0,066
P O-2	34,7	7,8	42,9	35,5	0,082	0.020	0.003	0.020	0,025	0,024	0,544	0,135	0,004	0,006	0,013	0,008	1,944	0,106	0,033
P P-2	35,4	7,4	43,1	36,1	0,060	0.020	0.003	0.020	0,021	0,024	0,143	0,100	0,005	0,009	0,011	0,007	1,756	0,102	0,021
P Q-2	31,8	10,8	65,1	29,0	0,113	0.020	0.003	0.020	0,002	0,027	0,650	0,115	0,005	0,031	0,010	-0,002	3,005	0,113	0,044
P R-2	30,9	10,2	50,4	28,4	0,096	0.020	0.003	0.020	0,010	0,025	0,624	0,126	0,015	0,017	0,011	0,002	3,100	0,109	0,044
P S-2	50,9	10,1	48,6	39,3	0,128	0.020	0.003	0.020	0,002	0,046	0,738	0,151	0,005	0,014	0,013	0,012	1,621	0,130	0,074
P T-2	39,7	7,9	63,0	54,8	0,108	0.020	0.003	0.020	0,001	0,047	0,709	0,114	0,004	0,010	0,021	0,011	1,671	0,127	0,041

Elements below the detection limits of ICP-OES

Sb	<Se	Cd	Co	Cr	As
<0,072	<0,068	<0,048	<0,32	-0,608	<0,32
0,007	<0.020	<0.003	<0.020	-0,038	0,008
0,007	<0.020	<0.003	<0.020	-0,010	<0.020
0,002	<0.020	0,099	<0.020	0,086	<0.020
-0,005	<0.020	0,030	<0.020	-0,007	<0.020
0,008	<0.020	<0.003	<0.020	-0,011	<0.020
-0,001	<0.020	<0.003	<0.020	-0,005	<0.020
0,008	<0.020	<0.003	0,048	-0,017	<0.020
0,005	<0.020	<0.003	<0.020	-0,015	<0.020
0,001	<0.020	<0.003	<0.020	0,086	<0.020
0,000	<0.020	<0.003	<0.020	-0,012	<0.020
0,003	<0.020	<0.003	<0.020	-0,012	<0.020
0,003	<0.020	<0.003	<0.020	-0,015	<0.020
0,002	<0.020	<0.003	<0.020	-0,001	<0.020
0,002	<0.020	<0.003	<0.020	-0,015	<0.020
0,003	<0.020	<0.003	<0.020	-0,011	<0.020
0,002	<0.020	<0.003	<0.020	-0,010	<0.020
-0,002	<0.020	<0.003	<0.020	-0,002	<0.020
0,001	<0.020	<0.003	<0.020	-0,019	<0.020
0,012	<0.020	0,003	<0.020	-0,031	<0.020
0,011	<0.020	<0.003	<0.020	-0,001	<0.020
0,012	<0.020	<0.003	<0.020	0,002	<0.020
0,007	<0.020	<0.003	<0.020	-0,021	<0.020
0,008	<0.020	<0.003	<0.020	-0,025	<0.020